# NOVEL STRATEGIES FOR CHARACTERIZING AND CONTROLLING THE STRESS RESPONSE OF *LISTERIA* SPP.

A Dissertation

Presented to the Faculty of the Graduate School

of Cornell University

in Partial Fulfillment of the Requirements for the Degree of

Doctor of Philosophy

by

Daina Lydia Ringus

August 2012

# NOVEL STRATEGIES FOR CHARACTERIZING AND CONTROLLING THE STRESS RESPONSE OF *LISTERIA* SPP.

Daina Lydia Ringus, Ph.D.

Cornell University 2012

The genus *Listeria* includes nine species, including the foodborne pathogen *Listeria monocytogenes*, which can cause serious illness in humans. *Listeria* spp. exist in urban and natural environments and are able to survive a diverse range of physiological conditions, to which the general stress response contributes. In *Listeria* spp. and other Gram-positive organisms, the general stress response is regulated by the alternative sigma factor sigma B ($\sigma^B$).

In these studies, we explored several novel methods of controlling and characterizing *Listeria* spp. in areas relevant to food safety, ranging from inactivation technologies to newly identified compounds for controlling the bacterial stress response. Specifically, the work presented here investigated: i) the use of Pulsed Light (PL), a nonthermal method, to inactivate *Listeria innocua* (a surrogate organism for *L. monocytogenes*) on packaging materials, ii) the transcriptional responses to stress of persistent and non-persistent strains of *L. monocytogenes* isolated from food processing environments as a possible mechanism of persistence, and iii) a novel small molecule inhibitor of $\sigma^B$ activity in *L. monocytogenes* and related *Bacillus subtilis*.

We found that PL was able to achieve inactivation of *L. innocua* up to 7.2 log CFU on low density polyethylene, and that inactivation was associated with the reflectance properties of the packaging materials that we tested. We found that *L. monocytogenes* strains from food processing plants classified as persistent did not induce higher transcript levels of four stress genes regulated by the transcriptional factors CtsR and $\sigma^B$ in response to salt stress compared to non-persistent strains. Finally, we determined that fluoro-phenyl-styrene-sulfonamide (FPSS), a

novel inhibitor of $\sigma^B$ activity, inhibits the activation of $\sigma^B$ in response to environmental and energy stresses in *B. subtilis*, and we conclude FPSS does not exert its inhibitory effect by interactions with the phosphatases RsbP or RsbU, or the members of the RsbV/RsbW/$\sigma^B$ partner switching model that is central to the regulation of $\sigma^B$. FPSS inhibits $\sigma^B$ activity by a yet unknown mechanism, and determining its mechanism of action will further our understanding of the regulation of $\sigma^B$.

## BIOGRAPHICAL SKETCH

Daina Lydia Ringus was born on August 5, 1983 near Chicago, IL as the youngest of three children to Dr. Julius Ringus and Lydia Ringus. Daina graduated from Yale University with a Bachelors of Art in literature in 2005. She spent the following year teaching English to grade school children in Cahors, France. While in France, Daina became interested in food production. Upon her return to the United States, she completed a second undergraduate degree (Bachelors of Science) in biochemistry at the University of Illinois at Chicago with the goal of pursuing a food science degree. During her time at UIC, Daina conducted undergraduate research with Dr. Donald Morrison studying *Streptococcus pneumoniae*. She began as a doctoral student at Cornell University in Food Science & Technology in 2008.

ACKNOWLEDGMENTS

I thank Dr. Kathryn Boor and Dr. Martin Wiedmann for their support and mentorship during my doctoral degree, and also my committee members Dr. Carmen Moraru and Dr. Dennis Miller, for their support. I also thank Dr. Ahmed Gaballa, an invaluable research mentor, and Dr. John Helmann for their help with my research.

In addition to my mentors, I thank the technicians of the Food Safety Lab, Maureen, Barbara, Esther, Sherry, Emily, and Steve; the postdocs, Teresa, Henk, Siyun, and Peter, and my labmates, Andrea, Courtenay, Haley, Kitiya, Laura, Lorraine, Matt R., Matt S., Pajau, Rachel, Sana, Travis, Tom, and Silin, for their support and friendship. I appreciate the support of my family, for their frequent visits to Ithaca and encouraging phone calls. I thank Reid Ivy for his support in and outside of the lab. Thank you to Stephanie Masiello, Dave Schuette, Céline Coquard Lenerz, and Tom Lenerz for their support and friendship throughout the past few years.

This work was supported by a USDA National Research Initiative grant (no. 2005-35201-15330 to K.J.B), a National Institutes of Health grant (no. 5R01AI052151-07), and by USDA National Needs Graduate Fellowship Competitive Grant No. 2007-38420-17751 from the National Institute of Food and Agriculture.

TABLE OF CONTENTS


| | | |
|---|---|---|
| CHAPTER 1 | Introduction | 1 |
| CHAPTER 2 | Pulsed Light inactivation of *Listeria innocua* on food packaging materials: inactivation kinetics and effect of surface roughness and reflectivity | 12 |
| CHAPTER 3 | Salt stress-induced transcription of $\sigma^B$- and CtsR-regulated genes in persistent and non-persistent L*isteria monocytogenes* strains from food processing plants | 34 |
| CHAPTER 4 | FPSS, a novel inhibitor of $\sigma^B$ activity, prevents the activation of $\sigma^B$ by environmental and energy stresses in *Bacillus subtilis* | 58 |
| CHAPTER 5 | Conclusions | 102 |
| APPENDIX 1 | Structure-activity relationships of FPSS analogs | 106 |

LIST OF FIGURES


| | | |
|---|---|---|
| Figure 1.1 | Comparison of *sigB* operons across species. | 3 |
| Figure 2.1 | PL inactivation of *L. innocua* on packaging coupons. | 22 |
| Figure 2.2 | Weibull predicted PL inactivation of *L. innocua* on packaging materials. | 26 |
| Figure 2.3 | Specular (A) and diffuse (B) reflection profiles of the packaging materials. | 27 |
| Figure 2.4 | Surface heating of coupons after PL. | 28 |
| Figure 2.5 | Water contact angles of coupons after PL treatment. | 29 |
| Figure 3.1 | Transcript levels, relative to transcript levels of 10403S at $t = 0$, of $\sigma^B$-regulated genes *gadD3* and *inlA* and CtsR-regulated genes lmo1138 and *clpB* before and after exposure ($t = 10$ min,) to BHI + 6% NaCl (w/v) at 37°C. | 42 |
| Figure 3.2 | Box plots of transcript levels, relative to transcript levels for 10403S at $t = 0$, of $\sigma^B$-regulated genes *gadD3* and *inlA* and CtsR-regulated genes lmo1138 and *clpB* before and after exposure ($t = 10$ min) to BHI + 6% NaCl (w/v) at 37°C, by persistence and lineage classifications. | 43 |
| Figure 3.3 | Induction of $\sigma^B$-regulated genes *gadD3* and *inlA* and CtsR-regulated genes lmo1138 and *clpB* after exposure to BHI + 6% NaCl (w/v) for 10 min at 37°C, by isolate. | 45 |
| Figure 3.4 | Box plots of induction of $\sigma^B$-regulated genes *gadD3* and *inlA* and CtsR-regulated genes lmo1138 and *clpB* after exposure to BHI + 6% NaCl (w/v) for 10 min at 37°C, by persistence and lineage classifications. | 46 |
| Figure 4.1 | Model of $\sigma^B$ regulation in *B. subtilis*. | 60 |
| Figure 4.2 | Effect of delayed addition of FPSS on salt-induced $\sigma^B$ activity. | 71 |

| | | |
|---|---|---|
| Figure 4.3 | Effect of FPSS on $\sigma^B$ activity by artificial induction. | 73 |
| Figure 4.4 | Effect of FPSS on $\sigma^B$ activity during entry into stationary phase. | 76 |
| Figure 4.5 | Effect of FPSS on $\sigma^B$ activity in response to azide stress. | 77 |
| Figure 4.6 | Effect of FPSS on $\sigma^B$ activity in response to phosphate limitation. | 78 |
| Figure 4.7 | Effect of FPSS on artificial induction of $\sigma^B$ activity by overexpression of RsbV. | 80 |
| Figure 4.8 | Effect of FPSS on $\sigma^B$ activation by growth at 16°C. | 82 |
| Figure 4.9 | Effect of FPSS on in vitro transcription of *L. monocytogenes* $\sigma^B$-dependent promoter. | 84 |
| Figure 4.10 | Stopped-flow fluorescence analysis of FPSS binding to *L. monocytogenes* $\sigma^B$ and RsbW. | 85 |
| Figure 4.11 | *sigB* transcript levels after addition of FPSS or DMSO in *L. monocytogenes* 10403SΔ*sigB*. | 87 |
| App. Figure 1 | Structures of FPSS analogs. Analogs of FPSS synthesized by B. Wang's group. | 106 |
| App. Figure 2 | Growth curves of *L. monocytogenes* 10403S with FPSS analogs WX-B-105 and WX-B-109. | 107 |
| App. Figure 3 | $\sigma^B$ activity of *B. subtilis* treated with FPSS analogs. | 108 |
| App. Figure 4 | Structural features of FPSS that contribution to inhibition of $\sigma^B$ activity and growth inhibition. | 109 |

LIST OF TABLES


| | | |
|---|---|---|
| Table 2.1 | Recovery losses for *L. innocua* on coupons of different packaging materials. | 19 |
| Table 2.2 | Weibull parameters for PL inactivation of *L. innocua* on packaging materials. | 23 |
| Table 2.3 | Surface roughness measurements of coupons. | 24 |
| Table 3.1 | Genes chosen in this study as reporters for activity of the transcriptional regulators $\sigma^B$ and CtsR. | 36 |
| Table 3.2 | *Listeria monocytogenes* strains used in this study. | 38 |
| Table 3.3 | Primers and probes used for qRT-PCR in this study. | 39 |
| Table 3.4 | Primers used for sequencing in this study. | 40 |
| Table 4.1 | Plasmids and strains used in this study. | 63 |
| Table 4.2 | Primers and probes used in this study. | 65 |
| Table 4.3 | Sporulation efficiency of *B. subtilis* treated with FPSS or DMSO. | 90 |

# CHAPTER 1

# INTRODUCTION

*Listeria monocytogenes* is a Gram-positive, non-sporeforming pathogen that can grow at temperatures as low as 0°C (35, 39) and at salt concentrations as high as 11% (17). The organism's ability to survive and replicate in conditions commonly used for preservation of food products presents food safety risks, and the vast majority of listeriosis cases are foodborne (30). According to the CDC, the incidence of listeriosis has not decreased since 2005 (7). Listeriosis symptoms can range from mild flu-like symptoms to meningitis, septicemia, and abortion in pregnant women. Furthermore, listeriosis has a relatively high mortality rate of 20-30% despite treatment with antibiotics (18-20). Therefore, *L. monocytogenes* remains a public health concern.

## ***Listeria*** **spp. prevalence and persistence**

Within the genus *Listeria*, nine species have been recognized, including three hemolytic species, *L. monocytogenes*, *L. ivanovii*, and *L. seeligeri*, and six non-hemolytic species, *L. innocua*, *L. welshimeri*, *L. grayi*, *L. rocourti*, *L. marthii*, and *L. fleischmannii* (2). *L. innocua* is a nonpathogenic species that is often used as a surrogate organism for *L. monocytogenes* during inactivation studies because of its genomic and growth requirement similarities (4, 10, 21).

*Listeria* spp. are widely prevalent (> 20% of positive samples) in natural and urban environments and are found in soil and water and on vegetation, sidewalks and floors, and human contact surfaces (29). *L. monocytogenes* and *L. innocua*, in particular, are significantly associated with urban environments (29). *L. monocytogenes* that is present in the natural environment can serve as a source of contamination of food processing facilities, entering via transmission by workers, on food supplies, or on equipment (14). Once inside these facilities, the

pathogen can contaminate packaging materials or food products after kill steps, or may establish in a particular niche within the environment, such as in drains or in hard-to-clean locations (6). *L. monocytogenes* persistence, defined as the organism's repeated presence over a prolonged period of sampling, is an important concern for food processors, and understanding the mechanisms of persistence may help control and prevent *L. monocytogenes* contamination of food products, which is especially of concern in ready-to-eat products that are not heated prior to consumption.

Novel methods such as Pulsed Light (PL) treatment have been investigated for nonthermal, chemical-free alternatives to conventional decontamination approaches. PL treatment utilizes brief pulses of high intensity broad spectrum light generated by inert gas discharge lamps. The technology has been shown to inactive vegetative bacteria, bacterial spores, and fungi on food products and food contact materials (24). In particular, PL inactivation of *Listeria* spp. has been shown on ready-to-eat sausages (37), chicken frankfurters (16), and stainless steel (42). These studies have shown that substrate properties impact the efficacy of PL treatment and should be considered when using PL for microbial inactivation.

***L. monocytogenes* stress response**

*L. monocytogenes* possesses several sigma factors that regulate transcription, including a primary sigma factor, sigma A, and four alternative sigma factors. Sigma factors are protein subunits of RNA polymerase (RNAP) that bind to core RNAP, allowing the holoenzyme to recognize specific binding sites (promoter sites) for initiation of transcription (5). The alternative sigma factor sigma B ($\sigma^B$) regulates the general stress response of *L. monocytogenes*, and the $\sigma^B$ regulon comprises over 150 directly regulated genes (15, 22, 27). $\sigma^B$ has been shown to be activated in response to heat, cold, acid, bile salt, and oxidative stress (1, 11, 15, 27, 34, 40, 41).

$\sigma^B$ has a significant role in this organism's response to changing environmental conditions, such as those encountered in food products and during gastrointestinal invasion.

The alternative sigma factor $\sigma^B$ is also activated by environmental stress and nutrient deprivation in the related organism *Bacillus subtilis* (see (12) for review). The regulation of $\sigma^B$ has been most extensively studied in *B. subtilis*, and many of the genes encoding Rsb (regulators of sigma B) proteins of the signal transduction pathways modulating $\sigma^B$ activity are conserved in other Gram-positive species including *L. monocytogenes, Staphylococcus aureus*, and *Bacillus cereus* (Figure 1.1). The *sigB* operon encodes proteins involved in the partner-switching mechanism first characterized in *B. subtilis*, which has also been demonstrated in *L. monocytogenes*, *S. aureus*, and *B. cereus*. (8, 25, 38).

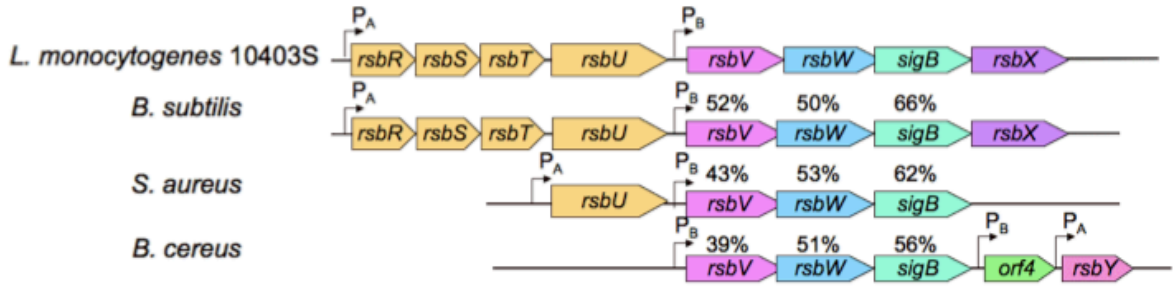


**Figure 1.1** Comparison of *sigB* operons across species. Arrows denote promoter sites ($P_A$, $\sigma^A$ promoter site; $P_B$, $\sigma^B$ promoter site). Percentages indicate % identity of amino acid sequences of corresponding proteins with *L. monocytogenes* 10403S, calculated using Uniprot BLAST.

In *L. monocytogenes*, $\sigma^B$'s regulation of genes that contribute to survival of stresses encountered during gastrointestinal stress and its modulation of key virulence genes suggest the sigma factor has a crucial role during intestinal adaptation. During gastrointestinal passage, ingested cells experience high acid conditions (pH ~2.0), followed by high osmolarity in the small intestine (equivalent to ~0.3 M NaCl) and bile detergent stress. Pre-adaptation to high

osmolarity has a protective effect on *L. monocytogenes* survival of bile stress, and suggests osmolarity may act as a signal for gut entry (32). $\sigma^B$ mediates the expression of genes necessary to survive these environmental stresses as well as genes involved in intestinal adaptation, including genes that encode the invasion proteins InlA and InlB and bile salt hydrolase (36). Furthermore, $\sigma^B$ appears to downregulate the expression of genes controlled by PrfA during intracellular infection, thus limiting cytotoxic effects during intracellular infection (23).

**Chemical biology: novel approaches to controlling and understanding pathogens**

The importance of $\sigma^B$ to *L. monocytogenes* stress survival and infection makes it a potential target for novel therapeutics. One approach to identifying compounds that target the protein is using chemical biology. Chemical biology relies on using small molecules as probes of biological systems and tools for drug discovery (33). High throughput screening (HTS) methods allow screening of libraries that contain several thousand compounds for a desired interaction or phenotype using cell-based or fragment-based reporter systems (9). Low throughput screening is then applied to further refine hits and define leads for drug or knowledge discovery (3).

Interactions of small molecule compounds with targets have been identified in several bacterial systems. For example, Hung et al. (13) used HTS to identify an inhibitor, "virstatin," of the transcriptional regulator ToxT in *Vibrio cholerae*. Treatment of *V. cholerae* cells with virstatin prevented intestinal colonization of infant mice after cells were delivered orogastrically. Other small molecule targets include the transcriptional regulator AlgR1 in *Pseudomonas aeruginosa* (28), *B. anthracis* lethal factor, and type III secretion system proteins (31). These examples illustrate previous successes of using small molecule compound libraries to identify interactions within bacterial systems.

Previous work done in our group identified a small molecule inhibitor, fluoro-phenyl-styrene-sulfonamide (FPSS), of the $\sigma^B$-regulated stress response in *L. monocytogenes* and *B. subtilis* (26). Approximately 57,000 compounds were screened for inhibition of $\sigma^B$ activity, measured indirectly via an *opuCA-gus* reporter fusion. From the 41 compounds chosen for secondary screening, 3 were chosen for follow-up based on information regarding mammalian cell toxicity information. An analog of the most effective of these 3 inhibitors (as determined by qRT-PCR analysis of a $\sigma^B$-dependent gene) was pursued, FPSS, since the original compound was unavailable for purchase. FPSS was: i) shown to inhibit $\sigma^B$ activity in *L. monocytogenes* and *B. subtilis*, ii) shown by microarray analysis to downregulate a large numbers of genes known to be upregulated by $\sigma^B$, iii) shown to inhibit bile hydrolase activity, and iv) shown to reduce *L. monocytogenes'* ability to invade Caco-2 human enterocyte cells. The mechanism by which FPSS inhibits $\sigma^B$ is yet unknown, and identifying its mode of action will be valuable to understanding its applications in these and other organisms

REFERENCES


1. **Begley, M., R. D. Sleator, C. G. M. Gahan, and C. Hill.** 2005. Contribution of three bile-associated loci, *bsh*, *pva*, and *btlB*, to gastrointestinal persistence and bile tolerance of *Listeria monocytogenes*. Infect Immun **73:**894-904.
2. **Bertsch, D., J. Rau, M. R. Eugster, M. C. Haug, P. A. Lawson, C. Lacroix, and L. Meile.** 2012. *Listeria fleischmannii* sp. nov., isolated from cheese. Int J Syst Evol Microbiol**:**ijs.0.036947-0.
3. **Bleicher, K. H., H.-J. Bohm, K. Muller, and A. I. Alanine.** 2003. Hit and lead generation: beyond high-throughput screening. Nat Rev Drug Discov **2:**369-378.
4. **Buchrieser, C., C. Rusniok, C., F. Kunst, P. Cossart, and P. Glaser, and Listeria Consortium.** 2003. Comparison of the genome sequences of *Listeria monocytogenes* and *Listeria innocua*: clues for evolution and pathogenicity. FEMS Immunol Med Microbiol **35:**207-213.
5. **Burgess, R. R., A. A. Travers, J. J. Dunn, and E. K. F. Bautz.** 1969. Factor stimulating transcription by RNA polymerase. Nature **221:**43-46.
6. **Carpentier, B., and O. Cerf.** 2011. Review - Persistence of *Listeria monocytogenes* in food industry equipment and premises. Intl J Food Microbiol **145:**1-8.
7. **CDC.** 2009. Preliminary FoodNet data on the incidence of infection with pathogens transmitted commonly through food --- 10 States, 2008. MMWR **58:**333-337.
8. **Chaturongakul, S., and K. J. Boor.** 2004. RsbT and RsbV contribute to $\sigma^B$-dependent survival under environmental, energy, and intracellular stress conditions in *Listeria monocytogenes*. Appl Environ Microbiol **70:**5349-5356.

9. **Clemons, P. A.** 2004. Complex phenotypic assays in high-throughput screening. Curr Opin Chem Biol **8:**334-338.

10. **Fairchild, T. M., and P. M. Foegeding.** 1993. A proposed nonpathogenic biological indicator for thermal inactivation of *Listeria monocytogenes*. Appl Environ Microbiol **59:**1247-1250.

11. **Ferreira, A., C. P. O'Byrne, and K. J. Boor.** 2001. Role of $\sigma^B$ in heat, ethanol, acid, and oxidative stress resistance and during carbon starvation in *Listeria monocytogenes*. Appl Environ Microbiol **67:**4454-4457.

12. **Hecker, M., J. Pané-Farré, and U. Völker.** 2007. SigB-dependent general stress response in *Bacillus subtilis* and related gram-positive bacteria. Microbiology **61:**215-236.

13. **Hung, D. T., E. A. Shakhnovich, E. Pierson, and J. J. Mekalanos.** 2005. Small-molecule inhibitor of *Vibrio cholerae* virulence and intestinal colonization. Science **310:**670-674.

14. **Ivanek, R., Y. T. Gröhn, and M. Wiedmann.** 2006. *Listeria monocytogenes* in multiple habitats and host populations: review of available data for mathematical modeling. Foodborne Path Disease **3:**319-336.

15. **Kazmierczak, M. J., S. C. Mithoe, K. J. Boor, and M. Wiedmann.** 2003. *Listeria monocytogenes* $\sigma^B$ regulates stress response and virulence functions. J Bacteriol **185:**5722-5734.

16. **Keklik, N. M., A. Demirci, V. M. Puri, and P. H. Heinemann.** 2012. Modeling the inactivation of *Salmonella* Typhimurium, *Listeria monocytogenes*, and *Salmonella* Enteritidis on poultry products exposed to Pulsed UV Light. J Food Prot **75:**281-288.

17. **Maria-Rosario, A., I. Davidson, M. Debra, A. Verheul, T. Abee, and I. R. Booth.** 1995. The role of peptide metabolism in the growth of *Listeria monocytogenes* ATCC 23074 at high osmolarity. Microbiology **141:**41-49.

18. **Mead, P. S., L. Slutsker, V. Dietz, L. F. McCaig, J. S. Bresee, C. Shapiro, P. M. Griffin, and R. V. Tauxe.** 1999. Food-related illness and death in the United States. Emerg Infect Dis **5:**607-25.

19. **Mitjà, O., C. Pigrau, I. Ruiz, X. Vidal, B. Almirante, A.-M. Planes, I. Molina, D. Rodríguez, and A. Pahissa.** 2009. Predictors of mortality and impact of aminoglycosides on outcome in listeriosis in a retrospective cohort study. J Antimicrob Chemother **64:**416-423.

20. **Mylonakis, E., E. L. Hohmann, and B. Calderwood.** 1998. Central nervous system infection with *Listeria monocytogenes*: 33 years' experience at a general hospital and review of 776 episodes from the literature. Medicine **77:**313.

21. **Nolan, D. A., D. C. Chamblin, and J. A. Troller.** 1992. Minimal water activity levels for growth and survival of *Listeria monocytogenes* and *Listeria innocua*. Intl J Food Microbiol **16:**323-335.

22. **Oliver, H., R. Orsi, L. Ponnala, U. Keich, W. Wang, Q. Sun, S. Cartinhour, M. Filiatrault, M. Wiedmann, and K. Boor.** 2009. Deep RNA sequencing of L. monocytogenes reveals overlapping and extensive stationary phase and sigma B-dependent transcriptomes, including multiple highly transcribed noncoding RNAs. BMC Genomics **10:**641.

23. **Ollinger, J., B. Bowen, M. Wiedmann, K. J. Boor, and T. M. Bergholz.** 2009. *Listeria monocytogenes* $\sigma^B$ modulates PrfA-mediated virulence factor expression. Infect Immun **77:**2113-2124.

24. **Oms-Oliu, G., O. Martín-Belloso, and R. Soliva-Fortuny.** 2010. Pulsed Light Treatments for Food Preservation: A Review. Food and Bioprocess Technology **3:**13-23.

25. **Palma, M., and A. L. Cheung.** 2001. Sigma B activity in *Staphylococcus aureus* is controlled by RsbU and an additional factor (s) during bacterial growth. Infect Immun **69:**7858-7865.

26. **Palmer, M. E., S. Chaturongakul, M. Wiedmann, and K. J. Boor.** 2011. The *Listeria monocytogenes* $\sigma^B$ regulon and its virulence-associated functions are inhibited by a small molecule. mBio **2:**e00241.

27. **Raengpradub, S., M. Wiedmann, and K. J. Boor.** 2008. Comparative analysis of the $\sigma^B$-dependent stress responses in *Listeria monocytogenes* and *Listeria innocua* strains exposed to selected stress conditions. Appl Environ Microbiol **74:**158-171.

28. **Roychoudhury, S., N. A. Zielinski, A. J. Ninfa, N. E. Allen, L. N. Jungheim, T. I. Nicas, and A. M. Chakrabarty.** 1993. Inhibitors of two-component signal transduction systems: inhibition of alginate gene activation in *Pseudomonas aeruginosa*. Proc Natl Acad Sci U S A **90:**965-9.

29. **Sauders, B. D., J. Overdevest, E. Fortes, K. Windham, Y. Schukken, A. Lembo, and M. Wiedmann.** 2012. Diversity of Listeria species in urban and natural environments. Appl Environ Microbiol **78:**4420-4430.

30. **Scallan, E., R. M. Hoekstra, F. J. Angulo, R. V. Tauxe, M.-A. Widdowson, S. L. Roy, J. L. Jones, and P. M. Griffin.** 2011. Foodborne illness acquired in the United States--major pathogens. Emerging Infectious Diseases **17:**7-15.

31. **Schepetkin, I. A., A. I. Khlebnikov, L. N. Kirpotina, and M. T. Quinn.** 2006. Novel small-molecule inhibitors of anthrax lethal factor identified by high-throughput screening. J Med Chem **49:**5232-5244.

32. **Sleator, R. D., D. Watson, C. Hill, and C. G. M. Gahan.** 2009. The interaction between *Listeria monocytogenes* and the host gastrointestinal tract. Microbiology **155:**2463-2475.

33. **Strausberg, R. L., and S. L. Schreiber.** 2003. From knowing to controlling: A path from genomics to drugs using small molecule probes. Science **300:**294-295.

34. **Sue, D., D. Fink, M. Wiedmann, and K. J. Boor.** 2004. $\sigma^B$-dependent gene induction and expression in *Listeria monocytogenes* during osmotic and acid stress conditions simulating the intestinal environment. Microbiology **150:**3843-3855.

35. **Tasara, T., and R. Stephan.** 2006. Cold stress tolerance of *Listeria monocytogenes*: A review of molecular adaptive mechanisms and food safety implications. J Food Prot **69:**1473-1484.

36. **Toledo-Arana, A., O. Dussurget, G. Nikitas, N. Sesto, H. Guet-Revillet, D. Balestrino, E. Loh, J. Gripenland, T. Tiensuu, and K. Vaitkevicius.** 2009. The *Listeria* transcriptional landscape from saprophytism to virulence. Nature **459:**950-956.

37. **Uesugi, A. R., and C. I. Moraru.** 2009. Reduction of *Listeria* on ready-to-eat sausages after exposure to a combination of pulsed light and nisin. J Food Prot **72:**347-353.

38. **van Schaik, W., M. H. Tempelaars, M. H. Zwietering, W. M. de Vos, and T. Abee.** 2005. Analysis of the role of RsbV, RsbW, and RsbY in regulating $\sigma^B$ activity in *Bacillus cereus*. J Bacteriol **187:**5846-5851.

39. **Walker, S. J., P. Archer, and J. G. Banks.** 2008. Growth of *Listeria monocytogenes* at refrigeration temperatures. J App Microbiol **68:**157-162.

40. **Wemekamp-Kamphuis, H. H., J. A. Wouters, P. P. de Leeuw, T. Hain, T. Chakraborty, and T. Abee.** 2004. Identification of sigma factor $\sigma^B$-controlled genes and their impact on acid stress, high hydrostatic pressure, and freeze survival in *Listeria monocytogenes* EGD-e. Appl Environ Microbiol **70:**3457-3466.

41. **Wiedmann, M., T. J. Arvik, R. J. Hurley, and K. J. Boor.** 1998. General stress transcription factor sigma B and its role in acid tolerance and virulence of *Listeria monocytogenes*. J Bacteriol **180:**3650-3656.

42. **Woodling, S. E., and C. I. Moraru.** 2005. Influence of surface topography on the effectiveness of pulsed light treatment for the inactivation of *Listeria innocua* on stainless-steel surfaces. J Food Sci **70:**345-351.

CHAPTER 2

# PULSED LIGHT INACTIVATION OF *LISTERIA INNOCUA* ON FOOD PACKAGING MATERIALS: INACTIVATION KINETICS AND EFFECT OF SURFACE ROUGHNESS AND REFLECTIVITY

*Submitted to: Journal of Food Engineering*

## ABSTRACT

Inactivation of *Listeria innocua* on food packaging materials by Pulsed Light (PL) treatment was investigated. Coupons of low density polyethylene (LDPE), high density polyethylene (HDPE), polyethylene-laminated ultra-metalized polyethylene terephthalate (MET), polyethylene-coated paperboard (TR), and polyethylene-coated aluminum foil paperboard laminate (EP) were inoculated with *L. innocua* cells in stationary growth phase. Inoculated coupons (~8 CFU/coupon) were treated with PL fluence of up to 8.0 J/cm$^2$, and survivors were determined. Reductions up to 7.2 ± 0.29, 7.1 ± 0.06, 4.4 ± 0.85, 4.5 ± 1.32, and 3.5 ± 0.82 log CFU/coupon were obtained on LDPE, HDPE, MET, TR, and EP, respectively. Inactivation data were used to determine Weibull kinetic parameters and predict inactivation in a wide range of fluence. Increasing surface reflectivity and surface roughness appeared to induce lower inactivation. Minimal surface heating was observed for all materials except MET, on which significant heating occurred. These results demonstrate the potential of PL as an effective method for decontaminating food packaging materials.

## INTRODUCTION

Decontamination of food packaging materials is necessary to ensure microbial safety and extend shelf life of food products, and is particularly important in aseptic applications. Currently,

hydrogen peroxide is used alone or in combination with heat to sanitize packages before filling in aseptic processes (1). One of the disadvantages of chemical disinfection is that residual chemicals may be left on the packaging material, which may alter the properties of the packaged food and, most importantly, may be detrimental for the consumers. Therefore, the food industry seeks alternative, non-chemical decontamination methods applicable for food packaging.

Pulsed Light (PL) treatment utilizes short pulses of broad white light, ranging from 200 to 1100 nm, to inactivate microorganisms. The inactivation of PL is mainly attributed to the bactericidal UV range of light < 400 nm (20). PL technology has features that recommend it for decontaminating packaging during aseptic processing, including: quick treatment time, no chemical residues, and recognition by the FDA for the treatment of food contact surfaces.

Several studies have investigated the use of PL to inactive microorganisms on solid substrates (3, 6, 11, 13, 14, 16, 18, 19). It has been hypothesized that physical properties of surfaces including surface topography and reflectivity affect the efficacy of PL inactivation. Surface roughness and crevices have been suggested as shielding cells during treatment, and surface hydrophobicity may influence the distribution of bacterial contaminants on surfaces, as inoculum containing hydrophilic organisms such as *Listeria monocytogenes* (10) may bead together and lead to more dense stacking of cells and potential shading effects. High reflectivity was observed to coincide with lowered inactivation by PL and continuous UV (19, 21). Woodling and Moraru (21) found lower PL inactivation of *L. innocua* on electropolished, highly reflective stainless steel than on less reflective stainless steel coupons, and Stannard et al. (13, 14) reported a similar trend using ultraviolet light for inactivation of spores on aluminum/ polyethylene laminated paperboard compared to less reflective paperboard/polyethylene laminate.

Studies investigating PL inactivation on and through packaging films (6-8) have shown PL to be effective for decontaminating common packaging materials. Minimal changes to the mechanical properties of packaging materials exposed to mild treatments of PL have been reported (7, 8), suggesting that PL may be a strategy for inactivating pathogenic bacteria on food products after packaging.

The objective of this study was to compare the effectiveness of PL for the inactivation of the challenge organism *L. innocua* on different food packaging materials. In this study, *L. innocua* served as a surrogate organism for *L. monocytogenes*. This particular strain of *L. innocua* has been shown to be slightly more resistant to PL treatment than a five-strain cocktail of *L. monocytogenes* (17). Furthermore, *L. monocytogenes* is one of the more PL resistant organisms (5). The use of *L. innocua* in this study allows for a direct comparison of inactivation on other solid substrates, including stainless steel (18, 21) and beef sausages (17). The chosen substrates represent common food packaging materials with similar surface hydrophobicity. Additionally, physical properties of the materials before and after treatment were evaluated to understand their effects on efficacy of microbial inactivation, as well as to determine the effects of PL on these materials' water contact angle and heating effects.

## MATERIALS AND METHODS

### *Bacterial cells and culture conditions*

A strain of *L. innocua* (FSL C2-008), stored at -80°C in 15% glycerol, was obtained from the Food Safety Laboratory at Cornell University (Ithaca, NY). A working stock was maintained on Tryptic Soy Agar (TSA; Difco, Becton Dickinson, Sparks, MD) slants, kept at 4°C. Cells from the working culture were streaked for isolation on TSA and used to inoculate 10 ml sterile

Brain Heart Infusion broth (BHI; Difco, Becton Dickinson), in order to achieve a high cell density. The culture was grown statically at 35 ± 2° C for 24 h to stationary phase, and transferred twice into fresh BHI using a 10 ul sterile transfer loop to achieve synchronized growth phases of passaged cells. Cultures were centrifuged at 3,700 *x g* for 10 min at 22°C, and the pellets were resuspended in 10 ml 0.1% sterile peptone (Difco, Becton Dickinson). Initial inoculum populations contained approximately 2 x $10^9$ CFU/ml.

*Coupon preparation and inoculation*

Rectangular (2.5 cm × 5 cm) coupons of the following materials were used: low density polyethylene (LDPE) (2 MIL poly bags; 0.04 mm thickness; Uline, Waukegan, IL), high density polyethylene (HDPE) (6.46 mm thickness; Regal Plastics, Dallas, TX), PET/LDPE/ultra metalized PET/LDPE/LLDPE metallocene bags (MET) (0.09 mm thickness); LDPE/paperboard/LDPE (TR) (0.46 mm thickness; TetraRex, Tetra Pak, Vernon Hills, IL), and PE/paperboard/PE/Al foil/TIE/PE (EP) (Alu board, 0.67 mm thickness; Elopak, New Hudson, MI). Prior to inoculation, all coupons except paperboard-containing materials were sonicated in a FS30H ultrasonic cleaner (Fisher Scientific, Pittsburgh, PA) containing 30:1 dilution of Fisherbrand Versa-Clean (Fisher Scientific) in deionized water for 30 min to remove dirt and debris. Cleaned coupons were rinsed with sterile deionized water and dried at room temperature on a laboratory bench. Before inoculation, dried coupons were sanitized by spraying with 70% ethanol and allowed to dry. To prevent seepage of fluids into the paperboard layer, the TR coupons were wiped with detergent solution and deionized water before air-drying. The cleaned TR coupons were sprayed with ethanol, dried on the bench, and cut into coupons using sterile scissors. Stainless steel coupons (mill finish; 5 cm × 10 cm) used as stages for coupons during

PL treatment were cleaned using the same procedure mentioned above, and autoclaved for 30 min at 121°C.

Dried, sterile packaging coupons were placed in sterile polystyrene Petri dishes (Fisherbrand) and inoculated with 0.5 ml of *L. innocua* culture in the stationary phase, delivered in 10 x 50 ul drops using a repeater pipette (Repeater Pipette Plus; Eppendorf). The concentration of the inoculum ($N_0$) was 2 x$10^9$ CFU/ml, determined by standard plate counting, as described in Section 2.4, resulting in a total inoculum load of 1 x $10^9$ CFU/coupon. Inoculated coupons were dried for 24 ± 1 h in a glass desiccator containing a supersaturated solution of $MgCl_2$× 6 $H_2O$ (Fisher Scientific), which maintained a headspace relative humidity of 32 ± 2%. The desiccator was kept in an incubator at 23 ± 1°C, to ensure consistent temperature during drying. These temperature and relative humidity conditions were optimized for reproducibility regarding the drying of inoculum and survivor losses.

*PL treatment and fluence measurements*

PL treatments were performed using a RS-3000C SteriPulse System (Xenon Corp., Woburn, MA). Inoculated coupons were placed on sterile stainless steel surfaces on a tray located 101.6 mm below the quartz lamp, centered underneath the focal point of the lamp. The coupons were treated with 1 to 12 pulses of light, at a fluence of 0.67 J/$cm^2$ per pulse (360 us). For all materials, the inoculated side of the coupons was placed facing the Xenon lamp, except for samples "LDPE through", which were treated with their inoculated side down to measure inactivation "through" the packaging film. Fluence measurements were taken using a pyroelectric head (PE25BBH) with a Nova II display (Ophir Optronics Inc., Wilmington, MA), with an aperture cover having a circular opening of 1 $cm^2$ and a pulse width setting of the meter of 1.0 ms. The pyroelectric head was placed 101.6 mm from the lamp source. Pauses of at least

30 s between measurements were allowed in order to prevent overheating of the pyroelectric head. Fluence measurements were performed in triplicate.

*Recovery and enumeration of survivors*

After PL treatment, coupons were placed into sterile 50 ml polypropylene centrifuge tubes (Fisherbrand, Fischer Scientific) containing 20 ml sterile TSB (a rich, nonselective medium for maximum recovery of damaged cells). The tubes were placed in the 23 ± 1°C incubator for 15 min to allow better recovery of the dried inocula before tubes were vortexed for 2 min at 3,000 rpm (Digital Vortex Mixer, Fischer Scientific). The recovery broth was serially diluted in Butterfield's phosphate buffer (BPB) and spread-plated on TSA. Plates were incubated at 35 ± 2° C for 48 h before counting the survivors (N). The concentration of the inoculum ($N_0$) was determined using the same procedure.

Accordingly, samples of the recovery of treatments yielding less than 20 CFU/plate were enumerated using the most probable number (MPN) technique following Swanson et al. (15). Samples of the recovery broth were serially diluted in BPB, and 1 ml aliquots of each dilution were transferred to 3 glass test tubes (150 x 16 mm) containing 9 ml TSB, which were incubated for 48 hrs at 35 ± 2° C. Positive tubes were presumptively identified by turbidity and further tested by streaking onto Modified Oxford media (Difco; Becton Dickinson) plates that were incubated for 24 hrs at 35 ± 2°C, and checked for black colonies with black halos, which indicated positive presence of *Listeria* spp.

*Evaluation of PL efficiency*

Microbial inactivation by PL was calculated as the logarithm of the survivor ratio, log ($N/N_0$). Recovery losses were determined using control coupons inoculated and dried but not treated with Pulsed Light, to account for the cells that either could not be recovered from the

inoculated coupons and for the cells that became nonviable during drying. The recovery losses for each type of surface are shown in Table 2.1.

Recovery losses were accounted for in calculating survivor ratios according to the formula (21):

$$\log\left(\frac{N}{N_0}\right) = \log\left(\frac{\text{Survivors}}{\text{Initial inoculum} \quad - \text{ Recovery loss}}\right) \qquad (1)$$

*Kinetic modeling of inactivation curves*

The non-linear Weibull model was used to describe inactivation kinetics. For microbial inactivation by Pulsed Light, the Weibull function takes the form (18):

$$\ln\left(\frac{N}{N_0}\right) = -\left(\frac{F}{\alpha}\right)^{\beta}, \text{ or } \log\left(\frac{N}{N_0}\right) = -\frac{1}{2.303}\left(\frac{F}{\alpha}\right)^{\beta} \qquad (2)$$

where $N/N_0$ represents the ratio of survivors after treatment over the initial number of organisms, $\alpha$ is the scale parameter, $\beta$ is the shape factor, which describes the shape of the survivor curve and F is the fluence ($J/cm^2$). The Weibull parameters $\alpha$ and $\beta$ were obtained by linearizing eq. (2). Specifically, $\log(\log(N/N_0))$ was plotted vs. log (F) and the Weibull parameters were obtained from the regression equation (3):

$$\log\left(\log\left(\frac{N}{N_0}\right)\right) = \beta \cdot \log(F) + \log(\alpha) \qquad (3)$$

**Table 2.1** Recovery losses for *L. innocua* on coupons of different packaging materials. Means of recovery losses (log (Initial inoculum –recovered CFU/coupon)) and SD are shown from three biological replicates.

| Material type | Recovery loss (log CFU/coupon ± SD) |
|---|---|
| LDPE direct | 1.0 ± 0.25 |
| LDPE through | 1.2 ± 0.39 |
| HDPE | 1.3 ± 0.11 |
| MET | 1.1 ± 0.28 |
| TR | 0.9 ± 0.12 |
| EP | 1.0 ± 0.26 |

*Heating effects*

Temperature changes as a result of PL treatment were determined by measuring the surface temperature on the coupons before and immediately (within 5 sec) after the treatment using an infrared thermometer (Fisher Scientific). All temperature measurements were performed in triplicate.

*Physical property analysis of the coupons*

Water contact angle measurements as a measure of hydrophobicity were performed using a CAM-PLUS contact angle meter (Chemsultants International, Inc., Mentor, OH) with reagent grade deionized water at room temperature on cleaned and sterilized coupons, as described elsewhere (3). All analyses were conducted both on untreated coupons (controls) and on coupons exposed to fluences ranging from 0.6 to 16.1 J/cm$^2$ (without inoculation). Two measurements per coupon were performed, and all measurements were conducted in triplicate.

Surface roughness profiles were measured using Veeco Dektak 6 M profilometer at the Nanobiotechnology Center at Cornell University. Ra, the average roughness, Rq, the root mean square roughness, and R10, the ten point roughness, the average height of the five highest local

maxima plus the average height of the five lowest local minimums, were measured on a 5 millimeter unit of the sample scanned with an applied stylus force of 4.47 mg. Each material was analyzed 3 times.

Specular and diffuse reflection profiles of the clean coupons were measured using a Fiber Optic Spectrometer HR 2000+CG-UV-NIR with a QR400-7-SR Reflection Probe (Ocean Optics, Inc.; Dunedin, FL). Specular reflection was measured by holding the probe at 90° from coupon surfaces with a CSH probe holder and a STAN-SSH standard (Ocean Optics). Diffuse reflection measurements were conducted using the same probe held at 45° relative to coupon surfaces, using a CSH-45 probe holder and a WS-1 standard (Ocean Optics).

*Statistical analysis*

Analysis of variance and post hoc Tukey's honest significant difference (HSD) tests were used to evaluate differences in inactivation, recovery losses, Weibull parameters, and physical properties among the different treatment levels and materials ($P < 0.05$). Student's t-test analysis was used to compare significantly different inactivation on opposing sides of LDPE ($p < 0.05$). All statistical analyses were performed using JMP 7.0 (SAS Institute Inc., Cary, NC).

## RESULTS AND DISCUSSION

### Inactivation of *L. innocua* on the packaging materials

As seen in the inactivation curves in Figure 1, inactivation of *L. innocua* increased with fluence in a non-linear fashion for all tested materials. The inactivation curves showed evidence of tailing, which is consistent with previous PL inactivation studies on solid surface substrates (18, 21). The treatment was most effective on HDPE and LDPE, with log reductions of 7.1 ± 0.06 and 7.2 ± 0.29 CFU, respectively, at the maximum fluence tested in this study (~8 J/cm$^2$).

Lower inactivation levels were achieved on EP, MET, and TR, with maximum inactivation of 3.5 ± 0.82, 4.4 ± 0.85, and 4.5 ± 1.32 log CFU, respectively. It is important to note that similar recovery losses, of around 1 log CFU, were obtained for all coupons (Table 2.1), with no statistically significant differences ($p > 0.05$) among materials. This indicates that differences in inactivation cannot be attributed to varying recovery losses of cells from the different materials. Based on the transparency of the LDPE, it was assumed that PL treatment may also be effective when applied through packaging, not only on the packaging surface directly exposed to the light. To test this hypothesis, this substrate was exposed to the treatment both by exposing the inoculated surface to the light ("LDPE direct" in Figure 2.1) or by flipping the inoculated coupon and treating it upside down ("LDPE through" in Figure 2.1). Both treatments yielded similar results, with no statistically significant differences ($p > 0.05$) in total inactivation between the two orientations of inoculum relative to the xenon lamp at any fluence level. This is an important result, consistent with previous work (7, 8) demonstrating PL inactivation of bacteria through LDPE, as it suggests that PL could potentially be used as a terminal, "through packaging" treatment, when LDPE is used as a packaging material.

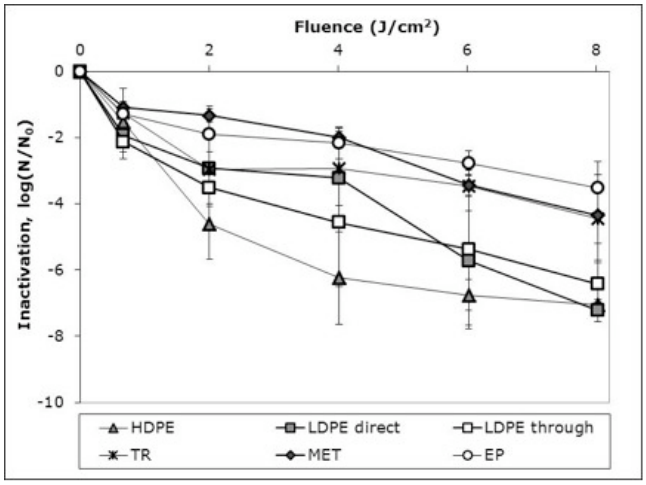


**Figure 2.1** PL inactivation of *L. innocua* on packaging coupons. Inoculum concentration on coupons ($N_0$) represents initial inoculum – recovery loss. Error bars show SD (n = 3).

Since in practical applications it is very useful to be able to estimate microbial inactivation at any given treatment (i.e., fluence in the case of PL treatment), the experimental inactivation data were used to generate kinetic parameters for inactivation of *L. innocua* on all packaging materials. The calculated shape ($\beta$) and scale ($\alpha$) parameters for the PL inactivation of *L. innocua* on the substrates are shown in Table 2.2. The Weibull model was able to represent quite accurately the survivor ratios for all substrates, and a good fit of the Weibull calculated inactivation with the experimental data was found. When interpreting the values in Table 2.2 it is important to note that a shape parameter $\beta > 1$ describes a concave down curve, $\beta < 1$ describes a concave up curve, and $\beta = 1$ describes the particular case of a linear inactivation curve. The shape parameters for all materials were <1, consistent with the concave shape of the inactivation curve. The values of $\alpha$, which reflects the magnitude of PL inactivation, varied among the different materials, with the lowest for MET and the highest for HDPE.

**Table 2.2** Weibull parameters for PL inactivation of *L. innocua* on packaging materials. Means of linear regression parameters calculated from three replicates ± SD.

| Substrate | Scale parameter $\alpha$ | Shape parameter $\beta$ | Goodness of fit ($r^2$) |
|---|---|---|---|
| LDPE direct | 1.93 ± 0.69[a,b] | 0.56 ± 0.28 | 0.76 ± 0.26 |
| LDPE through | 2.42 ± 0.39[a] | 0.46 ± 0.09 | 0.84 ± 0.04 |
| HDPE | 2.17 ± 0.45[a,b] | 0.65 ± 0.08 | 0.87 ± 0.07 |
| MET | 1.06 ± 0.18[b] | 0.60 ± 0.11 | 0.88 ± 0.02 |
| TR | 1.50 ± 0.46[a,b] | 0.50 ± 0.19 | 0.62 ± 0.21 |
| EP | 1.37 ± 0.33[a,b] | 0.40 ± 0.09 | 0.79 ± 0.03 |

[a,b]Letters indicate statistically significantly groups (Tukey's HSD; $p < 0.05$).

The calculated Weibull parameters were then used to predict values of PL inactivation for *L. innocua* in a fluence range of up to 12 J/cm$^2$, which is the maximum fluence allowed by the FDA on food products (CFR 21:179, 1996). The predicted inactivation curves for all materials are shown in Figure 2.2. For the polyethylene based packaging materials the predicted inactivation was over 7 log CFU (LDPE) and over 10 log CFU (HDPE) at 12 J/cm$^2$. This suggests that significantly higher inactivation can be reached by applying a fluence higher than the maximum of 8 J/cm$^2$ used in this study, whereas for the other materials the inactivation plateau was practically reached within the range of experimental fluence, and no substantial benefits could be achieved by using a higher fluence. The differences at what fluence the inactivation plateaus are reached may be a function of varying surface roughness of the packaging materials, and may indicate when all exposed cells are inactivated (Table 2.3).

**Table 2.3** Surface roughness measurements of coupons: Ra, average roughness, Rq, root square mean of roughness, and R10, ten point roughness. Values are means of three measurements per material.

| Material | Ra | Rq | R10 |
|---|---|---|---|
| LDPE | 44.2 | 58.9 | 212.7 |
| HDPE | 59.8 | 83.3 | 400.8 |
| MET | 218.2 | 320.9 | 1406.1 |
| TR | 1459.1 | 1845.8 | 5969.1 |
| EP | 4888.3 | 5888.1 | 21025.8 |

**Effect of the physical properties of substrates**

As mentioned above, one of the goals of this study was to compare microbial inactivation on food packaging materials with different surface properties in order to tease out subtleties relevant to the potential use of PL in packaging operations. Previous work on inactivation of *L. innocua* on stainless steel (21) and *B. subtilis* spores on paperboard packaging (13) has demonstrated lower PL inactivation on reflective surfaces as compared to less reflective surfaces. The specular reflectivity (light reflected at the same angle as the angle of incidence) and diffuse reflectivity (light reflected at a different angle than the angle of incidence) of the surfaces used in this study, for the spectral domain covered by the light emitted by the Xenon lamp, are shown in Figure 3. Reflection profiles indicate that MET and EP have the highest specular reflectivity, while TR has the highest diffuse reflectivity. In terms of their composition, all three are complex packaging materials, with MET and EP containing a metallic layer (Al), while TR consists of cardboard "sandwiched" between two layers of LPDE. These three highly reflective materials were those on which the lowest PL inactivation levels were achieved, which is in agreement with previous findings regarding a presumable negative influence of reflectivity on inactivation. This result appears counterintuitive, as reflective surfaces are typically associated with highly smooth

surfaces, which provide fewer opportunities for cell shading or hiding. However, surface roughness measurements of the surfaces (Table 2.3) demonstrated that, based on R10 roughness values, surface roughness of EP>TR>MET>HDPE>LDPE, indicating that the most reflective surfaces in this study were also the roughest. Surface roughness can provide shading for cells, and could explain the observed tailing of inactivation, consistent with previous work on surfaces (18, 21). Surface roughness alone, however, does not account for all differences in inactivation and may suggest that reflectivity can also play a role in determining inactivation efficacy. In a previous study, Stannard et al. (14) hypothesized that lower inactivation on aluminum foil-containing paperboard packaging may result from increased cell photoreactivation from the reflected light. Although it seems unlikely that this effect would be entirely responsible for the large differences in effectiveness (about 3 log CFU) between the most and least reflective surfaces, given the very short exposure time in PL (360 us of actual exposure to light per 0.67 J/cm$^2$), this possibility deserves further consideration.

**Effect of PL on the treated substrates**

One concern related to the application of PL treatment is surface heating, given the high amount of energy delivered to the surface – and dissipated on that surface – within a short period of time. Heating effects on these surfaces were determined for fluence levels up to 16 J/cm$^2$, which is twice the maximum dose used in the microbial inactivation study. Due to slight differences in room temperature and, consequently, the initial temperature of the coupons, the increase in temperature of the coupon surface is reported here (Figure 2.4). The average initial temperature of all coupons, across all experimental replicates and treatment conditions was 26.2 ± 0.8 °C.

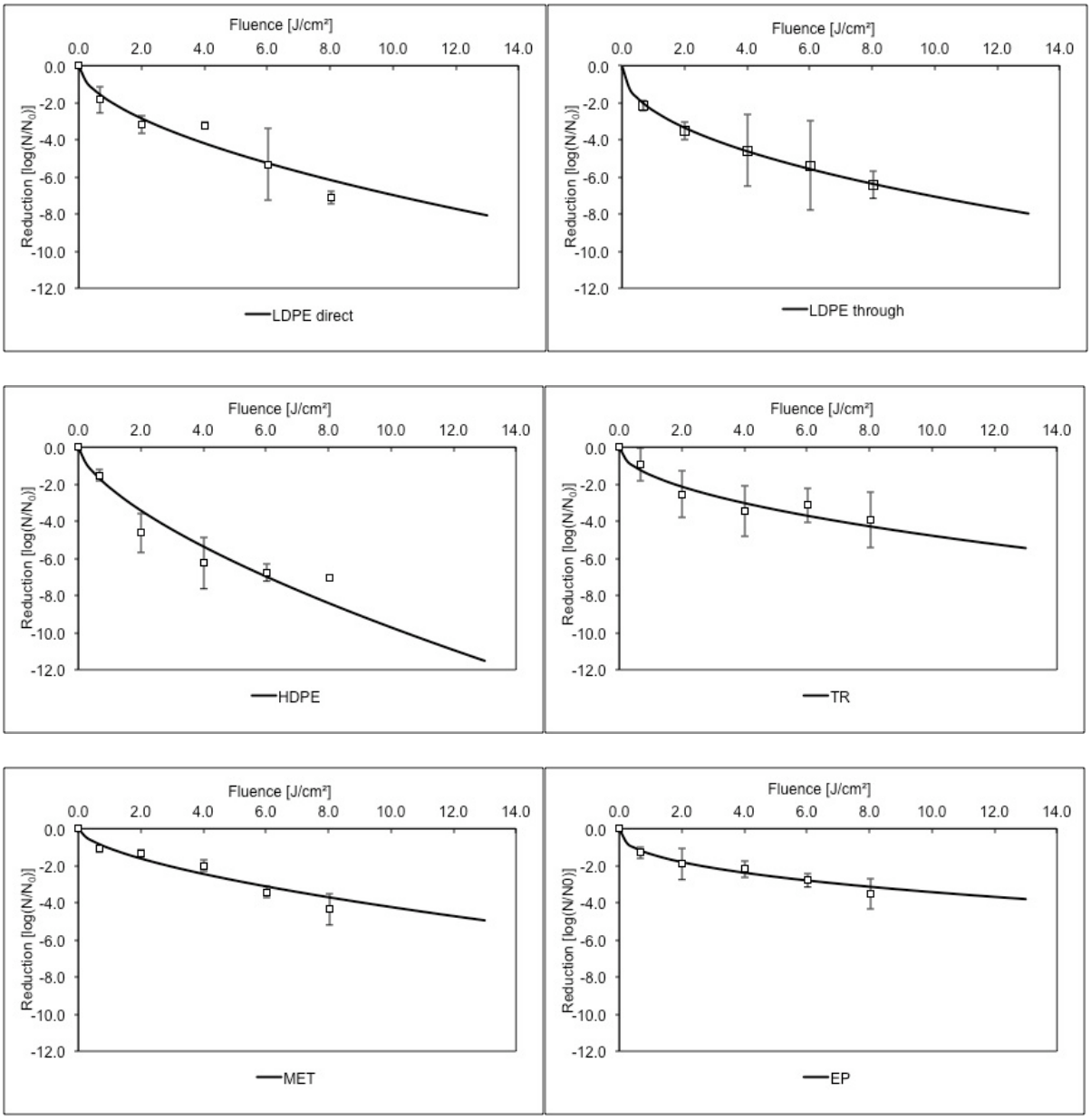


**Figure 2.2** Weibull predicted PL inactivation of *L. innocua* on packaging materials in solid lines, with mean experimental inactivations values with SD error bars (n = 3).

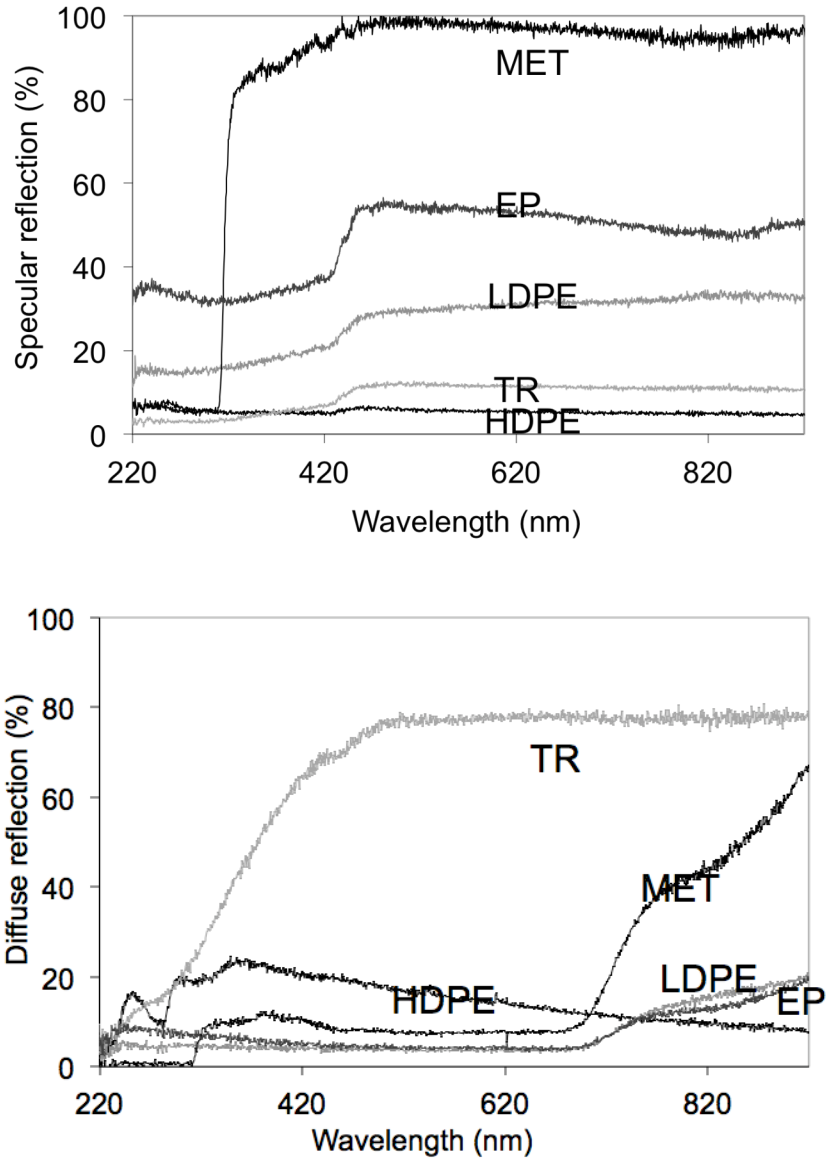


**Figure 2.3** Specular (A) and diffuse (B) reflection profiles of the packaging materials

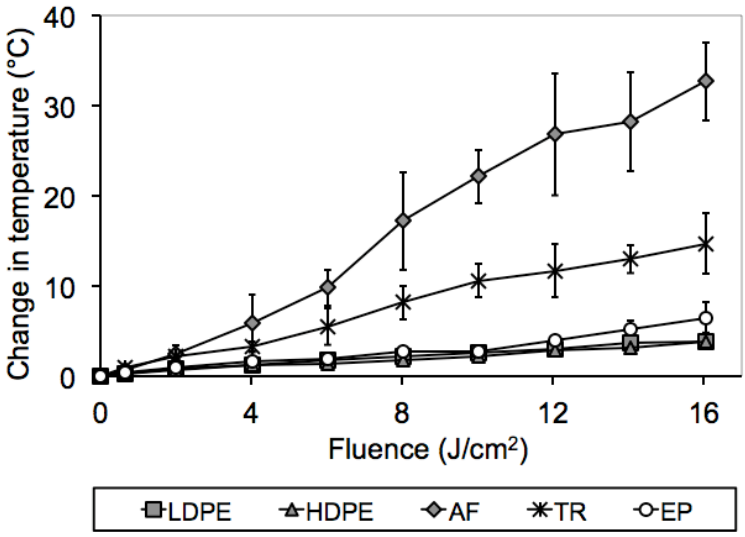


**Figure 2.4** Surface heating of coupons after PL. Error bars show SD (n = 3). Initial temperature of the coupons: ~ 26°C.

For the LDPE, HDPE and EP substrates, modest heating effects were observed. The temperature increase was only 2-3°C for treatments of ~8 J/cm$^2$ (12 pulses), and about twice as much for the treatments with ~16 J/cm$^2$ (24 pulses). Heating was highest on MET (about 20°C for the 8 J/cm$^2$ treatment and more than 30°C for the 16 J/cm$^2$ treatment), one of the materials on which the lowest inactivation was observed. This suggests that the material was also highly absorbent of heat, and thus it may not be very suitable for certain PL decontamination applications. The second material in terms of heating was TR, for which changes in temperature was about 50% less than those recorded for MET. The lack of correlation between observed heating effects and inactivation efficiency suggests heating of surfaces does not contribute to bacterial inactivation.

Since PL delivers a substantial dose of UV to the substrates, it is important to know whether or not the interaction between the light and the substrate will induce any changes in the

structural and physical properties of the materials. One way in which such effects can be probed is evaluation of the surface hydrophobicity, expressed by water contact angles. For instance, it has been reported before that a reduction in the hydrophobicity of certain surfaces can be caused by UV light (9). Changes in hydrophobicity can cause affect barrier properties (4) and bacterial adherence (2).

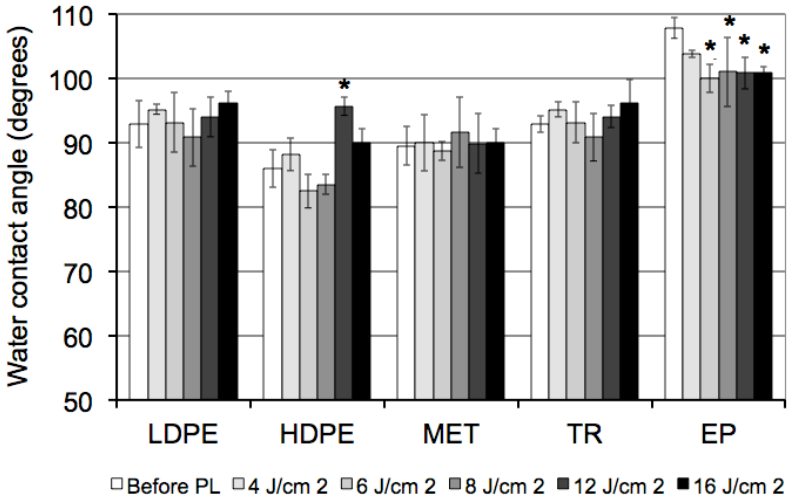


**Figure 2.5** Water contact angles of coupons after PL treatment. Error bars show SD (n = 6). Asterisks indicate means that differ significantly ($p < 0.05$) from the contact angle of untreated materials.

Water contact angles before and after PL treatment were measured to assess potential structural changes resulting from treatment (Figure 2.5). All surfaces used in this study were hydrophobic, with water contact angles > 80°. Contact angles only decreased significantly on EP ($p < 0.05$) after treatment at fluence of ≥ 6.0 J/cm$^2$ as compared to the values measured before PL treatment. This observed decrease may result from structural changes in uppermost packaging layers, possibly from photo-crosslinking or photo-oxidative degradation in the outer polymeric layer from exposure to UV (12). Additional effects, including changes in vapor transmission

rates or structural changes, should be examined for a more complete understanding of the impact of PL treatment on the integrity of packaging materials, or other food contact materials. Such an evaluation would be required in cases when a certain material may undergo repeated exposure to PL treatment, particularly for polymeric based materials that are known to interact with the UV component of the light spectrum.

## CONCLUSIONS

This study shows that PL is an effective decontaminating method for *L. innocua* cells on five types of food packaging materials. Treatments at a fluence level of about 8 J/cm$^2$ resulted in a reduction of *L. innocua* ranging from over 3 log CFU for complex, multi-layered packaging materials, to over 7 log CFU reduction on high density or low density polyethylene. Based on Weibull predictions, significantly higher inactivation may be reached by increasing the fluence for the polyethylene based materials, but not for the complex materials. Other noteworthy observations include the effectiveness of PL treatment through transparent polyethylene packaging, and the fact that highly reflective and rougher surfaces result in less inactivation than less reflective and smoother materials. An examination of treated the materials after PL treatment, including changes in water contact angles and surface heating, suggest minimal impact of the treatment on the exposed materials.

REFERENCES


1. **Ansari, M. I. A., and A. K. Datta.** 2003. An overview of sterilization methods for packaging materials used in aseptic packaging systems. Food and Bioproducts Processing **81:**57-65.
2. **Bower, C. K., J. McGuire, and M. A. Daeschel.** 1996. The adhesion and detachment of bacteria and spores on food-contact surfaces. Trends in Food Sci Tech **7:**152-157.
3. **Dunn, J., D. Burgess, and F. Leo.** 1997. Investigation of pulsed light for terminal sterilization of WFI filled blow/fill/seal polyethylene containers. PDA J Pharm Sci Technol **51:**111-115.
4. **Dury-Brun, C. c., P. Chalier, S. p. Desobry, and A. e. Voilley.** 2007. Multiple mass transfers of small volatile molecules Through flexible food packaging. Food Reviews Intl **23:**199-255.
5. **Gómez-López, V. M., F. Devlieghere, V. Bonduelle, and J. Debevere.** 2005. Factors affecting the inactivation of micro-organisms by intense light pulses. J Appl Microbiol **99:**460-470.
6. **Haughton, P. N., J. G. Lyng, D. J. Morgan, D. A. Cronin, S. Fanning, and P. Whyte.** 2011. Efficacy of high-intensity pulsed light for the microbiological decontamination of chicken, associated packaging, and contact surfaces. Foodborne Path Disease **8:**109-117.
7. **Keklik, N. M., A. Demirci, and V. M. Puri.** 2010. Decontamination of unpackaged and vacuum-packaged boneless chicken breast with pulsed ultraviolet light. Poult Sci **89:**570-581.

8. **Keklik, N. M., A. Demirci, and V. M. Puri.** 2009. Inactivation of *Listeria monocytogenes* on unpackaged and vacuum-packaged chicken frankfurters using pulsed UV-light. J Food Sci **74:**M431-M439.

9. **Li, B., and B. E. Logan.** 2005. The impact of ultraviolet light on bacterial adhesion to glass and metal oxide-coated surface. Colloids Surf B Biointerfaces **41:**153-161.

10. **Mafu, A. A., D. Roy, J. Goulet, and L. Savoie.** 1991. Characterization of physicochemical forces involved in adhesion of *Listeria monocytogenes* to surfaces. Appl Envir Microbiol **57:**1969-1973.

11. **McDonald, K. F., R. D. Curry, T. E. Clevenger, K. Unklesbay, A. Eisenstark, J. Golden, and R. D. Morgan.** 2000. A comparison of pulsed and continuous ultraviolet light sources for the decontamination of surfaces. IEEE Trans Plasma Sci **28:**1581-1587.

12. **Raab, M., L. Kotulák, J. Kolařík, and J. Pospíšil.** 1982. The effect of ultraviolet light on the mechanical properties of polyethylene and polypropylene films. J Appl Polymer Sci **27:**2457-2466.

13. **Stannard, C. J., J. S. Abbiss, and J. M. Wood.** 1985. Efficiency of treatments involving ultraviolet irradiation for decontaminating packaging board of different surface compositions. J Food Prot **48:**786-789.

14. **Stannard, C. J., J. S. Abiss, and J. M. Wood.** 1983. Combined treatment with hydrogen peroxide and ultra-violet irradiation to reduce microbial contamination levels in pre-formed food packaging cartons. J Food Prot **46:**1060-1064.

15. **Swanson, K. M. J., R. L. Petran, and J. H. Hanlin.** 2001. Culture Methods for Enumeration of Microorganisms, p. 53-62. *In* F. P. Downes and K. Ito (ed.),

Compendium of methods for the microbiological examination of foods, 4th ed. American Public Health Association, Washington, DC.

16. **Turtoi, M., and A. Nicolau.** 2007. Intense light pulse treatment as alternative method for mould spores destruction on paper-polyethylene packaging material. J Food Eng **83:**47-53.

17. **Uesugi, A. R., and C. I. Moraru.** 2009. Reduction of *Listeria* on ready-to-eat sausages after exposure to a combination of Pulsed Light and nisin. J Food Prot **72:**347-353.

18. **Uesugi, A. R., S. E. Woodling, and C. I. Moraru.** 2007. Inactivation kinetics and factors of variability in the pulsed light treatment of *Listeria innocua* cells. J Food Prot **70:**2518-2525.

19. **Warriner, K., G. Rysstad, A. Murden, P. Rumsby, D. Thomas, and W. M. Waites.** 2000. Inactivation of *Bacillus subtilis* spores on packaging surfaces by uv excimer laser irradiation. J Appl Microbiol **88:**678-685.

20. **Woodling, S. E., and C. I. Moraru.** 2007. Effect of spectral range in surface inactivation of *Listeria innocua* using broad-spectrum Pulsed Light. J Food Prot **70:**909-916.

21. **Woodling, S. E., and C. I. Moraru.** 2005. Influence of surface topography on the effectiveness of pulsed light treatment for the inactivation of *Listeria innocua* on stainless-steel surfaces. J Food Sci **70:**345-351.

CHAPTER 3

# SALT STRESS-INDUCED TRANSCRIPTION OF $\sigma^B$- AND CtsR-REGULATED GENES IN PERSISTENT AND NON-PERSISTENT *LISTERIA MONOCYTOGENES* STRAINS FROM FOOD PROCESSING PLANTS

*Published in Foodborne Pathog Dis. 2012. 9:198-206; Reprinted with permission.*

## ABSTRACT

*Listeria monocytogenes* is a foodborne pathogen that can persist in food processing environments. Six persistent and 6 non-persistent strains from fish processing plants and one persistent strain from a meat plant were selected to determine if expression of genes in the regulons of two stress response regulators, $\sigma^B$ and CtsR, under salt stress conditions is associated with the ability of *L. monocytogenes* to persist in food processing environments. Subtype data were also used to categorize the strains into genetic lineages I or II. qRT-PCR was used to measure transcript levels for two $\sigma^B$-regulated genes, *inlA* and *gadD3*, and two CtsR-regulated genes, lmo1138, and *clpB*, before and after ($t$ = 10 min) salt shock (i.e., exposure of exponential phase cells to BHI + 6% NaCl for 10 min at 37ºC). Exposure to salt stress induced higher transcript levels relative to levels under non-stress conditions for all four stress and virulence genes across all wildtype strains tested. Analysis of variance of induction data revealed that transcript levels for one gene (*clpB*) were induced at significantly higher levels in non-persistent strains compared to persistent strains ($p$ = 0.020; two-way ANOVA). Significantly higher transcript levels of *gadD3* ($p$ = 0.024; two-way ANOVA) and *clpB* ($p$ = 0.053; two-way ANOVA) were observed after salt shock in lineage I strains compared to lineage II strains. No clear association between stress gene transcript levels and persistence was detected. Our data are

consistent with an emerging model that proposes that establishment of *L. monocytogenes* persistence in a specific environment occurs as a random, stochastic event(s) rather than as a consequence of specific bacterial strain characteristics.

## INTRODUCTION

A number of studies have shown that *Listeria monocytogenes* can persist in food processing environments for months to years (14, 16, 31). Stress conditions encountered in food processing environments and food products can expose *L. monocytogenes* cells to conditions known to induce bacterial stress responses, including osmotic stress (2, 24, 43), oxidative stress (8, 13), and acid stress (13, 42, 43). Transcriptional regulators contributing to the stress response in *L. monocytogenes* include $\sigma^B$, an alternative sigma factor, which regulates > 150 genes involved in the general stress response of *L. monocytogenes* (24, 38, 42) and CtsR, a repressor of class III stress response genes, including genes encoding heat shock proteins (7, 17, 35). Increased piezotolerance of some *L. monocytogenes* isolates has been attributed to mutations in *ctsR* (19-21). Therefore, transcriptional regulators of stress response genes may contribute to varied stress responses in *L. monocytogenes* strains.

The goal of this study was to test the hypothesis that persistent and transient *L. monocytogenes* differ in baseline expression and induction of the $\sigma^B$ and CtsR regulons. Activity of $\sigma^B$ and CtsR was measured by using quantitative reverse transcriptase polymerase chain reaction (qRT-PCR) to measure transcript levels of (i) the reporter genes *inlA* and *gadA*, which are directly regulated by $\sigma^B$ (transcript levels of these genes serve as indirect measures of $\sigma^B$ activity) and (ii) the reporter genes lmo1138 and *clpB*, which are directly regulated by CtsR (transcript levels of these genes serve as indirect measures of CtsR activity). We hypothesized that persistent strains obtained from food processing environments would demonstrate higher

induction of $\sigma^B$- and CtsR-regulated genes after exposure to salt shock compared to non-persistent strains. The target genes (Table 3.1) used for the qRT-PCR experiments were chosen not because we hypothesized that they would be directly responsible for persistence, but to serve as appropriate reporters for the activity of these two key transcriptional regulators to provide insight into differences in expression of $\sigma^B$ and CtsR regulons based on classification of strains by persistence or lineage.

**Table 3.1** Genes chosen in this study as reporters for activity of the transcriptional regulators $\sigma^B$ and CtsR.

| Gene | Regulon | Reason for use in qRT-PCR assays | References |
|---|---|---|---|
| *gadD3* | $\sigma^B$ | Indicator for $\sigma^B$ activity; gene is solely $\sigma^B$ dependent | (11, 25, 44) |
| *inlA* | $\sigma^B$ | Indicator for $\sigma^B$ activity; *inlA* is solely $\sigma^B$ dependent under environmental stress conditions as shown in previous qRT-PCR studies (32); this gene is only co-regulated by PrfA if PrfA is active, such as in a PrfA* strain and inside the host | (24, 27, 32) |
| lmo1138 | CtsR | Indicator for CtsR activity; gene is solely CtsR-dependent | (17) |
| *clpB* | CtsR | Indicator for CtsR activity; gene is solely CtsR-dependent | (7, 17) |

## MATERIALS AND METHODS

*Bacterial strains and growth conditions*

A total of 6 persistent and 6 non-persistent isolates (**Table 3.2**) were selected from a 24-month longitudinal study of *L. monocytogenes* contamination patterns in 4 smoked fish plants (26). An isolate was considered to represent a persistent strain if multiple isolates belonging to

the same ribotype were recovered in the same plant ≥ 5 times and over a period > 3 months (30). Conversely, isolates representing a ribotype found only once in a plant during the course of the study were deemed representative of non-persistent strains. An additional persistent *L. monocytogenes* strain (FSL F6-154; previously J2818), which persisted in a food processing plant for > 10 years (40), was also included in our study. All isolates were classified to lineage based on ribotyping data (34). *L. monocytogenes* 10403S and selected isogenic mutant strains (17) were included as controls. Bacteria were grown from frozen stock cultures as previously described (39), except that cells were grown to mid-exponential phase ($OD_{600}$ = 0.4) after the final 1:100 dilution into 50 ml pre-warmed BHI.

*Salt shock experiments*

Salt shock experiments were performed as previously described (43), with modifications. Briefly, 4.5 ml aliquots of mid-exponential phase cells ($OD_{600}$ = 0.4) were collected from 50 ml cultures, and 10% phenol in ethanol was added to a final concentration of 1% phenol to stop transcription (5). To another 4.5 ml aliquot of the same culture, 4.5 ml of pre-warmed 12% NaCl (w/v) + BHI was added, and the culture was incubated for an additional 10 min at 37ºC with shaking, followed by addition of the phenol solution as described above. Phenol-treated samples were placed on ice and centrifuged within 5 min at 1,800 *x g* for 10 min at 4ºC. Pellets were kept on ice until RNA extraction, which immediately followed cell collection.

**Table 3.2** *Listeria monocytogenes* strains used in this study.

| Isolate | Ribotype | Lineage | Characteristics | Reference |
|---|---|---|---|---|
| 10403S | 1030A | II | Parent strain, serotype 1/2a | (6) |
| FSL A1-254 | 1030A | II | 10403SΔ*sigB* | (45) |
| FSL H6-190 | 1030A | II | 10403SΔ*ctsR* | (17) |
| FSL L4-060 | 1043A | I | Persistent | (26) |
| FSL L4-400 | 1052A | I | Persistent | (26) |
| FSL L4-408 | 1044A | I | Persistent | (26) |
| FSL L4-396 | 1039C | II | Persistent | (26) |
| FSL L4-386 | 1053A | II | Persistent | (26) |
| FSL L4-249 | 1039A | II | Persistent | (26) |
| FSL F6-154 | 1053A | II | Persistent | (40) |
| FSL L4-170 | 1038B | I | Non-persistent | (26) |
| FSL T1-392 | 1025A | I | Non-persistent | (26) |
| FSL L4-025 | 1042B | I | Non-persistent | (26) |
| FSL T1-041 | 1062D | II | Non-persistent | (26) |
| FSL T1-073 | 1023C | II | Non-persistent | (26) |
| FSL L4-151 | 1062A | II | Non-persistent | (26) |

*Total RNA isolation*

Cell pellets were resuspended in 1 ml TRI Reagent (Applied Biosystems, Foster City, CA), and manufacturer's instructions were followed to obtain purified total RNA after mechanical lysis with acid-washed 0.1 mm zirconium beads (Biospec, Bartlesville, OK) in a beadbeater (Mini-beadbeater-8; Biospec) for 4 min. RNA concentration and integrity was assessed as described elsewhere (4).

*TaqMan qRT-PCR*

cDNA was synthesized from total RNA (RIN value ≥ 7.0) treated with DNAse, following manufacturer's instructions (TURBO DNA-free; Applied Biosystems), in a reaction mixture

(100 ul) of TaqMan RT-PCR reagents with 500 ng total RNA. qPCR reactions were performed as previously described (4).

Transcript levels of four target genes (*gadD3* [lmo2434], *inlA*, lmo1138, and *clpB*) and one housekeeping gene (*rpoB*) were quantified, using the ABI Prism 7000 Sequence Detection System (Applied Biosystems), to indirectly measure the activity of the transcriptional regulators $\sigma^B$ and CtsR. TaqMan primers and probes (Table 3.3) were designed with Primer Express v1.0

**Table 3.3** Primers and probes used for qRT-PCR in this study.

| Gene | Name | Sequence (5'→3') |
|---|---|---|
| lmo1138 | DR32 lmo1138 Tqmn F | CATCCTTACCCAAAAATTGATTGAT |
| | DR33 lmo1138 Tqmn R | CGGCTAACTCCTGATTGATTTCC |
| | lmo1138 probe DR | CACGCACAGTGTTAAT |
| *gadD3* | DR26 gadA Tqmn F | TGAAGACGACAAGCGAAAACA |
| | DR27 gadA Tqmn R | GCTTTCTTCCTCAGATCCAAAGAG |
| | gadA Tqmn probe DR | AAAGTTATCGAATCCC |
| *inlA* | DR24 inlA Tqmn F | ACAAATGCTCAGGCAGCTACAAT |
| | DR25 inlA Tqmn R | CGTCTTCATTTTTTCCGCTAGAG |
| | inlA Tqmn probe DR | ACAAGATACTCCTATTAATC |
| *clpB,* | DR28 clpB lin1 Tqmn F | GGTGTAAACTATGGTCAAGCAATGA |
| lineage I | DR29 clpB lin1 Tqmn R | CGGCATCCCGCATCAA |
| | clpB lin1 probe DR | CCAAGCACTTTTTC |
| *clpB,* | DR30 clpB lin2 Tqmn F | CACAAAATCTAGCTATTGCATCAGAAC |
| lineage II | DR31 clpB lin2 Tqmn R | CAAAGTCGCTTTCTGTTAATAACACTTT |
| | clpB lin2 probe DR | TGACGTTGCACACGTT |
| *rpoB* | MS16 rpoB-F TqMn | CCGGACGTCACGGTAACAA |
| | MS18 rpoB-R TqMn | CAGGTGTTCCGTCTGGCATA |
| | rpoB MGB probe | TTATCTCCCGTATTTTACC |

software (Applied Biosystems) using target genes sequences obtained for all isolates used here (see Table 3.4 for primers). Separate *clpB* primer and probe sets were designed for lineage I and II strains due to high sequence divergence between lineages.

**Table 3.4** Primers used for sequencing in this study.

| Gene | Name | Sequence (5'→3') |
|---|---|---|
| lmo1138 | DR23 lmo1138-5' seq F | CCATTTTCGACCATTRTGATAAGATA |
| | DR21 lmo1138-5' seq R | TTTCRGACATGGAGTGACGGTTTTCGAGTG |
| *gadD3* | DR17 gadA-5' seq F | ATCAAACATAACGAACCTCCTTATAAGTACCATCG |
| | DR18 gadA-5' seq R | AGACCTCGTTTTTCCGCATKGTTACGCCAGCG |
| *inlA* | DR7 inlA-5' seq F | TTCGGATGCAGGAGAAAATC |
| | DR8 inlA-5' seq R | CCTGAAAGCGCACTAATATCAC |
| *clpB* | DR15 clpB-5' seq F | GGTCGTGATTAAGAAATTCAGAAGATCTGCCAACC |
| | DR16 clpB-5' seq R | GCTTCATAGTTTTCTTCTGCATTTTGAGAAGTCAC |
| *rpoB* | DR19 rpoB-5' seq F | AGGAAAMTTTTGATGMACGRTGTTT |
| | DR20 rpoB-5' seq R | TCTAGTTTTCCATTGAAGTAAACACCTGGAGAACG |

Transcript levels of the four target genes were normalized to the housekeeping gene *rpoB*. Induction, defined as fold change in transcript levels after salt shock ($t$ =10 min) relative to levels before salt shock ($t$ = 0), was calculated, using the Pfaffl method (41), for each biological replicate for each isolate. Efficiency values of primer and probe reactions were calculated for each isolate by including duplicate ten-fold dilutions of cDNA ($10^{-1}$ to $10^{-4}$) for each gene in reactions, and efficiency values were used in subsequent calculations. These values ranged from 91-100%, with a mean value and standard deviation of 98 ± 8%.

To compare mRNA transcript levels among isolates at both time points [i.e., before ($t$ = 0) and after salt-shock ($t$ = 10 min)], the $\Delta\Delta$-$C_t$ method (28) was used to calculate transcript levels relative to a calibrator sample, which was total RNA collected from *L. monocytogenes* 10403S during one biological replicate of salt shock. $C_t$ values obtained from this sample of 10403S cells collected at $t$ = 0 were used to calculate fold changes relative to expression levels of 10403S, using *rpoB* as an internal control. Thus, this relative quantification method represents transcript levels in arbitrary units of "fold change, relative to 10403S at $t$ = 0".

*Statistical analyses*

Induction and transcript levels relative to 10403S were analyzed using two-way analysis of variance (ANOVA) with JMP (JMP 9.0; SAS, Inc., Cary, NC). Data from two biological replicates of salt stress experiments for the 13 strains investigated were coded by persistence (N [Non-persistent] vs. P [Persistent]) or lineage (I vs. II) for each gene and used to determine effects of persistence, lineage or the interaction of lineage and persistence. Two biological replicates per strain were considered sufficient because we did not perform statistical analyses to compare transcript levels for individual strains. The following formula was used to determine effects of lineage and persistence and an interaction effect:

$$\text{fold change}_{gene} = \mu + \beta_{lineage} + \beta_{persistence} + \beta_{persistence*lineage} + \beta_0$$

Two-way ANOVA was performed on induction data and relative transcript level data separately. Data for transcript levels relative to 10403S were log transformed to fulfill ANOVA assumptions of normality.

## RESULTS

### Comparison of relative transcript levels of $\sigma^B$- and CtsR-regulated genes by persistence and lineage classifications of *L. monocytogenes* strains from food processing plants

Before salt shock, mean relative transcript levels, in exponential growth phase cells, of $\sigma^B$-regulated genes *gadD3* and *inlA* (in fold changes relative to 10403S at t = 0) ranged from 1.3 to 46.3 and 1.1 to 12.4, respectively, compared to 1.3 and 1.0 for 10403S (Figure 3.1). Mean relative transcript levels of CtsR-regulated genes lmo1138 and *clpB* ranged from 2.5 to 7.4 and 2.7 to 20.4, respectively, compared to 1.6 and 1.4 for 10403S. Statistical analysis of relative transcript levels before salt shock ($t = 0$) revealed no significant differences in transcript levels between persistent and non-persistent isolates for any of the four genes ($p > 0.05$; two-way ANOVA) (Figure 3.2). However, significantly higher *clpB* transcript levels were observed in

lineage I strains before salt stress ($p = 0.004$; two-way ANOVA). A significant interaction of persistence and lineage for relative transcript levels of *inlA* ($p = 0.028$; two-way ANOVA) before salt shock was also detected, but a contrast of the means showed no significant separation of the lineage/persistence pairings ($p > 0.05$; post-hoc Tukey HSD).

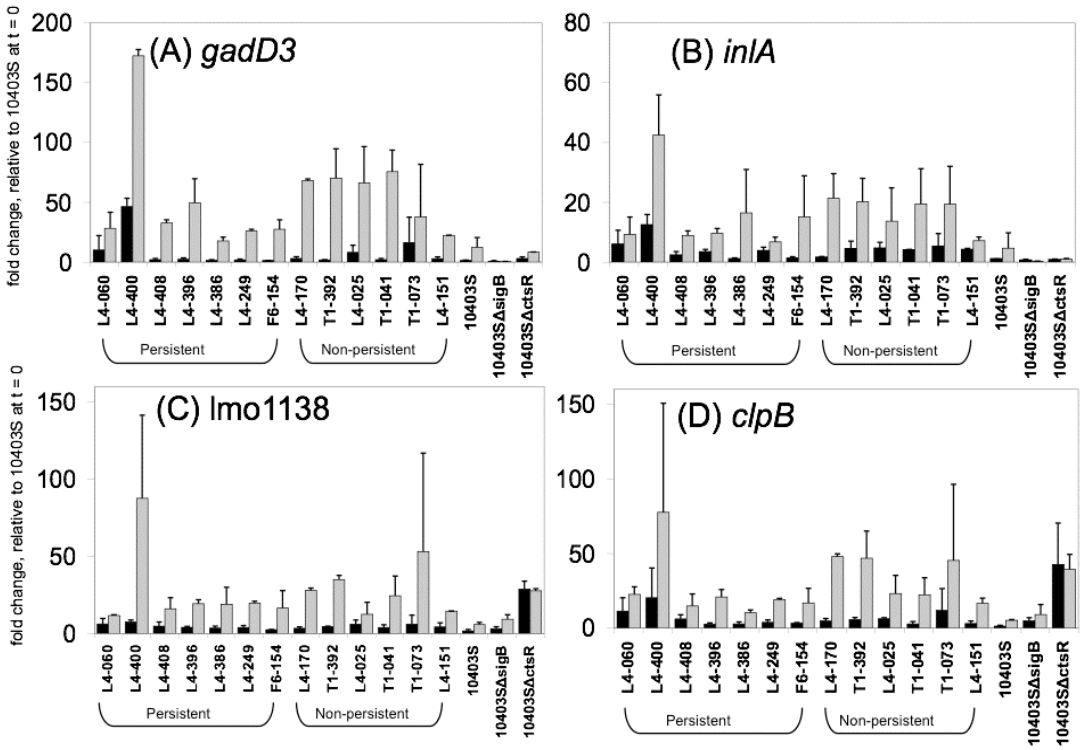


**Figure 3.1** Transcript levels, relative to transcript levels of 10403S at $t = 0$, of $\sigma^B$-regulated genes (A) *gadD3* and (B) *inlA* and CtsR-regulated genes (C) lmo1138 and (D) *clpB* before ($t = 0$, black bars) and after exposure ($t = 10$ min, gray bars) to BHI + 6% NaCl (w/v) at 37°C. Bars represent mean fold changes of transcript levels relative to transcripts obtained prior to salt shock from 10403S during one replicate of salt shock experiments, and error bars show standard deviations of two biological replicates per isolate. Relative fold changes to 10403S at $t = 0$ were calculated using the $\Delta\Delta$-$C_t$ relative quantification method (28). *rpoB* transcripts were used to normalize transcript levels.

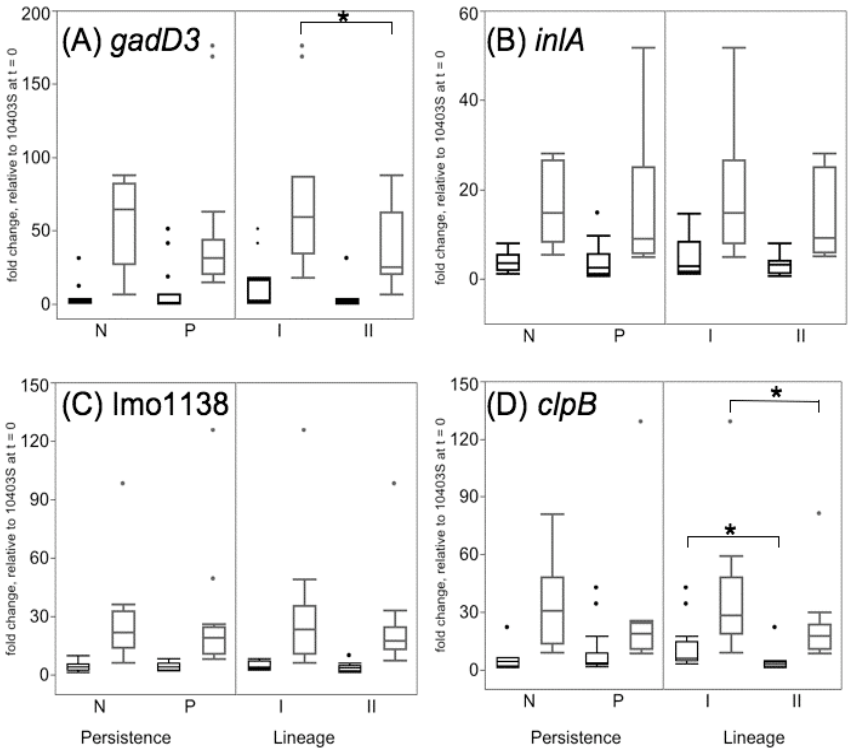


**Figure 3.2** Box plots of transcript levels, relative to transcript levels for 10403S at $t = 0$, of $\sigma^B$-regulated genes (A) *gadD3* and (B) *inlA* and CtsR-regulated genes (C) lmo1138 and (D) *clpB* before ($t = 0$, black boxes) and after exposure ($t = 10$ min, gray boxes) to BHI + 6% NaCl (w/v) at 37°C, by persistence (N = Non-persistent, P = Persistent) and lineage (I, II) classifications Boxes represent 25$^{th}$ and 75$^{th}$ percentiles with median line, and whiskers represent outermost data points that fall within upper quartile + 1.5*(interquartile range) and lower quartile – 1.5*(interquartile range) of individual data from two biological replicates per isolate. Outliers falling outside of this range are represented by points. Transcript levels were calculated using the $\Delta\Delta$-$C_t$ relative quantification method (28). *rpoB* transcripts were used to normalize transcript levels. Asterisks denote significant effects ($p \leq 0.05$) between groups linked by brackets as determined by two-way ANOVA. Data were log transformed prior to two-way ANOVA.

Relative transcript levels of $\sigma^B$-regulated genes *gadD3* and *inlA* after salt shock ranged from 17.6 to 172.5 and 6.7 to 42.5, respectively (for the 13 strains from food processing plants), compared to 12.3 and 4.6 for 10403S. Relative transcript levels of CtsR-regulated genes lmo1138 and *clpB* ranged from 11.7 to 87.6 and 10.3 to 77.6, respectively, compared to 5.8 and 5.26 for 10403S. These ranges also indicate considerable variation of transcript levels in response to salt shock for the strains from food processing plants. Analysis of relative transcript levels after salt shock ($t$ = 10 min) indicated higher relative transcript levels of *gadD3* ($p$ = 0.024; two-way ANOVA) for lineage I strains. Borderline significantly higher relative transcript levels of *clpB* ($p$ = 0.053; two-way ANOVA) were also observed in lineage I strains. Sequencing and analysis revealed no polymorphisms in the putative CtsR binding site upstream of *clpB*.

**Comparison of salt shock induction of $\sigma^B$- and CtsR-regulated genes by persistence and lineage classification of *L. monocytogenes* strains**

Individual induction fold changes of *gadD3, inlA,* lmo1138, and *clpB* (Figure 3.3) in all strains from food processing plants were > 1.0, indicating that the salt stress presented by our experimental conditions induced transcription of these genes. For $\sigma^B$-regulated genes, mean fold changes ranged from 3.7 to 44.6 for *gadD3* and from 1.7 to 16.6 for *inlA*. Induction, after salt shock, of *gadD3* and *inlA* in 10403S (9.8 and 4.4 fold change, respectively), but not in 10403SΔ*sigB* (0.5 and 1.0 fold change, respectively) confirmed $\sigma^B$ transcription of *gadD3* and *inlA* in response to salt stress. A two-way ANOVA found no significant effects of persistence or lineage on induction of either *gadD3* or *inlA* after salt shock ($p$ > 0.05; two-way ANOVA; Figure 3.4.

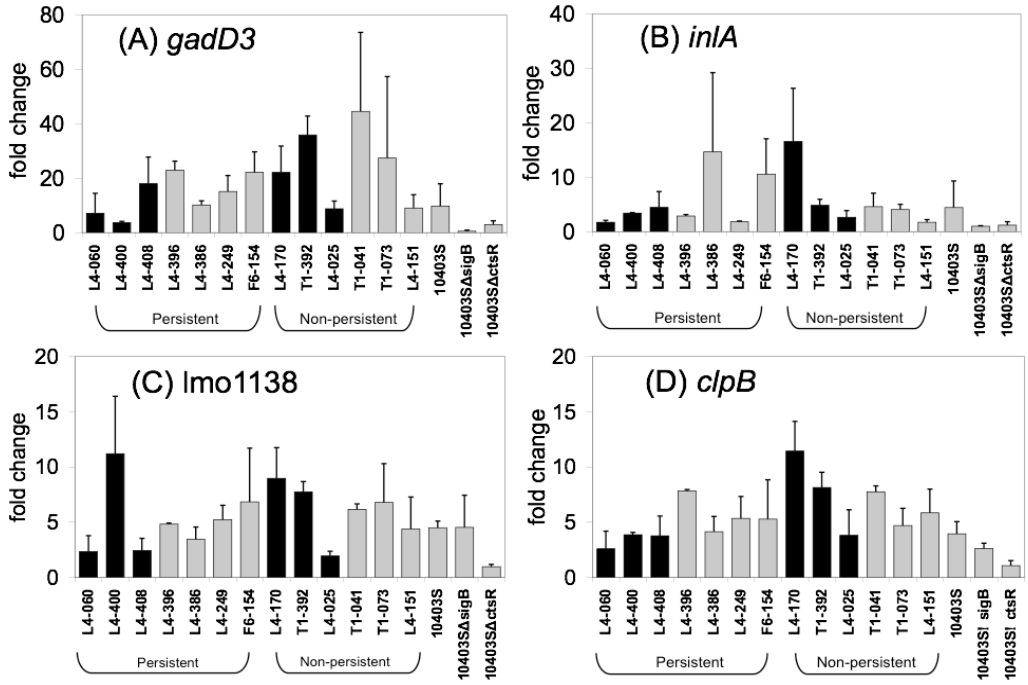


**Figure 3.3** Induction of $\sigma^B$-regulated genes (A) *gadD3* and (B) *inlA* and CtsR-regulated genes (C) lmo1138 and (D) *clpB* after exposure to BHI + 6% NaCl (w/v) for 10 min at 37°C, by isolate. Genetic lineages of isolates are represented by bar color (lineage I = black; lineage II = gray). Bars represent mean fold changes of transcript levels after salt shock relative to transcript levels prior to salt shock, and error bars show standard deviations of fold changes of two biological replicates calculated using the Pfaffl relative quantification method (41). *rpoB* transcripts were used to normalize transcript levels.

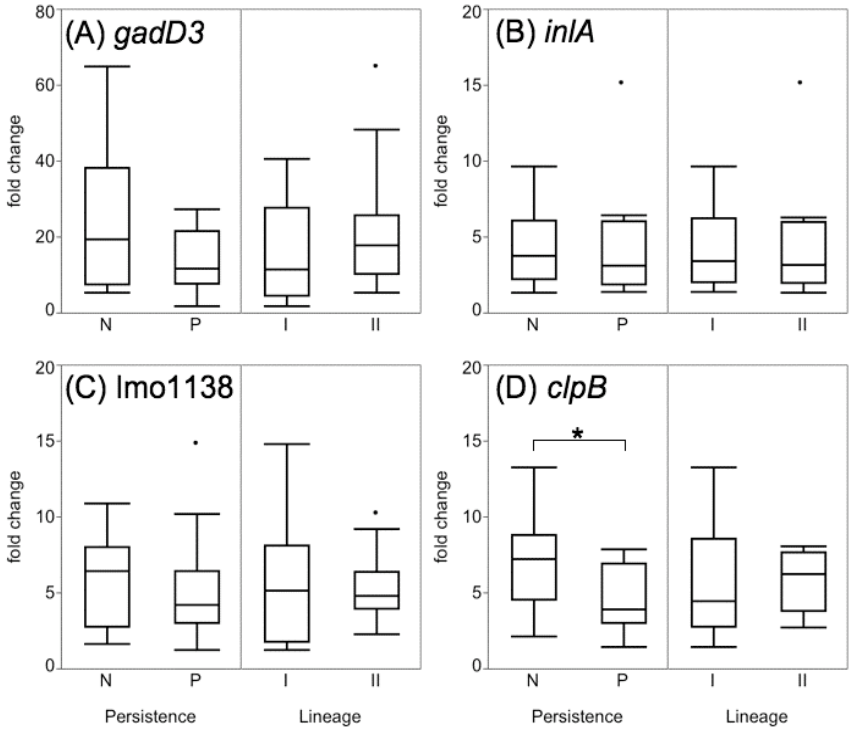


**Figure 3.4** Box plots of induction of $\sigma^B$-regulated genes (A) *gadD3* and (B) *inlA* and CtsR-regulated genes (C) lmo1138 and (D) *clpB* after exposure to BHI + 6% NaCl (w/v) for 10 min at 37°C, by persistence (N = Non-persistent, P = Persistent) and lineage (I, II) classifications. Boxes represent 25$^{th}$ and 75$^{th}$ percentiles with median line, and whiskers represent outermost data points that fall within upper quartile + 1.5*(interquartile range) and lower quartile – 1.5*(interquartile range) of individual data from two biological replicates per isolate. Outliers falling outside of this range are represented by points. Induction values were calculated using the Pfaffl relative quantification method (41). *rpoB* transcripts were used to normalize transcript levels. Asterisks denote significant effects ($p \leq 0.05$) between groups linked by brackets as determined by two-way ANOVA.

For CtsR-regulated genes, a two-way ANOVA found that induction of *clpB* after salt shock was significantly higher in non-persistent compared to persistent strains ($p = 0.020$; two-way ANOVA; Figure 3.4). No significant effects of persistence or lineage were observed on induction of lmo1138 after salt shock ($p > 0.05$; two-way ANOVA). Transcript levels of lmo1138 and *clpB* did not increase after salt shock in the Δ*ctsR* strain (fold change of 1.0 and 1.1, respectively) but increased in 10403S (4.5 and 3.9 fold change, respectively). Combined with the higher absolute transcript levels in the Δ*ctsR* strain (as compared to the parent strain 10403S, see Figure 3.1), these data support that CtsR represses transcription of these genes in the absence of stress conditions (17, 35) with complete derepression of lmo1138 and *clpB* before and after salt shock in the Δ*ctsR* strain. Induction of lmo1138 and *clpB* after salt shock in 10403SΔ*sigB*, with fold changes of 4.5 and 2.6, suggests that upregulation of these genes in response to salt shock is $\sigma^B$-independent.

**DISCUSSION**

Characterization of exponential phase transcript levels and salt induction of four stress response genes among 13 different *L. monocytogenes* isolates, representing strains that persisted in food processing plants and strains with no evidence of persistence, was performed to evaluate stress response gene expression patterns as well as CtsR and $\sigma^B$ activity in these strains. Overall our data indicate that (i) the $\sigma^B$-dependent genes *gadD3* and *inlA* and the CtsR-dependent genes lmo1138 and *clpB* are induced, across strains and lineages, after salt stress exposure; (ii) lineage I strains show higher transcript levels, as compared to lineage II strains, for some stress response genes (e.g., *gadD3* and *clpB*, after salt stress exposure); and (iii) *L. monocytogenes* isolates representing persistent and non-persistent strain do not differ in transcript levels or induction of the stress responsive genes *gadD3*, *inlA*, and lmo1138.

**$\sigma^B$-dependent genes *gadD3* and *inlA* and the CtsR-dependent genes lmo1138 and *clpB* are induced, across strains and lineages, after salt stress exposure**

The salt stress conditions used in this study consistently led to an increase in transcript levels of $\sigma^B$- and CtsR-regulated genes in a broad range of *L. monocytogenes* strains comprised of 12 ribotypes and two lineages. All four genes studied here showed higher relative transcript levels after salt shock in strains from food processing plants compared to the potentially laboratory-adapted strain 10403S. Induction of the $\sigma^B$-regulated genes *inlA* and *gadD3* across various salt concentrations (17, 37, 43) shows that induction of $\sigma^B$-regulated genes occurs over a large range of osmolarity, which may induce cross-protection of *L. monocytogenes* cells from additional stresses such as sanitizer treatment, low temperatures, or bile stress by "priming" cells with active $\sigma^B$ (3, 44). In addition to induction of $\sigma^B$ regulon members, we observed induction of CtsR-regulated genes in response to salt stress in all wildtype strains tested. Our finding that CtsR-regulated genes are induced by salt stress suggests that other stresses besides heat (7, 17, 35) lead to derepression of the CtsR regulon and indicates that some members of the CtsR regulon may contribute to salt stress response.

**Lineage I strains show higher transcript levels, as compared to lineage II strains, for some stress response genes (i.e., *gadD3* and *clpB*)**

Among several lineage-specific differences in transcript levels of genes chosen in this study, we observed higher *clpB* transcript levels in exponential phase cells before salt exposure in lineage I strains as compared to lineage II strains, as well as higher *gadD3* and *clpB* transcript levels after salt exposure in lineage I strains. GadD3 (Lmo2434) is one of three glutamate decarboxylases found in *L. monocytogenes* (11) that have been demonstrated to facilitate *L. monocytogenes* survival in low pH conditions, including gastric fluid (10, 11). ClpB has been

shown to be necessary for virulence in a mouse model (7). Our data suggest that either higher transcription of these genes or that these mRNA transcripts are more stable in lineage I strains. As we found no sequence differences in the CtsR binding sites of *clpB* (7, 17), genetic differences elsewhere in the chromosome are likely to be responsible for altered regulation of *clpB* in lineage I and II strains. It is also tempting to speculate that the difference in transcript levels between lineage I and II strains may relate to the potentially higher virulence potential of lineage I strains (9, 36, 46), which are more commonly associated with human *L. monocytogenes* isolates, as opposed to lineage II isolates, which are overrepresented among food isolates in many countries (15). The lineage differences in transcript levels identified here further support that that genetic relatedness may affect stress gene and virulence factor expression in *L. monocytogenes*, as previously observed (4, 33, 38).

**_L. monocytogenes_ isolates representing persistent and non-persistent strains do not differ in transcript levels or induction of the stress responsive genes _gadD3_, _inlA_, and lmo1138**

Our data found no evidence for a link between persistence and transcriptional response to one environmental stress, salt, as we observed only one gene, *clpB*, to be induced at significantly higher levels in non-persistent strains exposed to salt stress compared to persistent strains. Conceptual models explaining *L. monocytogenes* persistence in food processing environments include a model (1, 12, 22, 30) that certain *L. monocytogenes* strains or subpopulations (23) have some unique phenotypic characteristics (e.g., increased biofilm formation, sanitizer resistance, resistance to heat or acidic conditions) that facilitate establishment of a persistent population. An alternative model (14) is that most, if not all, *L. monocytogenes* can establish persistence if introduced into an appropriate niche (i.e., a location where they are protected from cleaning and sanitizers) at an opportune time. Some previous studies reported unique stress resistance

phenotypes for persistent strains (1, 29, 30), supporting the first model. Other studies, however, did not identify any differences in stress resistance between persistent and non-persistent strains (18, 22), consistent with our observations here that did not find evidence for increased transcript levels or enhanced induction of stress response genes in persistent strains. Our data support the model that establishment of persistence is not a reflection of specific strain characteristics. Future studies using a larger number of strains from food processing environments are needed to further support this model. Use of whole genomic transcriptomic and proteomics approaches can also lead to insights on transcriptional differences, other than $\sigma^B$ and CtsR regulation, that may exist between persistent and non-persistent strains.

REFERENCES


1. **Aase, B., G. Sundheim, S. Langsrud, and L. M. Rørvik.** 2000. Occurrence of and a possible mechanism for resistance to a quaternary ammonium compound in *Listeria monocytogenes*. Int J Food Microbiol **62:**57-63.
2. **Becker, L. A., M. S. Cetin, R. W. Hutkins, and A. K. Benson.** 1998. Identification of the gene encoding the alternative sigma factor $\sigma^B$ from *Listeria monocytogenes* and its role in osmotolerance. J Bacteriol **180:**4547-4554.
3. **Begley, M., C. G. M. Gahan, and C. Hill.** 2002. Bile stress response in *Listeria monocytogenes* LO28: adaptation, cross-protection, and identification of genetic loci involved in bile resistance. Appl Environ Microbiol **68:**6005-6012.
4. **Bergholz, T. M., H. C. den Bakker, E. D. Fortes, K. J. Boor, and M. Wiedmann.** 2010. Salt stress phenotypes in *Listeria monocytogenes* vary by genetic lineage and temperature. Foodborne Pathog Dis **7:**7492-7498.
5. **Bhagwat, A. A., R. P. Phadke, D. Wheeler, S. Kalantre, M. Gudipati, and M. Bhagwat.** 2003. Computational methods and evaluation of RNA stabilization reagents for genome-wide expression studies. J Microbiol Methods **55:**399-409.
6. **Bishop, D. K., and D. J. Hinrichs.** 1987. Adoptive transfer of immunity to *Listeria monocytogenes*. The influence of in vitro stimulation on lymphocyte subset requirements. J Immunol **139:**2005-2009.
7. **Chastanet, A., I. Derré, S. Nair, and T. Msadek.** 2004. *clpB*, a novel member of the *Listeria monocytogenes* CtsR regulon, is involved in virulence but not in general stress tolerance. J Bacteriol **186:**1165-1174.

8. **Chaturongakul, S., and K. J. Boor.** 2006. SigmaB activation under environmental and energy stress conditions in *Listeria monocytogenes*. Appl Environ Microbiol **72:**5197-5203.

9. **Chen, Y., W. H. Ross, M. J. Gray, M. Wiedmann, R. C. Whiting, and V. N. Scott.** 2006. Attributing risk to *Listeria monocytogenes* subgroups: dose response in relation to genetic lineages. J Food Prot **69:**335-344.

10. **Cotter, P. D., C. G. Gahan, and C. Hill.** 2001. A glutamate decarboxylase system protects *Listeria monocytogenes* in gastric fluid. Mol Microbiol **40:**465-475.

11. **Cotter, P. D., S. Ryan, C. G. Gahan, and C. Hill.** 2005. Presence of GadD1 glutamate decarboxylase in selected *Listeria monocytogenes* strains is associated with an ability to grow at low pH. Appl Environ Microbiol **71:**2832-2839.

12. **Earnshaw, A. M., and L. M. Lawrence.** 1998. Sensitivity to commercial disinfectants, and the occurrence of plasmids within various *Listeria monocytogenes* genotypes isolated from poultry products and the poultry processing environment. J Appl Microbiol **84:**642-648.

13. **Ferreira, A., C. P. O'Byrne, and K. J. Boor.** 2001. Role of $\sigma^B$ in heat, ethanol, acid, and oxidative stress resistance and during carbon starvation in *Listeria monocytogenes*. Appl Environ Microbiol **67:**4454-4457.

14. **Ferreira, V., J. Barbosa, M. Stasiewicz, K. Vongkamjan, A. Moreno Switt, T. Hogg, P. Gibbs, P. Teixeira, and M. Wiedmann.** 2011. Persistent *Listeria monocytogenes* in fermented meat sausage production facilities in Portugal represent diverse geno- and phenotypes. Appl Environ Microbiol **77:**2701-2715.

15. **Gray, M. J., R. N. Zadoks, E. D. Fortes, B. Dogan, S. Cai, Y. Chen, V. N. Scott, D. E. Gombas, K. J. Boor, and M. Wiedmann.** 2004. *Listeria monocytogenes* isolates from foods and humans form distinct but overlapping populations. Appl Environ Microbiol **70:**5833-5841.

16. **Holah, J. T., J. Bird, and K. E. Hall.** 2004. The microbial ecology of high-risk, chilled food factories; evidence for persistent *Listeria* spp. and *Escherichia coli* strains. J Appl Microbiol **97:**68-77.

17. **Hu, Y., S. Raengpradub, U. Schwab, C. Loss, R. Orsi, M. Wiedmann, and K. J. Boor.** 2007. Phenotypic and transcriptomic analyses demonstrate interactions between the transcriptional regulators CtsR and Sigma B in *Listeria monocytogenes*. Appl Environ Microbiol**:**7967-7980.

18. **Jensen, A., M. H. Larsen, H. Ingmer, B. F. Vogel, and L. Gram.** 2007. Sodium chloride enhances adherence and aggregation and strain variation influences invasiveness of *Listeria monocytogenes* strains. J Food Prot **70:**592-599.

19. **Joerger, R. D., H. Chen, and K. E. Kniel.** 2006. Characterization of a spontaneous, pressure-tolerant *Listeria monocytogenes* Scott A *ctsR* deletion mutant. Foodborne Pathog Dis **3:**196-202.

20. **Karatzas, K. A. G., V. P. Valdramidis, and M. H. J. Wells-Bennik.** 2005. Contingency locus in *ctsR* of *Listeria monocytogenes* Scott A: a strategy for occurrence of abundant piezotolerant isolates within clonal populations. Appl Environ Microbiol **71:**8390-8396.

21. **Karatzas, K. A. G., J. A. Wouters, C. G. M. Gahan, C. Hill, T. Abee, and M. H. J. Bennik.** 2003. The CtsR regulator of *Listeria monocytogenes* contains a variant glycine

repeat region that affects piezotolerance, stress resistance, motility and virulence. Mol Microbiology **49:**1227-1238.

22. **Kastbjerg, V. G., and L. Gram.** 2009. Model systems allowing quantification of sensitivity to disinfectants and comparison of disinfectant susceptibility of persistent and presumed nonpersistent *Listeria monocytogenes*. J Appl Microbiol **106:**1667-1681.

23. **Kastbjerg, V. G., D. S. Nielsen, N. Arneborg, and L. Gram.** 2009. Response of *Listeria monocytogenes* to disinfection stress at the single-cell and population levels as monitored by intracellular pH measurements and viable-cell counts. Appl Environ Microbiol **75:**4550-4556.

24. **Kazmierczak, M. J., S. C. Mithoe, K. J. Boor, and M. Wiedmann.** 2003. *Listeria monocytogenes* $\sigma^B$ regulates stress response and virulence functions. J Bacteriol **185:**5722-5734.

25. **Kazmierczak, M. J., M. Wiedmann, and K. J. Boor.** 2006. Contributions of *Listeria monocytogenes* sigmaB and PrfA to expression of virulence and stress response genes during extra-and intracellular growth. Microbiology **152:**1827-1838.

26. **Lappi, V. R., J. Thimothe, K. K. Nightingale, K. Gall, V. N. Scott, and M. Wiedmann.** 2004. Longitudinal studies on *Listeria* in smoked fish plants: impact of intervention strategies on contamination patterns. J Food Prot **67:**2500-2514.

27. **Lingnau, A., E. Domann, M. Hudel, M. Bock, T. Nichterlein, J. Wehland, and T. Chakraborty.** 1995. Expression of the *Listeria monocytogenes* EGD *inlA* and *inlB* genes, whose products mediate bacterial entry into tissue culture cell lines, by PrfA-dependent and -independent mechanisms. Infect Immun **63:**3896-3903.

28. **Livak, K. J., and T. D. Schmittgen.** 2001. Analysis of relative gene expression data using real-time quantitative PCR and the 2-ΔΔ-CT Method. Methods **25:**402-408.

29. **Lundén, J., T. Autio, A. Markkula, S. Hellstrom, and H. Korkeala.** 2003. Adaptive and cross-adaptive responses of persistent and non-persistent *Listeria monocytogenes* strains to disinfectants. Int J Food Microbiol **82:**265-272.

30. **Lundén, J., R. Tolvanen, and H. Korkeala.** 2008. Acid and heat tolerance of persistent and nonpersistent *Listeria monocytogenes* food plant strains. Lett Appl Microbiol **46:**276-280.

31. **Lundén, J. M., T. J. Autio, A. M. Sjöberg, and H. J. Korkeala.** 2003. Persistent and nonpersistent *Listeria monocytogenes* contamination in meat and poultry processing plants. J Food Prot **66:**2062-2069.

32. **McGann, P., M. Wiedmann, and K. J. Boor.** 2007. The alternative sigma factor $\sigma^B$ and the virulence gene regulator PrfA both regulate transcription of *Listeria monocytogenes* internalins. Appl Environ Microbiol **73:**2919-2930.

33. **Moorhead, S. M., and G. A. Dykes.** 2003. The role of the *sigB* gene in the general stress response of *Listeria monocytogenes* varies between a strain of serotype 1/2a and a strain of serotype 4c. Curr Microbiol **46:**461-466.

34. **Nadon, C. A., D. L. Woodward, C. Young, F. G. Rodgers, and M. Wiedmann.** 2001. Correlations between molecular subtyping and serotyping of *Listeria monocytogenes*. J Clin Microbiol **39:**2704-2707.

35. **Nair, S., I. Derré, T. Msadek, O. Gaillot, and P. Berche.** 2000. CtsR controls class III heat shock gene expression in the human pathogen *Listeria monocytogenes*. Mol Microbiol **35:**800-811.

36. **Norton, D. M., J. M. Scarlett, K. Horton, D. Sue, J. Thimothe, K. J. Boor, and M. Wiedmann.** 2001. Characterization and pathogenic potential of *Listeria monocytogenes* isolates from the smoked fish industry. Appl Environ Microbiol **67:**646-653.

37. **Olesen, I., F. K. Vogensen, and L. Jespersen.** 2009. Gene transcription and virulence potential of *Listeria monocytogenes* strains after exposure to acidic and NaCl stress. Foodborne Pathog Dis **6:**669-680.

38. **Oliver, H. F., R. H. Orsi, M. Wiedmann, and K. J. Boor.** 2010. *Listeria monocytogenes* $\sigma^B$ has a small core regulon and a conserved role in virulence but makes differential contributions to stress tolerance across a diverse collection of strains. Appl Environ Microbiol **76:**4216-4232.

39. **Ollinger, J., M. Wiedmann, and K. J. Boor.** 2008. $\sigma^B$- and PrfA-dependent transcription of genes previously classified as putative constituents of the *Listeria monocytogenes* PrfA regulon. Foodborne Pathog Dis **5:**281-293.

40. **Orsi, R., M. Borowsky, P. Lauer, S. Young, C. Nusbaum, J. Galagan, B. Birren, R. Ivy, Q. Sun, L. Graves, B. Swaminathan, and M. Wiedmann.** 2008. Short-term genome evolution of *Listeria monocytogenes* in a non-controlled environment. BMC Genomics **9:**539.

41. **Pfaffl, M. W.** 2001. A new mathematical model for relative quantification in real-time RT-PCR. Nucleic Acids Res **29:**e45.

42. **Raengpradub, S., M. Wiedmann, and K. J. Boor.** 2008. Comparative analysis of the $\sigma^B$-dependent stress responses in *Listeria monocytogenes* and *Listeria innocua* strains exposed to selected stress conditions. Appl Environ Microbiol **74:**158-171.

43. **Sue, D., D. Fink, M. Wiedmann, and K. J. Boor.** 2004. $\sigma^B$-dependent gene induction and expression in *Listeria monocytogenes* during osmotic and acid stress conditions simulating the intestinal environment. Microbiology **150:**3843-3855.

44. **Wemekamp-Kamphuis, H. H., J. A. Wouters, P. P. de Leeuw, T. Hain, T. Chakraborty, and T. Abee.** 2004. Identification of sigma factor $\sigma^B$- controlled genes and their impact on acid stress, high hydrostatic pressure, and freeze survival in *Listeria monocytogenes* EGD-e. Appl Environ Microbiol **70:**3457-3466.

45. **Wiedmann, M., T. J. Arvik, R. J. Hurley, and K. J. Boor.** 1998. General stress transcription factor $\sigma^B$ and its role in acid tolerance and virulence of *Listeria monocytogenes*. J Bacteriol **180:**3650-3656.

46. **Wiedmann, M., J. L. Bruce, C. Keating, A. E. Johnson, P. L. McDonough, and C. A. Batt.** 1997. Ribotypes and virulence gene polymorphisms suggest three distinct *Listeria monocytogenes* lineages with differences in pathogenic potential. Infect Immun **65:**2707-2716

CHAPTER 4

# FPSS, A NOVEL INHIBITOR OF $\sigma^B$ ACTIVITY, PREVENTS THE ACTIVATION OF $\sigma^B$ BY ENVIRONMENTAL AND ENERGY STRESSES IN *BACILLUS SUBTILIS*


## ABSTRACT

Sigma B ($\sigma^B$) is an alternative sigma factor that regulates the general stress response in *Bacillus subtilis* and many other Gram-positive organisms. Activation of $\sigma^B$ in response to environmental stress, energy stress, and growth at high and low temperatures occurs via different signal transduction pathways in *B. subtilis*. We determined the effects of fluoro-phenyl-styrene-sulfonamide (FPSS), a previously identified novel small molecule inhibitor of *Listeria monocytogenes* $\sigma^B$ activity, in *B. subtilis* under various stress conditions to investigate its mechanism for inhibiting $\sigma^B$ activity. FPSS prevented energy stress induction of $\sigma^B$ activity during entry into stationary phase and delayed $\sigma^B$ activity in response to phosphate limitation and azide stress. We also found that FPSS inhibited chill induction (growth at 16°C) of $\sigma^B$ activity in a Δ*rsbV* strain, indicating that RsbU, RsbP, and RsbV are not exclusive targets of FPSS. FPSS did not inhibit $\sigma^B$ activity when induction of $\sigma^B$ was artificially induced by uncoupling expression of the *sigB* operon from its autoregulatory feedback loop, suggesting FPSS prevents the activation of $\sigma^B$ but not $\sigma^B$-dependent transcription. We investigated the partner-switching module RsbV/RsbW/$\sigma^B$ as a potential target of FPSS using in vitro transcription and stopped-flow fluorescence analysis, and found no evidence to indicate direct binding of FPSS to either RsbW or $\sigma^B$. qRT-PCR analysis showed that the addition of FPSS did not decrease *sigB* transcript levels with or without the addition of stress in *L. monocytogenes*, suggesting FPSS does not block transcription of the *sigB* operon. Finally, FPSS did not significantly affect ($p >$

0.05) sporulation in *B. subtilis* when added during exponential growth, suggesting that in these conditions, FPSS does not affect the ribosomally associated protein Obg or the SpoIIA/SpoIIAB partner switching module required for sporulation. Our findings indicate FPSS's ability to inhibit $\sigma^B$ activation occurs through a yet unknown mechanism, and appears to work outside of the members of the previously characterized regulatory proteins controlling $\sigma^B$ activity.

## INTRODUCTION

Sigma B ($\sigma^B$) is an alternative sigma factor that regulates the general stress response in *Bacillus subtilis*, and is conserved in many related Gram-positive bacteria including the pathogens *Listeria monocytogenes*, *Staphylococcus aureus*, and *Bacillus anthracis*. Activation of $\sigma^B$ leads to a rapid, coordinated stress response of more than 100 genes in *L. monocytogenes* (40, 47) and *B. subtilis* (39, 46) that allow the organisms to respond to changing physiological conditions. In addition to its regulation of the stress response, $\sigma^B$ regulates virulence factors in *L. monocytogenes* (38, 42), *B. anthracis* (23), and *S. aureus* (8, 27), suggesting the alternative sigma factor might serve as a potential target for intervention strategies during infection by these pathogens.

$\sigma^B$ activity is tightly regulated in *B. subtilis* by three distinct pathways that integrate responses to stress, in contrast to *L. monocytogenes* that regulates $\sigma^B$ via one pathway (reviewed in (25); Figure 4.1). In *B. subtilis*, one pathway relays the response to environmental stresses such as high salt, acid, and ethanol stress through a 1.8 MDa multiprotein complex called the stressosome comprising the RsbS antagonist, RsbR coantagonists, and the RsbT serine/threonine kinase (19, 30, 36). In stressed cells, the kinase RsbT phosphorylates the antagonist RsbS and

coantagonist RsbRA, allowing RsbT to be released from the stressosome to which it is normally bound. Once free, RsbT activates the phosphatase RsbU (21, 24, 54, 58).

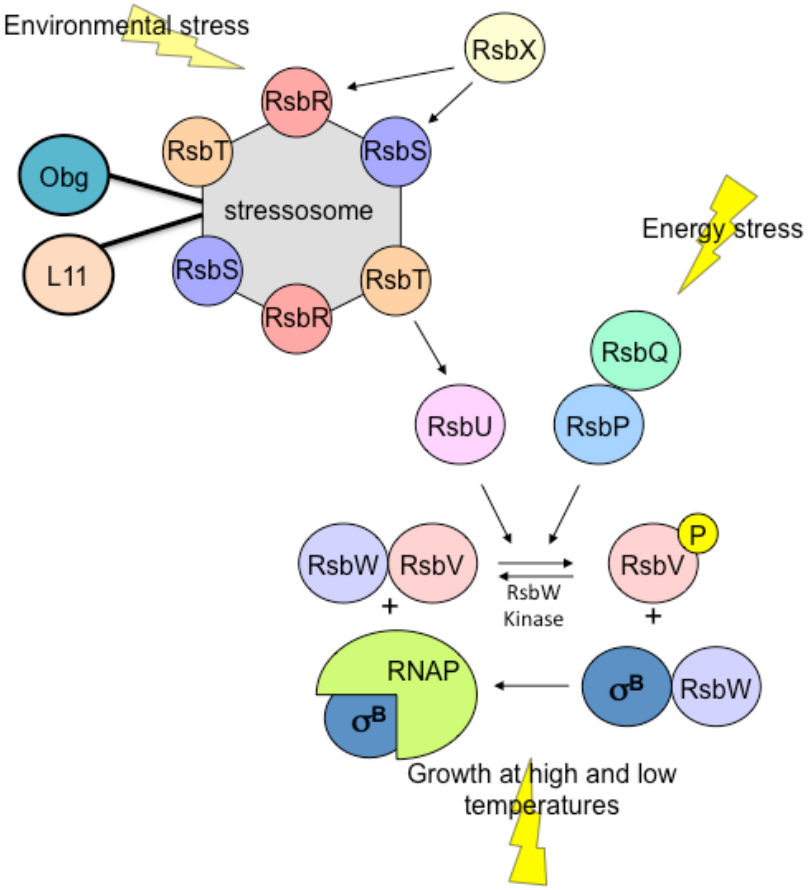


**Figure 4.1** Model of $\sigma^B$ regulation in *B. subtilis*. Modified from Hecker et al. (25). The stressosome senses environmental energy signals and activates the positive regulator, RsbU, which dephosphorylates RsbV-P. Unphosphorylated RsbV binds to RsbW, freeing $\sigma^B$. RsbQ and RsbP sense energy stress, activating the phosphatase function of RsbP that dephosphorylates RsbV-P. Growth at high and low temperatures leads to $\sigma^B$ activation independently of RsbV. References are noted in the text.

Active RsbU dephosphorylates phosphorylated anti-anti-sigma factor, RsbV-P, which allows RsbV to bind to the anti-sigma factor, RsbW and promoting $\sigma^B$'s release from RsbW. In a

second branch, energy stresses, such as glucose, ATP and GTP limitation, and phosphate starvation, are sensed by RsbP and RsbQ (13, 53, 60). The phosphatase RsbP dephosphorylates RsbV-P, again resulting in the release of $\sigma^B$ from RsbW. Finally, growth at high and low temperatures activates $\sigma^B$ independently of RsbT/RsbU/RsbV in a yet not fully understood manner (12, 26).

In contrast, activation of *L. monocytogenes* $\sigma^B$ in response to environmental and energy stresses occurs through a single pathway via the stressosome. *L. monocytogenes* lacks genes encoding homologs of RsbP and RsbQ (15, 16). Replacement of the four *B. subtilis rsbR* paralogs with *L. monocytogenes rsbR* within the *sigB* operon in *B. subtilis* allows for the activation of $\sigma^B$ by energy stresses, indicating that this paralog can integrate responses to energy and environmental stresses. Other work supports this model of $\sigma^B$ regulation by a single pathway in *L. monocytogenes*, since RsbU and RsbT have been shown to be necessary for the activation of $\sigma^B$ in response to both environmental and energy stresses (15, 16, 50).

Our group previously used highthroughput screening of small molecule libraries to identify a novel inhibitor of $\sigma^B$ activity, fluoro-phenyl-styrene-sulfonamide (FPSS), in *L. monocytogenes* (44). We showed that FPSS also inhibits induction of $\sigma^B$ activity by an environmental stress, 0.3 M NaCl, in *B. subtilis*. Because FPSS inhibits $\sigma^B$ activity in *L. monocytogenes* and *B. subtilis*, we hypothesized the small molecule operates through a similar mechanism in the related organisms that share highly conserved *sigB* operons (22) but communicate stress signals through different regulatory pathways. To deduce the mechanism by which FPSS inhibits $\sigma^B$ activity, we performed a series of genetic and biochemical experiments targeting previously identified regulatory pathways of $\sigma^B$ in *B. subtilis*, focusing our work in this organism because $\sigma^B$ regulation is better characterized than in *L. monocytogenes*.

We show that FPSS inhibits or delays *B. subtilis* $\sigma^B$ activation by both environmental and energy stresses, providing evidence that the small molecule does not interfere with the Rsb (regulators of sigma B) proteins of these separate pathways. We also show that FPSS inhibits $\sigma^B$ activity during growth at 16°C in a Δ*rsbV* strain, suggesting an RsbV-independent mechanism. By artificially inducing $\sigma^B$ activity using a strain with an inducible promoter upstream of *rsbV-rsbW-sigB*, we demonstrate that FPSS prevents the activation of $\sigma^B$ and not $\sigma^B$-dependent transcription, a hypothesis supported by in vitro transcription data showing no effect of FPSS on transcription from a $\sigma^B$-dependent promoter. Finally, we demonstrate that FPSS does not block transcription of the *sigB* operon in *L. monocytogenes* by qPCR or sporulation in *B. subtilis*. Our results suggest that FPSS prevents the activation of $\sigma^B$ through an unknown mechanism that operates separately from the characterized regulatory proteins investigated in this study.

## MATERIALS AND METHODS

### *Bacterial strains and genetic methods*

All strains used in this study are listed in Table 4.1. Strains PB2, PB198, PB206, PB213, and PB345 were provided by C. Price (University of California, Davis). Strains (renamed FSL B2-273 and FSL B2-274 for this study) for overexpressing $His_6$-SigB and $His_6$-SigA were provided by W. Goebel (Universität Würzburg, Germany).

To generate proteins $His_6$-tagged at the N-terminus, *L. monocytogenes rsbV* and *rsbW* were amplified using primers DR42 and DR43 and DR48 and DR49 (sequences listed in Table 4.2), respectively, and subcloned into *Kpn*I and *Pst*I sites in pQE30 (Qiagen, Valencia, CA). The resulting plasmids, pDLR3 and pDLR4, were used to transform *E. coli* M15 [pREP4] cells (Qiagen) by electroporation. Inserted sequences were confirmed by sequencing at the Cornell University Life Sciences Core Laboratory. Strains expressing *B. subtilis rsbV* were constructed

by inserting PCR amplified gene fragments into the pCK35 vector (58) at *Hind*III and *Sph*I sites. Constructions were verified by sequencing. The resulting plasmid pDLR2 was transformed by

**Table 4.1** Plasmids and strains used in this study.

| Plasmid or strain | Relevant genotype | Source or construction |
|---|---|---|
| Plasmids | | |
| pDLR1 | $P_{fri\ Lm\ SigA1\ SigB}$ in pUC19; $Ap^R$ | This study |
| pDLR2 | $P_{spac}$ *rsbV*$_{Bs}$; $Neo^R$ | This study |
| pDLR3 | $P_{spac}$ *rsbV*$_{Lm}$; $Ap^R$ | This study |
| pDLR4 | $P_{spac}$ *rsbW*$_{Lm}$; $Ap^R$ | This study |
| pCK35 | $P_{spac}$ *rsbR*$^-$ *rsbS*$^-$ *rsbT*$^+$; $Neo^R$ | (58) |
| pUC19 | high copy number cloning vector; $Ap^R$ | (59) |
| pQE30 | N-His$_6$ expression vector, $P_{T5}/O_{lac}$, ColEI ori, $Ap^R$ | Qiagen |
| *B. subtilis* strains | | |
| FSL B2-303 | $P_{spac}$ *rsbV*$_{Bs}$ *amyE::ctc-lacZ trpC2* | pDLR2→PB198 |
| FSL B2-304 | $P_{spac}$ *rsbV*$_{Bs}$ *amyE::ctc-lacZ trpC2 sigBΔ3::spc trpC2* | pDLR2→PB345 |
| FSL PB206 | *rsbVΔl amyE::pDH32-ctc* | (11) |
| PB2 | *trpC2* | (45) |
| PB198 | *amyE::ctc-lacZ trpC2* | (11) |
| PB345 | *amyE::ctc-lacZ trpC2 sigBΔ3::spc trpC2* | (10) |
| PB213 | $P_{spac}$ (*rsbV*$^+$ *rsbWΔl sigB*$^+$ *rsbX*$^+$) *amyE::*pDH32-*ctc trpC2* | (11) |
| *E. coli* strains | | |
| FSL B2-273 | M15 pREP4 pQE30hisSigA$_{Lm}$ | (48) |
| FSL B2-274 | M15 pREP4 pQE30hisSigB$_{Lm}$ | (48) |
| FSL B2-300 | M15 pREP4 pQE30hisrsbV$_{Lm}$ | pDLR3→PB198 |
| FSL B2-301 | M15 pREP4 pQE30hisrsbWs$_{Lm}$ | pDLR4→PB198 |
| FSL B2-302 | TOP10 pUC19-$P_{fri\ Lm}$ | pDLR1→TOP10 |
| TOP10 | F$^-$ *mcrA* Δ(*mrr-hsdRMS-mcrBC*) φ80*lacZ*ΔM15 Δ*lacX74 recA1 araD139* Δ(*ara-leu*)*7697 galU galK rpsL* (Str$^r$) *endA1 nupG* | Invitrogen |
| *L. monocytogenes* strains | | |
| 10403S | Wildtype; serotype 1/2a | (9) |
| 10403SΔ*sigB* | Δ*sigB* | (55) |

electroporation (57) into strains PB198 and PB345. A 276 bp PCR fragment containing SigA2- and SigB-dependent promoter elements from the *L. monocytogenes fri* promoter region (43) was cloned into PUC19 at *Hind*III and *Xba*I sites, and transformed into *E. coli* TOP10 cells (Invitrogen, Carlsbad, CA), resulting in strain FSL B2-302. Chloramphenicol (10 ug/ml), streptomycin (100 ug/ml), kanamycin (25 ug/ml), ampicillin (100 ug/ml), and neomycin (5 ug/ml) were included as appropriate.

*Overproduction and purification of $\sigma^B$ and $\sigma^A$ for in vitro transcription*

$His_6$-SigB and $His_6$-SigA proteins were overexpressed from strains FSL B2-273 and FSL B2-274. Cells were grown in 500 mL Luria broth (LB) containing ampicillin and kanamycin at 37°C with shaking (225 rpm). At OD 0.7-1.0, 1 mM IPTG was added. Cells were pelleted by centrifugation (10,000 *x g*, 4°C, 15 min) after 3-4 hours of growth with isopropyl-β-D-thiogalactopyranoside (IPTG) and frozen at -80°C. To purify proteins, cell pellets were thawed and resuspended in 5 ml lysis buffer (20 mM Tris, pH 8.0, 0.5 M NaCl, 5 mM imidazole, 6 M guanidine hydrochloride, 1 mM β-mercaptoethanol, 1 mg/ml lysozyme). Cells were sonicated (4

**Table 4.2** Primers and probes used in this study.

| Primer or probe | Sequence (5'→3') | Source |
|---|---|---|
| DR1 FRI Fwd | CGAAGCTTCACCTGAAAGCGGTGAGAAT | This study |
| DR2 FRI Rev | CTCTAGACCAGTGTGGAAACCATCACA | This study |
| DR34 rsbV Fwd | GATAAGCTTAAAGCAACTAGTGATTTGAAGG AAAA | This study |
| DR35 rsbV Rev | GATGCATGCCGGCACTTTCATTTCGATGT | This study |
| DR42 HisRsbV Fwd | GGCAGGGGTACCATGAATATTAGTATAGAAA TAAAAGAACGTGATAC | This study |
| DR43 HisRsbV Rev | ACTTGTCTGCAGCAAATTTTGTCATGCATTGT TGCG | This study |
| DR48 HisRsbW Fwd | GACACAGGTACCATGGCAACAATGCATGA | This study |
| DR49 HisRsbW Rev | GCTTGTCTGCAGTTCGCCTCTTTATCAGGTTG A | This study |
| *sigB* Taqman F | GCCGCTTACCAAGAAAATGG | (Chaturongakul, unpublished) |
| *sigB* Taqman R | TTCGGGCGATGGACTCTACT | (Chaturongakul, unpublished) |
| *sigB* MGB probe | ATCAAGACGCCCAATAT | (Chaturongakul, unpublished) |
| *rpoB* Taqman F | CCGGACGTCACGGTAACAA | (6) |
| *rpoB* Taqman R | CAGGTGTTCCGTCTGGCATA | (6) |
| *rpoB* MGB probe | CCGGACGTCACGGTAACAA | (6) |

Restriction sites are underlined.

x 20 sec on, 1 min off at 33 W) on ice and the lysate was centrifuged (10,000 *x g*, 4°C, 15 min) to remove cell debris. Supernatants were applied to a Ni-NTA column (HisTrap HP, GE Lifesciences, Pittsburgh, PA) using a 10 ml syringe. On-column refolding was performed using a stepwise gradient of buffer [20 mM Tris (pH 8.0), 0.5 M NaCl, 5 mM imidazole, 1 mM β-mercaptoethanol] containing decreasing concentrations of urea. Following elution, protein fractions were analyzed using SDS-PAGE and Coomassie blue staining (Simplyblue, Invitrogen). Fractions containing target protein were concentrated (Vivaspin 2, 10 KDa MWCO,

GE Lifesciences) and exchanged into protein storage buffer [10 mM Tris (pH 8.0), 10 mM $MgCl_2$, 0.1 mM EDTA, 0.1 mM DTT, 0.1 M NaCl, 50% glycerol], and stored at -20°C.

*Overproduction and purification of RsbW and $\sigma^B$ for stopped-flow fluorescence analysis*

$His_6$-RsbW and $His_6$-SigB were overexpressed, and proteins were batch purified using Ni-NTA resin (PrepEase Histidine-tagged High Specificity Purification Resin, Affymetrix, Santa Clara, CA) according to manufacturer's instructions. Fractions containing the target protein were purified on a Superdex 200 FPLC column using HEPES buffer [20 mM HEPES (pH 7.5), 100 mM NaCl, 10% glycerol] and stored at -80°C.

*Growth conditions and β-galactosidase assays*

All *B. subtilis* strains were grown with shaking (225 rpm) in 300 ml Nephelo flasks (Nephelo, BellCo, Vineland, NJ). Strains PB213, FSL B2-303, and FSL B2-304 were grown in buffered LB (10). For azide and salt stress experiments, strains grown overnight in LB at 37°C were diluted (1:25) into fresh 30 ml of LB, then passaged again (1:25) into fresh LB (30 ml) at mid exponential phase ($O.D._{600}$ 0.2). At $O.D._{600}$ 0.2, sodium azide (200 mM) or sodium chloride (5 M NaCl) was added to a final concentration of 2 mM or 0.3 M, respectively. FPSS (44) [(E)-*N*-(4-fluorophenyl)-2-phenylethenesulfonamide; Enamine Ltd., Kiev, Ukraine) stock solutions (10 mM) were diluted in dimethyl sulfoxide (DMSO; Sigma-Aldrich, St. Louis, MO) and filtered with 0.2 um nylon membrane syringe filters (Acrodisc, Pall, Port Washington, NY). FPSS was added to a final concentration of 64 uM, except where noted differently. For cold growth experiments, FPSS or an equal volume of DMSO was added to exponential phase cultures (at $OD_{600}$ 0.2) grown in LB at 37°C before moving them to 16˚C with shaking (225 rpm). Phosphate limitation experiments were conducted in a synthetic medium (60). Low phosphate (0.15 mM) synthetic medium (30 ml) with FPSS or DMSO was inoculated with 1.2 ml of culture (1:25)

grown in the same medium overnight. Beginning at $O.D._{600}$ 0.2, samples were removed at regular intervals. β-galactosidase activity assays were performed using the method described by Kenney and Moran (29), using cell permeabilization with choloroform. $OD_{600}$ values of cell suspensions were used to calculate Miller units, while protein concentration by Bradford assay (Biorad, Hercules, CA) was used to calculate β-galactosidase specific activity. At least two biological replicates were performed for each experiment.

*In vitro transcription assays*

Phenol-chloroform purified PCR product (amplified using primers DR1 and DR2 and plasmid pDLR1) was used as DNA template for in vitro transcription assays. In vitro transcription initiated from the SigA2- and SigB-dependent promoters of the *L. monocytogenes fri* promoter results in RNA fragments of 185 and 120 bp, respectively. Reaction mixtures (40 ul) containing in vitro transcription buffer [10 mM Tris-HCl (pH 7.8), 10 mM $MgCl_2$, 0.5 mM EDTA, 1 mM DTT, 7.5 mM KCl, and 10 ug/ml acetylated BSA], $His_6$-SigA or $His_6$-SigB, and FPSS or DMSO were incubated at room temperature for 5 min. Purified *B. subtilis* RNA polymerase was added to the mixtures for a final concentration of 150 nM. PCR product (330 ng) was added, followed by incubation at 37°C for 10 min. Transcription reactions were started by adding a mixture of NTPs [approximately 12 nmol of each ATP, CTP, GTP, and UTP and 1.7 nmol [$\alpha$-$^{32}$P]-UTP (6,000 Ci $mmol^{-1}$)] and incubated at 37°C for 10 min. Reactions were stopped by adding 60 ul of stop solution (0.5 M sodium acetate, 17 mM EDTA). RNA was precipitated by adding 2 ul glycogen (Glycoblue, Invitrogen) and 330 ul EtOH, followed by overnight storage at -20°C. RNA was collected by centrifugation at 16,000 *x g* for 10 min, washed with 70% EtOH, and resuspended in formamide loading dye. Samples were heated at 95°C for 5 min and

loaded in a 6% TBE-urea gel for separation. Transcripts were visualized using a phosphoimager screen.

*RNA extraction, cDNA synthesis, and qRT-PCR*

*L. monocytogenes* strain FSL A1-254 was streaked from frozen stocks onto BHI plates and incubated overnight at 37°C. An isolated colony was used to inoculate 5 ml BHI, which was incubated at 37°C overnight with shaking (225 rpm). An aliquot of 50 ul was transferred from this culture to 5 ml fresh, prewarmed BHI (1:100) and grown to $OD_{600}$ 0.4. An aliquot of 300 ul was transferred to two Nephelo flasks containing 300 ml prewarmed BHI and grown until $OD_{600}$ 0.4. An aliquot of culture (5 ml) was removed from each culture and added to 5 ml RNAprotect (Qiagen) to stop transcription. To the remaining cultures, 64 uM FPSS or an equal volume of DMSO was added, and the flasks were returned to the incubator. After 15 min, another 5 ml was removed and treated as above. Salt (0.3 M NaCl, final concentration) was added to the cultures, and the cultures returned to the incubator. After 15 min, a final 5 ml aliquot was removed and treated as above. Cells were pelleted at 3,600 *x g* for 10 min at 4°C after 5 min at room temperature in RNAprotect. Pellets were kept on ice until RNA extraction, performed as previously described (5). cDNA was synthesized as described elsewhere (41). Taqman qPCR was performed on $10^{-1}$, $10^{-2}$, and $10^{-3}$ dilutions of cDNA using *sigB* and *rpoB* (6) primers and probes (sequences in Table 4.2). A standard curve was generated using genomic chromosomal DNA isolated from *L. monocytogenes* 10403S. Copy numbers of *sigB* transcript levels were calculated from standard curves and normalized to *rpoB* transcript levels, as described in Sue et al. (51).

*Sporulation assays*

Sporulation of *B. subtilis* was induced by nutrient exhaustion in 2XSG medium (34). Isolated colonies were used to inoculate 20 ml 2XSG medium in a 300 ml flask for overnight growth at 37°C with shaking (225 rpm), and at $OD_{600}$ 0.2, 200 ul of culture was added to fresh 20 ml medium containing 64 uM FPSS or an equivalent volume of DMSO, and grown as above. After 24 hr, 1 ml of culture was heated at 80°C for 20 min and serially diluted in phosphate buffer saline (PBS) for plating onto LB agar. Plates were incubated at 37°C for 24 hr. Sporulation efficiency was determined as CFU/ml of heated samples normalized to CFU/ml of unheated samples.

*Stopped-flow fluorescence analysis*

Binding of FPSS to RsbW and $\sigma^B$ was measured using the proteins' intrinsic Trp and Tyr fluorescence signal with a KinTek SF2004 stopped-flow fluorimeter. The excitation wavelength was set at 280 nm and emission was monitored using a 305 nm bandpass filter. Proteins were dialyzed into 50 mM Tris-HCl (pH 7.4) overnight, quantified by Bradford assay, and diluted with dialysate, with 5% DMSO added to match the DMSO concentration present in FPSS solutions. FPSS was diluted to 5 uM in dialysate. For single-mix experiments, each shot involved 1:1 mixing of 40 uL aliquots of protein and small molecule and then collection of 1,000 points over the time period. Reactions were conducted at 22°C.

*Statistical analysis*

Statistical analysis of *sigB* transcript levels from three biological replicates was performed using t-tests at each time point with a statistical significance value of $p < 0.05$ (JMP 9.0, SAS, Inc., Cary, NC). Sporulation efficiencies of three biological replicates were analyzed for statistically significant differences ($p < 0.05$) using a t-test between treatments within each strain (JMP 9.0).

## RESULTS

### FPSS interferes with the activation of $\sigma^B$

In previous work, we showed that the addition of FPSS to mid-exponential phase *B. subtilis* prevents induction of $\sigma^B$ activity during exposure to salt (0.3 M NaCl) (44), as monitored by a well-characterized $\sigma^B$-dependent single copy *ctc-lacZ* transcriptional fusion (11). To determine whether FPSS prevents $\sigma^B$ activity by altering the activation of $\sigma^B$ (meaning its switch between an inactive, bound state to its free, active state) or by inhibiting the sigma factor's activity, i.e., its transcriptional function once $\sigma^B$ is released from its antagonist RsbW, we measured the effect of adding FPSS 15 min after induction of $\sigma^B$ activity by 0.3 M NaCl. We hypothesized that if FPSS affects the activation of $\sigma^B$ rather than its ability to associate with RNA polymerase (RNAP) or the recruitment of holoenzyme RNAP to $\sigma^B$-dependent promoter sites, addition of FPSS after induction of $\sigma^B$ activity should not affect the development of $\sigma^B$ activity in response to an environmental stress. We observed a similar accumulation of β-galactosidase enzyme in cultures treated with FPSS after exposure to salt compared to control cultures treated with DMSO, the solvent in which our stock solutions of FPSS are dissolved (Figure 4.2). Consistent with our previous work we saw no $\sigma^B$ activity in cultures treated with 64 uM FPSS prior to the addition of salt. The absence of an effect of FPSS on $\sigma^B$ activity once $\sigma^B$ is activated by salt suggests that FPSS inhibits the activation of $\sigma^B$, rather than interfering with $\sigma^B$-dependent transcription once $\sigma^B$ is active and promoting transcription from $\sigma^B$-dependent binding sites.

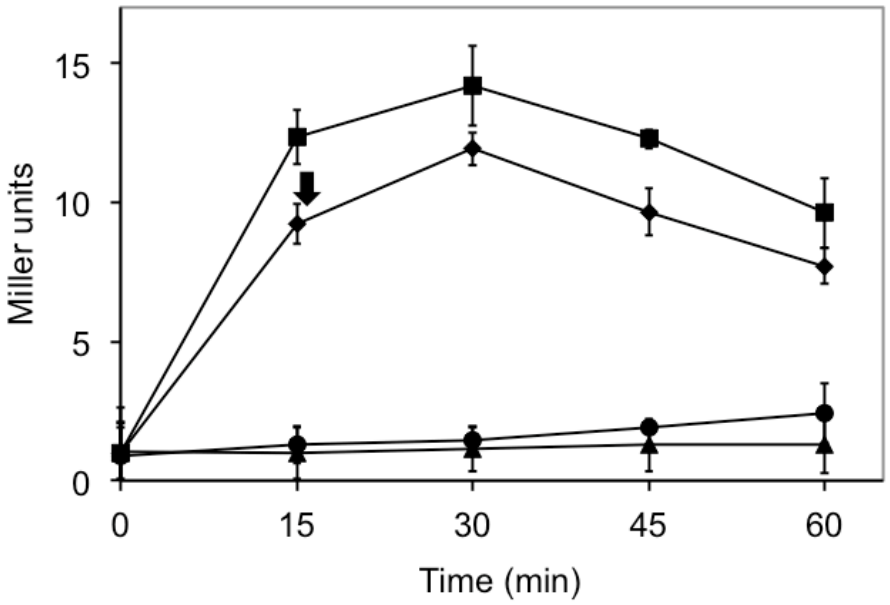


**Figure 4.2** Effect of delayed addition of FPSS on salt-induced $\sigma^B$ activity. At mid-exponential phase ($OD_{600}$ 0.2), PB198 (*amyE::ctc-lacZ trpC2)* grown in LB at 37°C was treated with: $H_2O$ and DMSO (●), 0.3 M NaCl and DMSO (■), 0.3 M NaCl and 64 uM FPSS (▲), or 0.3 M NaCl, and 64 uM FPSS was added after 15 min sampling (indicated by arrow) (◆). Mean β-galactosidase activity with range bars of two biological replicates is shown.

We used genetic experiments to further investigate whether FPSS affects $\sigma^B$'s transcriptional role as an RNAP subunit, or alternatively, the post-translational regulation of $\sigma^B$ (activation of $\sigma^B$). In *B. subtilis* and *L. monocytogenes*, the gene encoding $\sigma^B$ lies within an eight gene operon, *$P_A$-rsbR-rsbS-rsbT-rsbU-$P_B$-rsbV-rsbW-sigB-rsbX*, known as the *sigB* operon (28, 56). A $\sigma^B$-dependent promoter lies upstream of *sigB*, creating an autoregulatory feedback loop once $\sigma^B$ becomes active. By using *B. subtilis* strain PB213 (11), which contains an inducible promoter upstream of the *rsbV-rsbW-sigB*, we uncoupled $\sigma^B$ regulation from the signal

transduction cascade and from its autoregulation. Addition of IPTG to PB213 induces $\sigma^B$ activity, as measured by a $\sigma^B$-dependent reporter fusion, in this *rsbW* null mutant (11), presumably by increasing the amount of active, unbound $\sigma^B$ in the absence of the anti-sigma factor antagonist. The upregulation of *rsbX* along with the other genes downstream of this strain's $P_{spac}$ promoter has no observed negative feedback consequences on $\sigma^B$ activity because the phosphatase RsbX exerts its negative regulatory function on members of the stressosome (17, 54), which are not involved in regulating $\sigma^B$ activity in this strain.

As shown in Figure 4.3, the presence of 64 uM FPSS immediately before the addition of 1 mM IPTG had no effect on $\sigma^B$ activity in this strain compared to a parallel control culture treated with DMSO, in which $\sigma^B$ activity was rapidly induced upon addition of IPTG. This result again demonstrates that FPSS has no effect on $\sigma^B$'s transcriptional function once $\sigma^B$ has become active. These results provide additional evidence to support our hypothesis that FPSS interferes with the regulation of $\sigma^B$ rather than its transcription-mediating role once released from RsbW and consequently active.

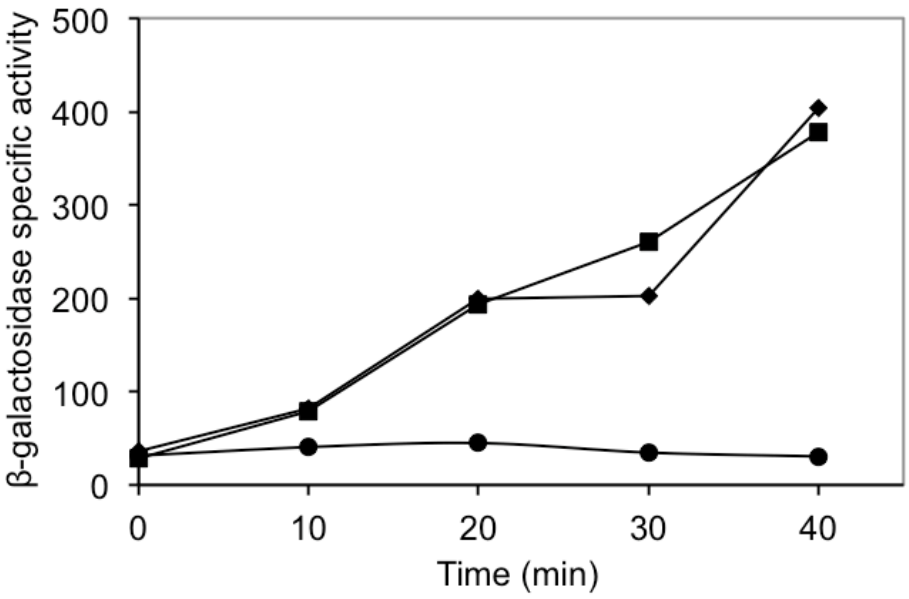


**Figure 4.3** Effect of FPSS on $\sigma^B$ activity by artificial induction. PB213 [$P_{spac}$ (*rsbV*$^+$ *rsbW*Δ*l sigB*$^+$ *rsbX*$^+$) *amyE::*pDH32-*ctc trpC2*] was grown in BLB at 37°C with shaking (225 rpm). At $OD_{600}$ 0.4 (*t* = 0), 64 uM FPSS or DMSO, then IPTG (1 mM final concentration) or $dH_2O$, were added. β-galactosidase activity of PB213 with $H_2O$ and DMSO (●), IPTG and DMSO (■), and IPTG and FPSS (◆) is shown. Samples were removed at regular intervals. Results from a representative sample are shown.

**FPSS inhibits $\sigma^B$ in response to energy stress**

Energy stresses, caused by entry into stationary phase, limitation of phosphate or glucose, and a drop in ATP levels, induce $\sigma^B$ activity in *B. subtilis* through a different signal transduction pathway than environmental stresses that requires the phosphatase RsbP to dephosphorylate RsbV-P (53, 54, 60). A null *rsbP* strain demonstrates normal induction of $\sigma^B$ activity in

response to high salt and ethanol exposure (53), indicating it is not a necessary regulatory protein for $\sigma^B$ activity in response to environmental stress. Therefore, we investigated whether FPSS inhibits $\sigma^B$ activity in response to energy stresses in order to determine by deductive reasoning whether FPSS interacts with a member of the stressosome or the phosphatase RsbU. We hypothesized that if FPSS interferes with the function of the members of the environmental stress pathway, then the energy stress response should be unaffected. We assayed three energy stress conditions, entry into stationary phase, phosphate limitation, and azide stress, in the presence of FPSS to deduce the compound's effect on the energy stress regulatory pathway.

The presence of FPSS prevented the induction of $\sigma^B$ activity during entry into stationary phase (Figure 4.4) in PB198 cells grown at 37°C in LB, an effect that lasted for at least 5 hours after entry into stationary phase. The addition of FPSS prior to the addition of sodium azide (2 mM), which inhibits ATP synthesis, induced $\sigma^B$ activity in the DMSO-treated control culture once growth ceased (Figure 4.5). The FPSS-treated culture also showed induction of $\sigma^B$ activity about 4 hours after the DMSO-treated culture, despite a concurrent cessation in growth in both cultures. Finally, we grew strain PB198 in synthetic medium with limited phosphate (15 uM) to induce phosphate starvation, and treated parallel cultures with 0, 32, 64, or 128 uM FPSS. We observed a delay in $\sigma^B$ activity in cultures treated with FPSS, as well as decreased activity dependent on the concentration of FPSS added to the cultures (Figure 4.6). The addition of 64 uM and 128 uM FPSS resulted in ~46% and ~24% activity of the wild type, respectively.

The perturbation of normal $\sigma^B$ activity in response to these three energy stresses implies that FPSS does not interfere with the function of the positive regulator RsbU or upstream members of the stressosome, which are not required for the response to this type of energy stresses (54). Together with our data showing that FPSS prevents environmental stress activation

of $\sigma^B$, these findings allow us to conclude that FPSS does not affect either RsbP or RsbQ, which are not required for $\sigma^B$ activity in response to salt stress (53). We hypothesize that the delayed $\sigma^B$ activity observed in azide-treated and phosphate-starved cultures might be related to nucleotide levels in these conditions. In high ATP conditions, RsbW's kinase function phosphorylates RsbV, inactivating it and preventing it from binding to RsbW (1, 60). A drop in ATP levels is critical for the activation of $\sigma^B$ in response to energy stresses, and we hypothesize that the delayed induction of $\sigma^B$ activity that we observed in response to azide stress and phosphate starvation might result from the lack of ATP needed to phosphorylate and thus deactivate RsbV in these conditions (61), an effect that might be separate from FPSS's mechanism of inhibiting $\sigma^B$ activation. Alternatively, the small molecule might be titrated or inactivated eventually in cells growing in these conditions by its target, an effect we do not observe in response to salt stress or entry into stationary phase during growth in LB.

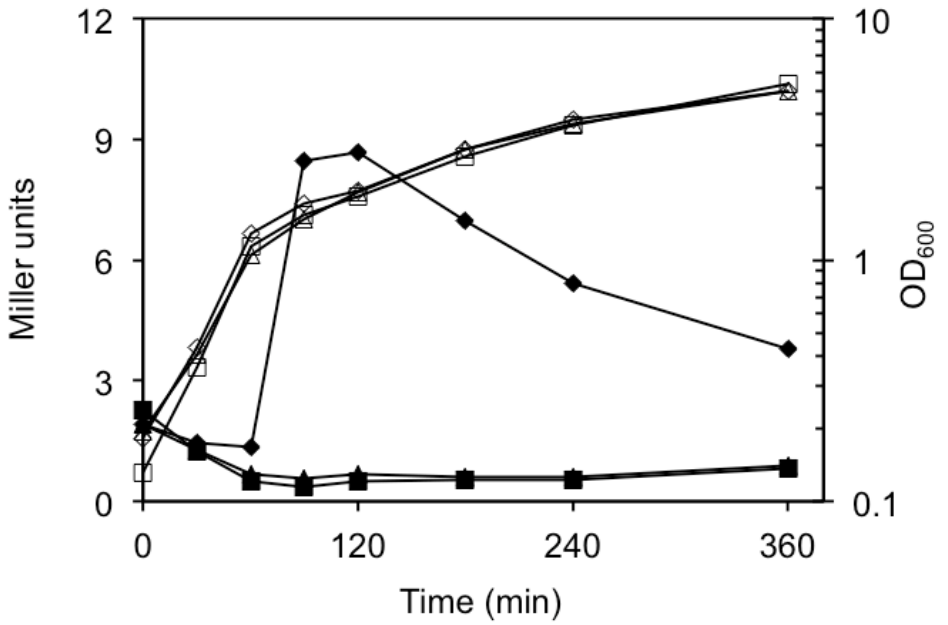


**Figure 4.4** Effect of FPSS on $\sigma^B$ activity during entry into stationary phase. Strains PB198 (*amyE::ctc-lacZ trpC2)* and PB345 (*amyE::ctc-lacZ trpC2 sigBΔ3::spc trpC2)* were grown in LB at 37°C with shaking (225 rpm). At mid-exponential phase ($OD_{600}$ 0.2), a 1.5 ml aliquot was removed, and 64 uM FPSS (▲) or an equal volume of DMSO (◆) was added to PB198, and PB345 was treated with DMSO (■). Samples were removed at indicated intervals. β-galactosidase activity (closed symbols) and cell growth, measured by $OD_{600}$ (open symbols), of one representative sample are shown.

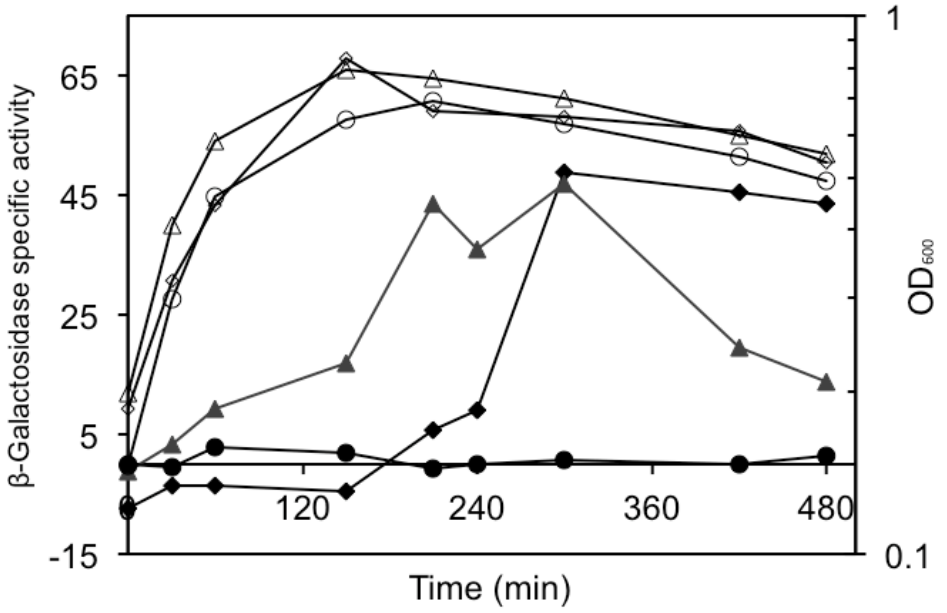


**Figure 4.5.** Effect of FPSS on $\sigma^B$ activity in response to azide stress. Strains PB198 (*amyE::ctc-lacZ trpC2)* and PB345 (*amyE::ctc-lacZ trpC2 sigBΔ3::spc trpC2)* were grown in LB at 37°C with shaking (225 rpm) to mid-exponential phase. At $OD_{600}$ 0.2 ($t$ = 0), PB198 was treated with sodium azide (final concentration, 2 mM) and 64 uM FPSS (◆) or an equal volume of DMSO (▲). Samples were removed at regular intervals. β-galactosidase activity (closed symbols) and cell growth, monitored by $OD_{600}$ (open symbols) from a representative sample are shown.

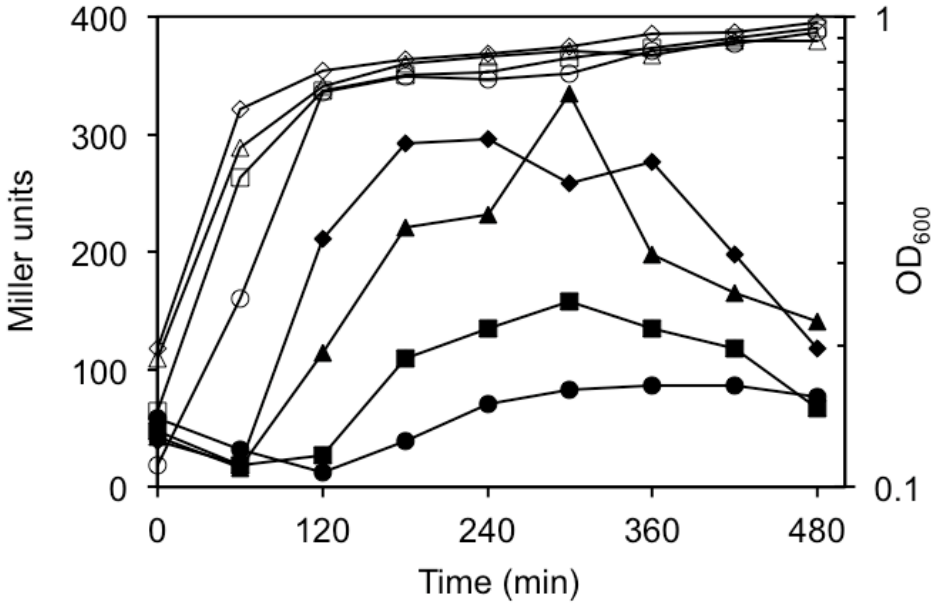


**Figure 4.6.** Effect of FPSS on $\sigma^B$ activity in response to phosphate limitation. PB198 (*amyE::ctc-lacZ trpC2)* was grown in LB at 37°C with shaking (225 rpm) in low phosphate (15 uM) defined medium with 32 uM FPSS (▲), 64 uM FPSS (■), and 128 uM FPSS (●), or an equal volume of DMSO as that added to the culture treated with 128 uM FPSS (◆). Samples were removed after regular intervals at $OD_{600}$ 0.2 ($t$ = 0). β-galactosidase activity (closed symbols) and cell growth, measured by $OD_{600}$ (open symbols), from a representative assay are shown.

The result that FPSS inhibited $\sigma^B$ activity in response to both environmental and energy stresses led us to investigate whether FPSS interacts with members of the signal transduction cascade downstream of the phosphatases RsbU and RsbP: the partner switching module RsbV/RsbW/$\sigma^B$. Specifically, we hypothesized that if FPSS bound to RsbV, it might prevent

RsbV from binding to RsbW and thus prevent the release of $\sigma^B$. If RsbV is the target of FPSS, then the addition of FPSS should prevent artificial induction of $\sigma^B$ activity caused by overexpressing RsbV. To test this notion, we constructed a plasmid carrying *rsbV* under an inducible promoter, modifying the pCK35 vector used by Yang et al. (58) to artificially induce $\sigma^B$ activity by overexpressing the positive regulator RsbT. We determined the minimum concentration of IPTG necessary to reproducibly induce $\sigma^B$ activity, 15 uM, in an effort to prevent potential saturation of FPSS by RsbV that might occur from using a higher concentration of IPTG that could mask its inhibitory effect. FPSS (64 uM) added to mid-exponential phase cultures prior to the addition of IPTG prevented the artificial induction of $\sigma^B$ activity by overexpression of RsbV that we observed in a control culture treated with DMSO ( Figure **4.7**). This result suggests that FPSS might bind to either RsbV or another member of the partner switching module to interfere with the release of $\sigma^B$ from RsbW in response to stress.

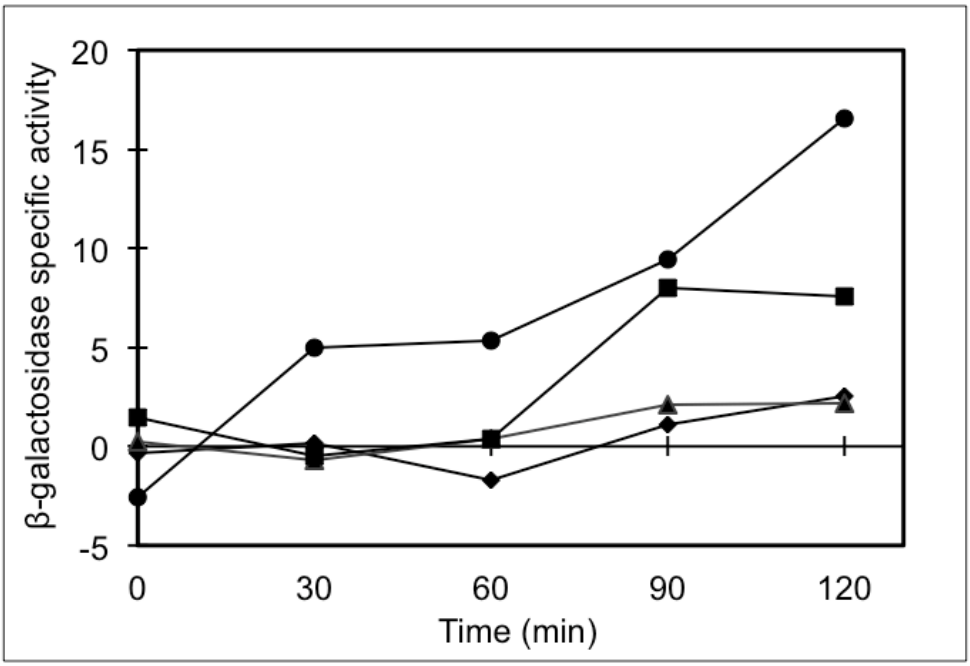


**Figure 4.7** Effect of FPSS on artificial induction of $\sigma^B$ activity by overexpression of RsbV. Cells were grown in BLB at 37°C with shaking (225 rpm). At $OD_{600}$ 0.2 ($t$ = 0), a 1.5 ml aliquot was removed, and 64 uM FPSS or DMSO, and IPTG (15 uM final concentration) or $dH_2O$, were added. β-galactosidase activity of B2-303 (*amyE::ctc-lacZ trpC2* pDLR2) with $H_2O$ and DMSO (■); B2-303 with IPTG and DMSO (●); B2-303 with IPTG and FPSS (◆); and B2-304 (*sigBΔ3*::*spc amyE::ctc-lacZ trpC2* pDLR2) with IPTG and DMSO (▲) are shown. Samples were removed at regular intervals. Results from a representative sample are shown.

**FPSS prevents chill induction of $\sigma^B$ activity**

Growth at high (51°C) and low (16°C) temperatures induces $\sigma^B$ activity independently of the RsbT/RsbU/RsbV pathway in *B. subtilis* (12, 26), indicating that induction of $\sigma^B$ activity in these conditions does not depend on the phosphorylation state of RsbV. To determine whether

FPSS prevents induction of $\sigma^B$ by an interaction with RsbV, or is dependent on the phosphorylation state of RsbV, we tested whether FPSS could prevent "chill induction" of $\sigma^B$ activity. If FPSS does interact with RsbV to disrupt the release $\sigma^B$ from RsbW, we expected to see no effect of FPSS on $\sigma^B$ activity during growth at 16°C in *B. subtilis*. Conversely, if FPSS interacts in an RsbV-independent manner, we expected to see inhibition of $\sigma^B$ activity in a Δ*rsbV* mutant during cold growth. We grew *B. subtilis* PB198 and Δ*rsbV* strain PB206 (11) at 37°C cells in LB, shifted them to 16°C, and monitored $\sigma^B$ activity (Figure 4.8). DMSO-treated PB198 and PB206 showed induction of $\sigma^B$ activity approximately 18 hours after a shift to 16°C, compared to cultures treated with 64 uM FPSS prior to the temperature shift. The inhibition of $\sigma^B$ activity by FPSS in a *B. subtilis* strain lacking *rsbV* suggests a mechanism independent of RsbV and independent of the signal transduction pathways that lead to the dephosphorylation of RsbV-P.

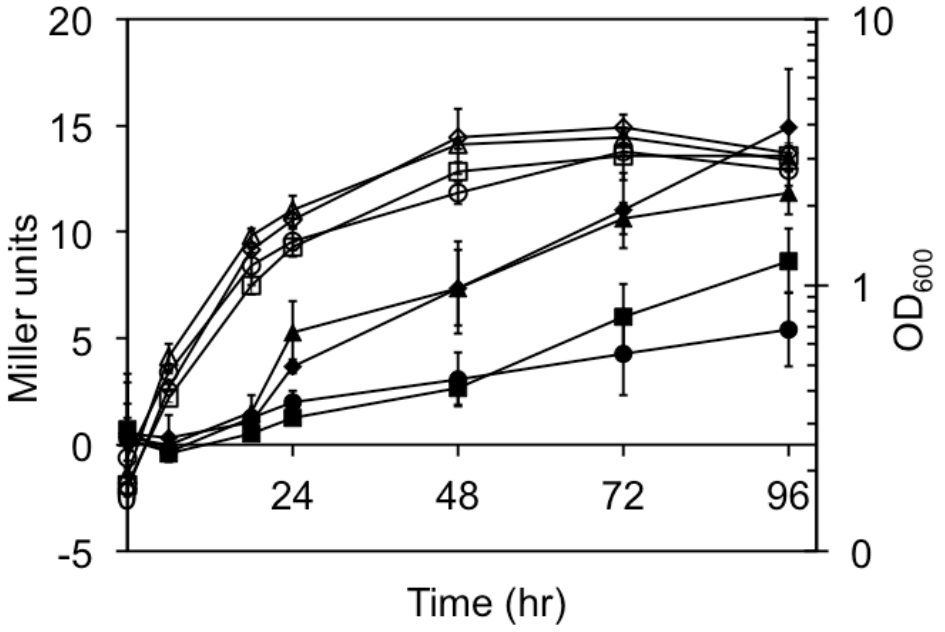


**Figure 4.8.** Effect of FPSS on $\sigma^B$ activation by growth at 16°C. Strains PB198 (*amyE::ctc-lacZ trpC2)* and PB206 (*rsbV*Δ*l amyE::pDH32-ctc*) were grown at 37°C with shaking (225 rpm) in LB until mid-exponential phase ($OD_{600}$ 0.2). Strains were treated with 64 uM or an equal volume of DMSO then transferred to 16°C with shaking (225 rpm): PB198 treated with DMSO (◆); PB198 with 64 uM FPSS (■); PB206 (▲) with DMSO; and PB206 with 64 uM FPSS (●) is shown. Mean β-galactosidase activity (closed symbols) and cell growth, monitored by $OD_{600}$ (open symbols), with range bars of two biological replicates are shown.

**FPSS does not bind directly to $\sigma^B$ to prevent transcription from a $\sigma^B$ promoter site**

Since our β-galactosidase assays led us to rule out the members of the three pathways of the signal transduction cascade regulating $\sigma^B$ activity as potential targets of FPSS responsible for inhibition of $\sigma^B$ activity, we investigated potential direct binding of the small molecule to $\sigma^B$.

The results of adding FPSS to *B. subtilis* in which $\sigma^B$ activity was artificially or already induced strongly suggested that FPSS affects regulation of $\sigma^B$, but we proposed the use of a reductionist in vitro transcription system to explore any potential binding of FPSS to $\sigma^B$. If FPSS binds directly to $\sigma^B$, it might interfere with the sigma factor's ability to bind to RNAP or its release from RsbW. We performed in vitro transcription assays containing *B. subtilis* RNAP, $His_6$-tagged *L. monocytogenes* $\sigma^B$ or $\sigma^A$ (as a control), and a fragment of the *L. monocytogenes fri* promoter region containing one $\sigma^B$- and one $\sigma^A$-dependent promoter site (43). If FPSS binds directly to the sigma factor, the addition of FPSS would lead to a reduced amount of transcript produced from the $\sigma^B$ promoter in a reaction compared to a control reaction to which DMSO was added.

The hybrid *B. subtilis* -*L. monocytogenes* RNAP holoenzyme successfully transcribed from both *L. monocytogenes* promoter sites (Figure 4.9). Control reactions without any added sigma factors indicated that residual *B. subtilis* $\sigma^A$ contained in the purified RNAP protein fraction initiated transcription from the *L. monocytogenes* $\sigma^A$-dependent promoter site (lane 11), but the addition of exogenous, purified *L. monocytogenes* sigma factors promoted higher transcript levels from the template's $\sigma^A$-and $\sigma^B$- promoter sites (lanes 12 and 13), even in the presence of DMSO (lanes 14 and 15). We performed two titration experiments to test the effect of FPSS on transcription from a $\sigma^B$-dependent promoter site. In the first titration experiment, increasing amounts of $\sigma^B$ added to reactions caused higher levels of transcripts to be produced from the $\sigma^B$ promoter (lanes 1-5). Transcription in these reactions from the $\sigma^B$-dependent promoter site the effect was uninhibited by the presence of FPSS up to ~1,000 fold the concentration of $\sigma^B$ and *B. subtilis* RNAP (lanes 6-10). In the second experiment, titration with increasing amounts of FPSS relative to $\sigma^B$ up to 1,000-fold higher (lanes 17-21) did not inhibit

transcription relative to a control reaction containing with DMSO (Lane 16). Since the RNAP-$\sigma^B$ holoenyzme was able to transcribe from a $\sigma^B$-dependent promoter despite the presence of a relatively high concentration of FPSS, these data provide support in addition to our evidence from the delayed addition of FPSS to a salt-treated culture (Figure 4.2) that FPSS does not prevent the binding of $\sigma^B$ to core RNAP and does not prevent recognition of $\sigma^B$-dependent promoter sites.

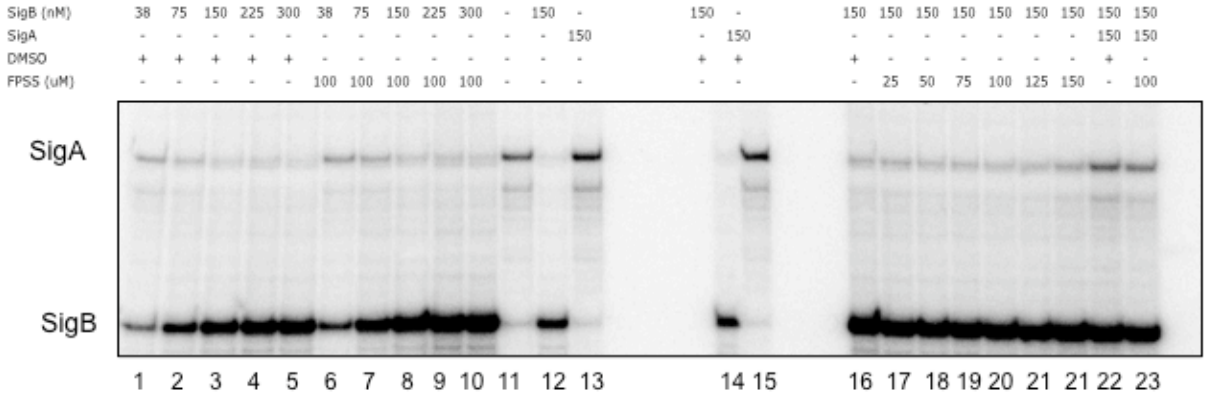


**Figure 4.9** Effect of FPSS on in vitro transcription of *L. monocytogenes* $\sigma^B$ -dependent promoter. Left lanes: *B. subtilis* RNAP (150 nM) was added to reactions containing varying concentrations of $\sigma^B$ (37.5, 75, 150, 225, or 300 nM) in the presence of DMSO (lanes 1-6) or 100 uM FPSS (lanes 7-10). Control reactions (lanes 12-13) indicate sigma factor-initiated transcription from both promoters, even in the presence of DMSO (lanes 14 and 15). Right lanes: *B. subtilis* RNAP (150 nM) was added to reactions containing $\sigma^B$ (150 nM) in the presence of DMSO (lane 16) or varying concentrations of FPSS (25, 50, 75, 100, 125, or 150 uM; lanes 17-21).

To further test the possibility that FPSS binds to either $\sigma^B$ or RsbW to interfere with $\sigma^B$ activity, we used stopped-flow fluorescence analysis to measure potential binding of FPSS to these proteins in vitro. This method measures changes in the fluorescence of proteins upon

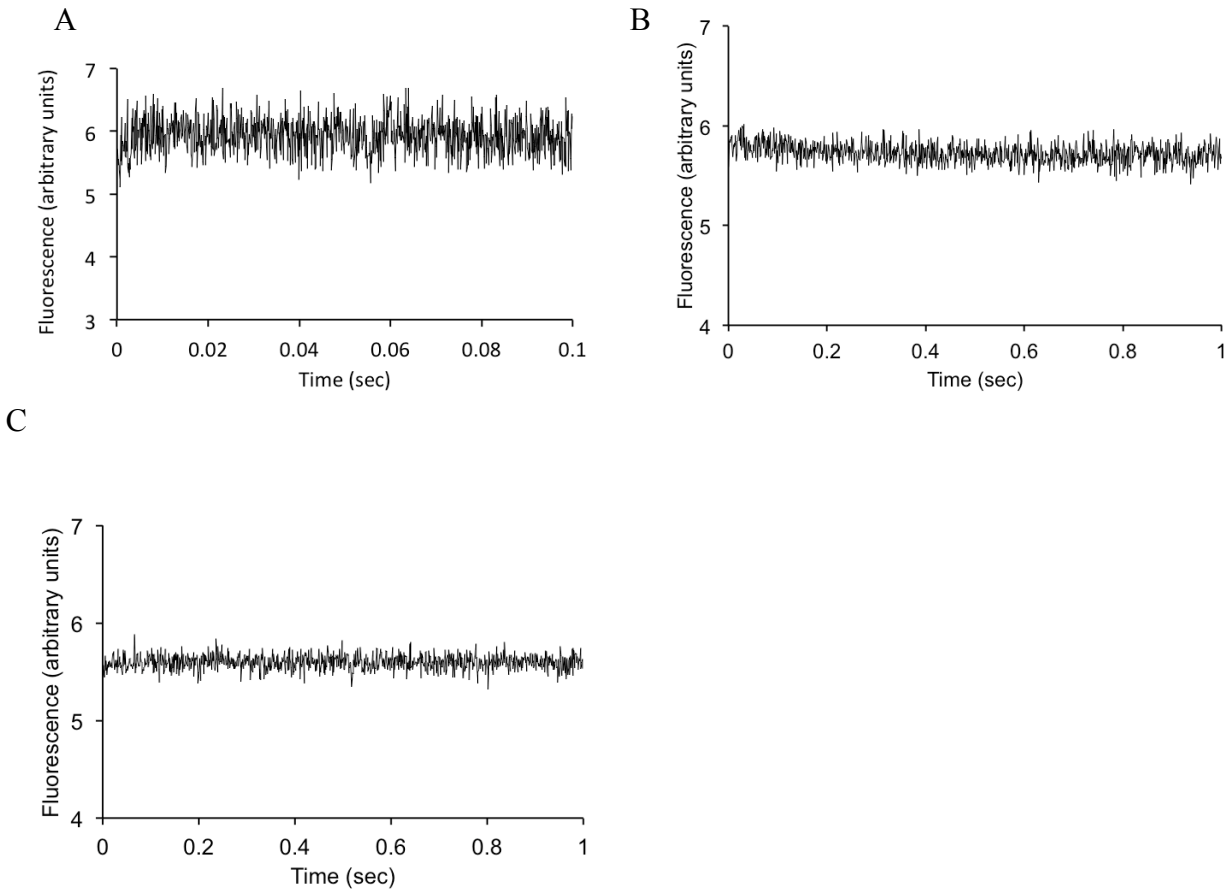


**Figure 4.10** Stopped-flow fluorescence analysis of FPSS binding to *L. monocytogenes* $\sigma^B$ and RsbW. (A) and (B) Rapid mixing of 1:1 aliquots of 2 uM $His_6$-$\sigma^B$ with 5 uM FPSS. (C) Rapid mixing of 4 uM $His_6$-RsbW with 5 uM FPSS. Proteins and FPSS were in 50 mM Tris-HCl, pH 7.4, and reactions were conducted at 21°C. Excitation wavelength was set at 280 nm and emission was measured using a 305 nm bandpass filter.

mixing with ligands. Rapid mixing assays of $His_6$-tagged purified *L. monocytogenes* RsbW (4 uM) and $\sigma^B$ (2 uM) with FPSS (5 uM) (Figure 4.10) demonstrated no changes in the fluorescence of the proteins, suggesting an absence of binding in these in vitro conditions.

**FPSS does not prevent the transcription of *sigB* in vivo**

One potential way FPSS could inhibit $\sigma^B$ activity is by blocking transcription of the gene encoding the sigma factor. Binding sites for global regulators of carbon metabolism and nitrogen metabolism, CcpA and TnrA, lie upstream of *rsbV* in *B. subtilis* (18). Mutations in these DNA sequences alter $\sigma^B$ activity in response to a variety of stresses, including ethanol stress, glucose and phosphate starvation (18). To determine whether FPSS might inhibit $\sigma^B$ activity by blocking transcription of *sigB*, either via one of these repressor proteins or by some other mechanism, we measured *sigB* transcript levels in *L. monocytogenes* 10403SΔ*sigB*. Our *sigB* Taqman qRT-PCR primers and probe detect a signal in this null mutant because the construction left ~200 bp of the 5' end of the gene intact (55). Using the Δ*sigB* strain allowed us to monitor *sigB* transcript levels in response to FPSS addition and to an environmental stress without positive upregulation by the autoregulatory feedback loop formed by the $\sigma^B$-dependent promoter found upstream of *rsbV*.

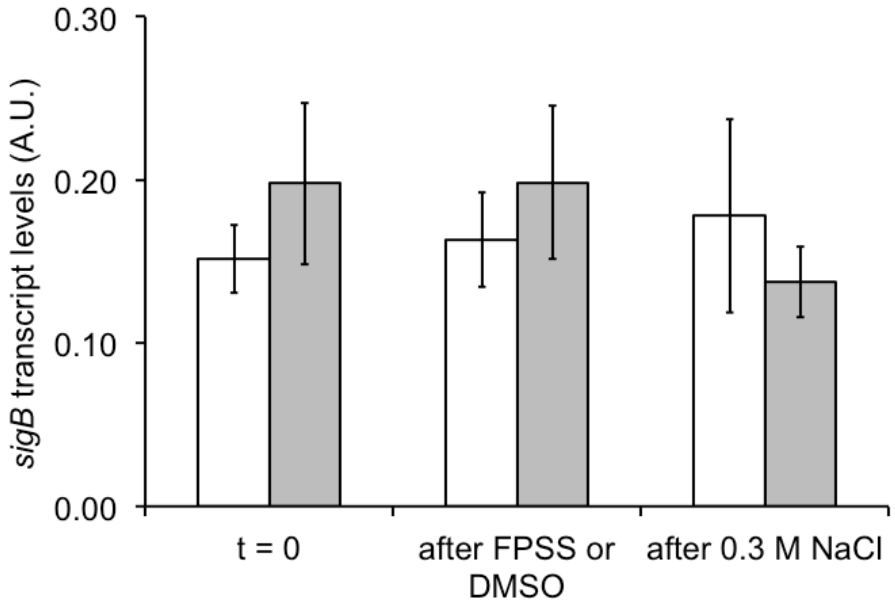


**Figure 4.11** *sigB* transcript levels after addition of FPSS or DMSO. *L. monocytogenes* 10403SΔ*sigB* was grown in BHI at 37°C with shaking (225 rpm). At $OD_{600}$ 0.4, 5 ml of culture was removed and added to 5 ml RNAprotect (Qiagen) to stop transcription prior to RNA isolation ($t$ =0). FPSS (64 uM) or an equal volume of DMSO was added to remaining cultures. After 15 min, another 5 ml aliquot was removed for RNA isolation ("after FPSS or DMSO"). Salt (0.3 M NaCl, final concentration) was added to both cultures, and after 15 min, another 5 ml of culture was collected ("after 0.3 M NaCl). Mean values of *sigB* transcript levels (in arbitrary units) from a DMSO-treated culture (white bars) and a FPSS-treated culture (gray bars) with standard deviation error bars are shown, calculated from three biological replicates. *sigB* transcript copy numbers were normalized to *rpoB* copy numbers to calculate relative transcript levels.

We asked the question of whether the addition of FPSS causes a drop in the transcript levels of *sigB* with and without exposure to a sudden environmental stress, 0.3 M NaCl, compared to a DMSO-control treated culture of *L. monocytogenes*. A mid-exponential phase culture of *L. monocytogenes* 10403SΔ*sigB* was exposed to 64 uM FPSS or DMSO, and RNA was collected from an aliquot was removed after 15 min of exposure to the compounds. Next, we added salt and again collected RNA from a sample of the culture collected 15 min after exposure to salt. This experimental setup allowed us to see if the addition of FPSS alone decreased *sigB* transcript levels in exponential phase *L. monocytogenes* cells, and also if the presence of FPSS during stress exposure affected *sigB* transcript levels. We saw no significant differences ($p > 0.05$; t-test) of copy numbers of *sigB* transcripts at any of the three time points: t = 0, after addition of FPSS or DMSO, and after addition of salt, between treatments (Figure 4.11). These findings indicate FPSS does not operate at a transcriptional level to inhibit transcription of *sigB*, thus preventing $\sigma^B$ activity during mid-exponential phase growth or in response to a sudden environmental stress.

**FPSS does not prevent sporulation in *B. subtilis***

Partner switching modules paralogous to the RsbV/RsbW/$\sigma^B$ complex control other sigma factors in *B. subtilis*. In particular, the activity of the first sporulation-specific sigma factor, $\sigma^F$, is regulated by an anti-sigma factor and an anti-anti sigma factor, SpoIIAB and SpoIIAA, homologous to RsbW and RsbV, respectively (1, 2). Some "cross-talk" occurs between the paralogous systems' kinases, SpoIIAB and RsbW, and their substrate anti-sigma factors (14). Therefore, we sought to determine whether the effect of FPSS might also inhibit $\sigma^F$ activity.

In addition to this other partner switching module, we sought to investigate whether FPSS affects sporulation to test for any effects on Obg, an essential GTP binding protein in *B. subtilis* necessary for growth, sporulation, and environmental stress activation of $\sigma^B$ activity (31, 49). Obg's growth and stress activation functions are separable and attributed to two separate regions of the protein (32), suggesting one function might be altered without impairing the other. Furthermore, Obg's association with ribosomal complexes (33) and interaction with RsbW in a yeast two-hybrid assay (32) led us to explore whether FPSS might somehow interact with Obg to disrupt $\sigma^B$ activity.

To test whether any of these proteins' functions might be perturbed by FPSS, we examined the small molecule's effect on *B. subtilis* sporulation. Deletion of *sigB* has been shown to have no effect on sporulation (7), so accordingly we did not expect FPSS inhibition of $\sigma^B$ activity to inhibit sporulation unless it exerted its effects on another system. We assayed Δ*sigB* mutant strain PB345 in addition to PB198 to verify any effects on sporulation would be independent of $\sigma^B$. PB198 and PB345 were grown in sporulation medium (2XSG) supplemented with FPSS or DMSO for 24 hr at 37°C, then heated at 80°C for 20 min. Neither strain showed a significantly different sporulation efficiency ($p > 0.05$; t-test) when grown in the presence of DMSO compared to 64 uM FPSS (Table 4.3). While possible that FPSS might be titrated by a potential target at the high cell densities at which sporulation occurred, these results do not suggest that FPSS interferes with the partner switching module SpoIIAB-SpoIIAA or Obg when added to exponentially growing cells at the same concentration (64 uM) that prevents $\sigma^B$ activity during entry into stationary phase.

**Table 4.3** Sporulation efficiency of *B. subtilis* treated with FPSS or DMSO.

| Strain | Treatment | Mean sporulation efficiency (%)[a] |
|---|---|---|
| PB198 (*amyE::ctc-lacZ trpC2*) | DMSO | 72.1 (11.0) |
| PB198 (*amyE::ctc-lacZ trpC2*) | 64 uM FPSS | 70.7 (11.1) |
| PB345 (*amyE::ctc-lacZ trpC2 sigBΔ3::spc trpC2*) | DMSO | 51.6 (19.8) |
| PB345 (*amyE::ctc-lacZ trpC2 sigBΔ3::spc trpC2*) | 64 uM FPSS | 60.3 (8.1) |

[a]Mean sporulation efficiency was calculated from three biological replicates. Standard deviations are shown in parentheses. T-tests of treatments within strain were performed on sporulation efficiency values ($p > 0.05$; JMP 9.0).

## DISCUSSION

$\sigma^B$ regulates the general stress response in *B. subtilis* through a variety of pathways (25). We have probed the mechanism of action of a novel inhibitor of $\sigma^B$ activity, FPSS (44), by measuring its effect on $\sigma^B$ activity in response to environmental, energy, and growth at cold temperature. FPSS prevents or delays induction of $\sigma^B$ activity controlled by all three pathways, allowing us to deduce that none of the regulatory proteins belonging to these pathways are exclusive targets of FPSS.

Central to the regulation of $\sigma^B$ in response to energy and sudden environmental stress in *B. subtilis* is the dephosphorylation of the anti-anti-sigma factor, RsbV, a member of the partner switching module directly responsible for controlling the free or bound state of $\sigma^B$ (3, 4, 11). The phosphorylation state of RsbV serves as the main switch that determines the binding partner of the anti-sigma factor RsbW. Unphosphorylated RsbV has a higher affinity for RsbW than $\sigma^B$ (20), but RsbW's kinase function keeps a majority of RsbV phosphorylated at baseline expression levels of the *sigB* operon in unstressed cells (35). The phosphatases RsbU and RsbP desphosphorylate RsbV-P and modulate $\sigma^B$ activity in a tightly controlled circuit, countering RsbW's antagonistic role (35). In *B. subtilis*, RsbU and RsbP function independently, responding

to separate stress sensing components. Our finding that the response to stress controlled by both pathways possessing these phosphatases is inhibited by FPSS allows us to conclude that neither RsbU nor RsbP is a direct target of FPSS. Additionally, we conclude that neither the stressosome nor RsbQ, the upstream regulatory proteins that interact with RsbU and RsbQ, respectively, that communicate stress signals to the phosphatases are exclusive targets of FPSS.

Growth at 16°C induces $\sigma^B$ activity more gradually than rapid environmental stresses like exposure to salt (12). $\sigma^B$ activity in response to cool temperatures is induced independently of RsbV's phosphorylation state, since $\sigma^B$ activity increases even in a Δ*rsbV* mutant (12). We confirmed this previously observed "chill induction," and found FPSS inhibited $\sigma^B$ activity in these conditions in both wild type and Δ*rsbV* strains. While the activation of $\sigma^B$ during cold growth is not yet full understood, induction of $\sigma^B$ activity appears to occur independently of RsbV's phosphorylation state, providing further evidence that FPSS affects neither phosphatases RsbP or RsbU to exert its effect on $\sigma^B$ activity. We also conclude that RsbV is not a target of FPSS based on these data.

We explored whether FPSS affects $\sigma^B$ pre- or post-activation, in other words, whether it exerts an effect before or after the freeing of $\sigma^B$. Our results from artificial induction of $\sigma^B$ activity by overexpressing the *sigB* operon suggest that FPSS disrupts the freeing of $\sigma^B$ from RsbW that normally occurs in response to stress, not by inhibiting the transcriptional activity of $\sigma^B$ once freed. We failed to provide evidence for direct binding of FPSS to $\sigma^B$ or RsbW in vitro, strongly suggesting that FPSS does not inhibit $\sigma^B$ activity by direct binding to the sigma factor in vivo. Therefore, we tentatively conclude that FPSS's mechanism of inhibiting $\sigma^B$ activity is not a result of direct binding to members of the partner switching module.

Our findings suggest that there may be another necessary component for $\sigma^B$ activation that we did not investigate in our study. We have observed a slight growth inhibition of *B. subtilis* and *L. monocytogenes* wildtype and Δ*sigB* strains treated with concentrations of FPSS (our work, unpublished), which may suggest that the small molecule has a universal effect and affects other cellular systems besides the $\sigma^B$ regulon. Another possibility may be that FPSS interferes with the signals upstream of the stress-sensing pathways investigated in this study, such as the production or perception of some stress-communicating ligand that can be sensed by PAS domains (52) found in *B. subtilis* RsbP-PAS, as hypothesized by Nadezhdin et al. (37). Identifying FPSS's target will be crucial to understanding how $\sigma^B$ activity is regulated in *B. subtilis* and *L. monocytogenes*, and how similar homologous systems are regulated in other Gram-positive organisms.

REFERENCES


1. **Alper, S., A. Dufour, D. A. Garsin, L. Duncan, and R. Losick.** 1996. Role of adenosine nucleotides in the regulation of a stress-response transcription factor in *Bacillus subtilis*. J Mol Biol **260:**165-177.
2. **Alper, S., L. Duncan, and R. Losick.** 1994. An adenosine nucleotide switch controlling the activity of a cell type-specific transcription factor in *B. subtilis*. Cell **77:**195-205.
3. **Benson, A. K., and W. G. Haldenwang.** 1993. *Bacillus subtilis* sigma B is regulated by a binding protein (RsbW) that blocks its association with core RNA polymerase. Proc Natl Acad Sci U S A **90:**2330-2334.
4. **Benson, A. K., and W. G. Haldenwang.** 1993. Regulation of sigma B levels and activity in *Bacillus subtilis*. Journal of Bacteriology **175:**2347-2356.
5. **Bergholz, T. M., B. Bowen, M. Wiedmann, and K. J. Boor.** 2012. *Listeria monocytogenes* shows temperature-dependent and -independent responses to salt stress, including responses that induce cross-protection against other stresses. Appl Environ Microbiol **78:**2602-2612.
6. **Bergholz, T. M., H. C. den Bakker, E. D. Fortes, K. J. Boor, and M. Wiedmann.** 2010. Salt stress phenotypes in *Listeria monocytogenes* vary by genetic lineage and temperature. Foodborne Path Disease **7:**1537-1549.
7. **Binnie, C., M. Lampe, and R. Losick.** 1986. Gene encoding the sigma 37 species of RNA polymerase sigma factor from *Bacillus subtilis*. Proc Natl Acad Sci U S A **83:**5943-5947.

8. **Bischoff, M., P. Dunman, J. Kormanec, D. Macapagal, E. Murphy, W. Mounts, B. Berger-Bachi, and S. Projan.** 2004. Microarray-based analysis of the *Staphylococcus aureus* sigmaB regulon. J Bacteriol **186:**4085-4099.

9. **Bishop, D. K., and D. J. Hinrichs.** 1987. Adoptive transfer of immunity to *Listeria monocytogenes*. The influence of in vitro stimulation on lymphocyte subset requirements. J Immunol **139:**2005-2009.

10. **Boylan, S. A., A. R. Redfield, and C. W. Price.** 1993. Transcription factor sigma B of *Bacillus subtilis* controls a large stationary-phase regulon. J Bacteriol **175:**3957-3963.

11. **Boylan, S. A., A. Rutherford, S. M. Thomas, and C. W. Price.** 1992. Activation of *Bacillus subtilis* transcription factor sigma B by a regulatory pathway responsive to stationary-phase signals. J Bacteriol **174:**3695-3706.

12. **Brigulla, M., T. Hoffmann, A. Krisp, A. Volker, E. Bremer, and U. Volker.** 2003. Chill induction of the SigB-dependent general stress response in *Bacillus subtilis* and Its contribution to low-temperature adaptation. J Bacteriol **185:**4305-4314.

13. **Brody, M. S., K. Vijay, and C. W. Price.** 2001. Catalytic function of an α/β hydrolase is required for energy stress activation of the $\sigma^B$ transcription factor in *Bacillus subtilis*. J Bacteriol **183:**6422-6428.

14. **Carniol, K., T.-J. Kim, C. W. Price, and R. Losick.** 2004. Insulation of the $\sigma^F$ Regulatory System in *Bacillus subtilis*. Journal of Bacteriology **186:**4390-4394.

15. **Chaturongakul, S., and K. J. Boor.** 2004. RsbT and RsbV contribute to $\sigma^B$-dependent survival under environmental, energy, and intracellular stress conditions in *Listeria monocytogenes*. Appl Environ Microbiol **70:**5349-5356.

16. **Chaturongakul, S., and K. J. Boor.** 2006. $\sigma^B$ activation under environmental and energy stress conditions in *Listeria monocytogenes*. Appl Environ Microbiol **72:**5197-5203.

17. **Chen, C.-C., R. J. Lewis, R. Harris, M. D. Yudkin, and O. Delumeau.** 2003. A supramolecular complex in the environmental stress signalling pathway of *Bacillus subtilis*. Mol Microbiol **49:**1657-1669.

18. **Choi, S.-K., and M. H. Saier.** 2010. Transcriptional regulation of the *rsbV* promoter controlling stress responses to ethanol, carbon limitation, and phosphorous limitation in *Bacillus subtilis*. Intl J Microbiol **2010:**263410.

19. **Delumeau, O., C.-C. Chen, J. W. Murray, M. D. Yudkin, and R. J. Lewis.** 2006. High-Molecular-Weight complexes of RsbR and paralogues in the environmental signaling pathway of *Bacillus subtilis*. J Bacteriol **188:**7885-7892.

20. **Delumeau, O., R. J. Lewis, and M. D. Yudkin.** 2002. Protein-protein interactions that regulate the energy stress activation of $\sigma^B$ in *Bacillus subtilis*. J Bacteriol **184:**5583-5589.

21. **Eymann, C., S. Schulz, K. Gronau, D. Becher, M. Hecker, and C. W. Price.** 2011. In vivo phosphorylation patterns of key stressosome proteins define a second feedback loop that limits activation of *Bacillus subtilis* $\sigma^B$. Mol Microbiol **80:**798-810.

22. **Ferreira, A., M. Gray, M. Wiedmann, and K. J. Boor.** 2004. Comparative genomic analysis of the *sigB* operon in *Listeria monocytogenes* and in other Gram-positive bacteria. Curr Microbiol **48:**39-46.

23. **Fouet, A., O. Namy, and G. Lambert.** 2000. Characterization of the operon encoding the alternative sigma B factor from *Bacillus anthracis* and its role in virulence. J Bacteriol **182:**5036-5045.

24. **Gaidenko, T. A., X. Bie, E. P. Baldwin, and C. W. Price.** 2011. Substitutions in the presumed sensing domain of the *Bacillus subtilis* stressosome affect its basal output but not response to environmental signals. J Bacteriol **193:**3588-3597.

25. **Hecker, M., J. Pané-Farré, and U. Völker.** 2007. SigB-dependent general stress response in *Bacillus subtilis* and related gram-positive bacteria. Microbiology **61:**215-236.

26. **Holtmann, G., M. Brigulla, L. Steil, A. Schutz, K. Barnekow, U. Volker, and E. Bremer.** 2004. RsbV-independent induction of the SigB-dependent general stress regulon of *Bacillus subtilis* during growth at high temperature. J Bacteriol **186:**6150-6158.

27. **Horsburgh, M. J., J. L. Aish, I. J. White, L. Shaw, J. K. Lithgow, and S. J. Foster.** 2002. $\sigma^B$ modulates virulence determinant expression and stress resistance: characterization of a functional *rsbU* strain derived from *Staphylococcus aureus* 8325-4. J Bacteriol **184:**5457-5467.

28. **Kalman, S., M. L. Duncan, S. M. Thomas, and C. W. Price.** 1990. Similar organization of the *sigB* and *spoIIA* operons encoding alternate sigma factors of *Bacillus subtilis* RNA polymerase. J Bacteriol **172:**5575-5585.

29. **Kenney, T. J., and C. P. Moran Jr.** 1987. Organization and regulation of an operon that encodes a sporulation-essential sigma factor in *Bacillus subtilis*. J Bacteriol **169:**3329-3339.

30. **Kim, T.-J., T. A. Gaidenko, and C. W. Price.** 2004. In vivo phosphorylation of partner switching regulators correlates with stress transmission in the environmental signaling pathway of *Bacillus subtilis*. J Bacteriol **186:**6124-6132.

31. **Kok, J., K. A. Trach, and J. A. Hoch.** 1994. Effects on *Bacillus subtilis* of a conditional lethal mutation in the essential GTP-binding protein Obg. J Bacteriol **176:**7155-7160.

32. **Kuo, S., B. Demeler, and W. G. Haldenwang.** 2008. The growth-promoting and stress response activities of the *Bacillus subtilis* GTP binding protein Obg are separable by mutation. J Bacteriol **190:**6625-6635.

33. **Kuo, S., S. Zhang, R. L. Woodbury, and W. G. Haldenwang.** 2004. Associations between *Bacillus subtilis* $\sigma^B$ regulators in cell extracts. Microbiology **150:**4125-4136.

34. **Leighton, T. J., and R. H. Doi.** 1971. The stability of messenger ribonucleic acid during sporulation in *Bacillus subtilis*. J Biol Chem **246:**3189-3195.

35. **Locke, J. C. W., J. W. Young, M. Fontes, M. J. H. Jiménez, and M. B. Elowitz.** 2011. Stochastic pulse regulation in bacterial stress response. Science **334:**366-369.

36. **Marles-Wright, J., T. Grant, O. Delumeau, G. van Duinen, S. J. Firbank, P. J. Lewis, J. W. Murray, J. A. Newman, M. B. Quin, P. R. Race, A. Rohou, W. Tichelaar, M. van Heel, and R. J. Lewis.** 2008. Molecular achitecture of the "Stressosome," a signal integration and transduction hub. Science **322:**92-96.

37. **Nadezhdin, E. V., M. S. Brody, and C. W. Price.** 2011. An α/β hydrolase and associated Per-ARNT-Sim domain comprise a bipartite sensing module coupled with diverse output domains. PLoS ONE **6:**e25418.

38. **Nadon, C. A., B. M. Bowen, M. Wiedmann, and K. J. Boor.** 2002. Sigma B contributes to PrfA-mediated virulence in *Listeria monocytogenes*. Infect Immun **70:**3948-3952.

39. **Nannapaneni, P., F. Hertwig, M. Depke, M. Hecker, U. Mäder, U. Völker, L. Steil, and S. A. F. T. van Hijum.** Defining the structure of the general stress regulon of

*Bacillus subtilis* using targeted microarray analysis and random forest classification. Microbiology **158:**696-707.

40. **Oliver, H., R. Orsi, L. Ponnala, U. Keich, W. Wang, Q. Sun, S. Cartinhour, M. Filiatrault, M. Wiedmann, and K. Boor.** 2009. Deep RNA sequencing of L. monocytogenes reveals overlapping and extensive stationary phase and sigma B-dependent transcriptomes, including multiple highly transcribed noncoding RNAs. BMC Genomics **10:**641.

41. **Oliver, H. F., R. H. Orsi, M. Wiedmann, and K. J. Boor.** 2010. *Listeria monocytogenes* $\sigma^B$ has a small core regulon and a conserved role in virulence but makes differential contributions to stress rolerance across a diverse collection of strains. Appl Environ Microbiol **76:**4216-4232.

42. **Ollinger, J., B. Bowen, M. Wiedmann, K. J. Boor, and T. M. Bergholz.** 2009. *Listeria monocytogenes* $\sigma^B$ modulates PrfA-mediated virulence factor expression. Infect Immun **77:**2113-2124.

43. **Olsen, K. N., M. H. Larsen, C. G. M. Gahan, B. Kallipolitis, X. A. Wolf, R. Rea, C. Hill, and H. Ingmer.** 2005. The Dps-like protein Fri of *Listeria monocytogenes* promotes stress tolerance and intracellular multiplication in macrophage-like cells. Microbiol **151:**925-933.

44. **Palmer, M. E., S. Chaturongakul, M. Wiedmann, and K. J. Boor.** 2011. The *Listeria monocytogenes* $\sigma^B$ regulon and its virulence-associated functions are inhibited by a small molecule. mBio **2:**e00241.

45. **Price, C. W., and R. H. Doi.** 1985. Genetic mapping of *rpoD* implicates the major sigma factor of *Bacillus subtilis* RNA polymerase in sporulation initiation. Mol Gen Genet **201:**88-95.

46. **Price, C. W., P. Fawcett, H. Ceremonie, N. Su, C. K. Murphy, and P. Youngman.** 2001. Genome-wide analysis of the general stress response in *Bacillus subtilis*. Mol Microbiol **41:**757-774.

47. **Raengpradub, S., M. Wiedmann, and K. J. Boor.** 2008. Comparative analysis of the $\sigma^B$-dependent stress responses in *Listeria monocytogenes* and *Listeria innocua* strains exposed to selected stress conditions. Appl Environ Microbiol **74:**158-171.

48. **Rauch, M., Q. Luo, S. Muller-Altrock, and W. Goebel.** 2005. SigB-dependent *in vitro* transcription of *prfA* and some newly identified genes of *Listeria monocytogenes* whose expression is affected by PrfA *in vivo*. J Bacteriol **187:**800-804.

49. **Scott, J. M., and W. G. Haldenwang.** 1999. Obg, an essential GTP binding protein of *Bacillus subtilis*, is necessary for stress activation of transcription factor sigma B. J Bacteriol **181:**4653-4660.

50. **Shin, J.-H., M. S. Brody, and C. W. Price.** 2010. Physical and antibiotic stresses require activation of the RsbU phosphatase to induce the general stress response in *Listeria monocytogenes*. Microbiology **156:**2660-2669.

51. **Sue, D., D. Fink, M. Wiedmann, and K. J. Boor.** 2004. $\sigma^B$-dependent gene induction and expression in *Listeria monocytogenes* during osmotic and acid stress conditions simulating the intestinal environment. Microbiology **150:**3843-3855.

52. **Taylor, B. L., and I. B. Zhulin.** 1999. PAS domains: internal sensors of oxygen, redox potential, and light. Microbiol Mol Biol Rev **63:**479-506.

53. **Vijay, K., M. S. Brody, E. Fredlund, and C. W. Price.** 2000. A PP2C phosphatase containing a PAS domain is required to convey signals of energy stress to the $\sigma^B$ transcription factor of *Bacillus subtilis*. Mol Microbiol **35:**180-188.

54. **Voelker, U., A. Voelker, B. Maul, M. Hecker, A. Dufour, and W. G. Haldenwang.** 1995. Separate mechanisms activate sigma B of *Bacillus subtilis* in response to environmental and metabolic stresses. J Bacteriol **177:**3771.

55. **Wiedmann, M., T. J. Arvik, R. J. Hurley, and K. J. Boor.** 1998. General stress transcription factor sigma B and its role in acid tolerance and virulence of *Listeria monocytogenes*. J Bacteriol **180:**3650-3656.

56. **Wise, A. A., and C. W. Price.** 1995. Four additional genes in the *sigB* operon of *Bacillus subtilis* that control activity of the general stress factor sigma B in response to environmental signals. J Bacteriol **177:**123-33.

57. **Xue, G.-P., J. S. Johnson, and B. P. Dalrymple.** 1999. High osmolarity improves the electro-transformation efficiency of the gram-positive bacteria *Bacillus subtilis* and *Bacillus licheniformis*. J Microbiol Methods **34:**183-191.

58. **Yang, X., C. M. Kang, M. S. Brody, and C. W. Price.** 1996. Opposing pairs of serine protein kinases and phosphatases transmit signals of environmental stress to activate a bacterial transcription factor. Genes Dev **10:**2265.

59. **Yanisch-Perron, C., J. Vieira, and J. Messing.** 1985. Improved M13 phage cloning vectors and host strains: nucleotide sequences of the M13mp18 and pUC19 vectors. Gene **33:**103-119.

60. **Zhang, S., and W. G. Haldenwang.** 2005. Contributions of ATP, GTP, and redox state to nutritional stress activation of the *Bacillus subtilis* $\sigma^B$ transcription factor. J Bacteriol **187:**7554-7560.

61. **Zhang, S., and W. G. Haldenwang.** 2003. RelA is a component of the nutritional stress activation pathway of the *Bacillus subtilis* transcription factor $\sigma^B$. J Bacteriol **185:**5714-5721.

# CHAPTER 5

# CONCLUSIONS

Because *L. monocytogenes* can grow at refrigeration temperatures and can cause severe illness and even death in susceptible populations, this foodborne pathogen remains an important food safety concern. Its ability to be transmitted throughout food systems requires several steps: initial contamination of food processing environments, contamination of food after lethal processing steps or in their absence during processing, and the ability to survive the various stresses during any of these stages of transmission. The work presented here addresses these various aspects of transmission and stress survival by a range of applied and basic research approaches.

Our first objective was to measure the efficacy of PL inactivation on food packaging materials. We show that high levels of inactivation (> 7 log CFU) of Gram-positive vegetative cells (*L. innocua*) can be achieved on packaging materials, and through some materials with low absorbance in the UV range such as low density polyethylene. Our inactivation data were consistent with previous PL inactivation studies that demonstrated inactivation curves achieved by PL can be modeled using Weibull kinetics. We also show that substrate characteristics – in particular, specular reflection – appear to influence inactivation kinetics.

These results demonstrate that any commercial uses of PL should be validated on a case-by-case basis to ensure that the treatment meets desired inactivation targets for a specific substrate. Future work exploring the use of PL for decontamination of packaging materials should measure the effects of PL on other packaging properties, such as water vapor and oxygen transmission, which are important performance criteria for packaging applications.

The second objective of this work was to investigate mechanisms of persistence of *L. monocytogenes* in food processing environments. The question of why some strains of this foodborne pathogen are able to persist while others are only found sporadically continues to be a pressing question for the food industry that seeks to eliminate persistent *L. monocytogenes* from food processing facilities.

In the second study, we proposed a transcriptional mechanism and hypothesized that an elevated stress response might allow certain strains to survive the stresses encountered in a food processing facility better than other strains with less elevated stress responses. Quantification of transcript levels of four genes regulated by two stress regulators, CtsR and $\sigma^B$, in response to high salt conditions in 13 strains from food processing plants did not reveal a trend of higher induction of these genes by persistent strains compared to non-persistent strains. Therefore, we found no evidence to support our initial hypothesis. This work adds to the growing body of literature unable to identify specific mechanisms that are consistently associated with *L. monocytogenes* persistence in food processing environments and supports a stochastic model, in which strains establish niches randomly, rather than by demonstrating specific phenotypes that give them an advantage over other strains.

Finally, our third objective was target deconvolution of FPSS, a novel inhibitor of $\sigma^B$ activity. The initial approach to identify compounds that inhibit $\sigma^B$ activity was a cell-based assay in which ~57,000 compounds were screened for a phenotypic effect, i.e., decreased $\sigma^B$ activity as measured by a $\sigma^B$-dependent transcriptional reporter fusion. Two common problems exist in cell-based drug discovery: i) identifying the specific target of a compound that results in a desired phenotype and ii) recognizing any other, unanticipated targets in addition to the targeted system. Identifying the target of compounds inhibiting $\sigma^B$ presents potential challenges

because of its complex post-translation regulation. We hypothesized that FPSS might exert its inhibitory effect on $\sigma^B$ activity through a less obvious mechanism than direct binding to the sigma factor, such as binding to one of the proteins responsible for its regulation (i.e., Rsb proteins and partner switching module RsV/RsbW/$\sigma^B$).

We have explored all the regulatory proteins known to date to be necessary for $\sigma^B$ activity in response to stress in *B. subtilis* as exclusive targets of FPSS without identifying FPSS's mechanism of action. Though we examined binding of FPSS to RsbW with stopped-flow fluorescence analysis, additional work should address the partner switching module, particularly RsbW, using in vivo and in vitro methods to more confidently rule out this complex as a target of FPSS. A problem in our target deconvolution work has been the relatively small size of FPSS (MW 277.31) compared to the protein targets we have investigated, limiting the techniques available to detect direct binding of FPSS to proteins and to label FPSS with a minimally disrupting probe. For example, pull-down assays with biotin or fluorescently labeled FPSS were unsuccessful in pulling down any unique proteins (D. Ringus, data not shown), which may be the result of the probes interfering with binding, a weak interaction, or a non-protein target.

Future work should explore better methods for labeling FPSS and transcriptomics and proteomics of FPSS-treated cells. Identifying other methods that allow for the labeling of FPSS in a less intrusive way (such as isotopic labeling) may provide a more effective means to hone in on the cellular target. Using highthroughput methods such as RNA-Seq and quantitative proteomics (iTraq) may be used to shed light on FPSS's transcriptional and translation perturbations, and can confirm the observations presented here. For example, phosphoproteomics can determine the phosphorylation state of Rsb proteins in the presence of FPSS to confirm our conclusion that FPSS inhibits $\sigma^B$ activity regardless of RsbV's phosphorylation state.

The target of FPSS remains elusive and highly intriguing, as identifying this mystery target will add to our understanding of the complexity of regulation of $\sigma^B$ in *B. subtilis*, *L. monocytogenes*, and other Gram-positive organisms. It is not surprising that such a crucial yet resource intensive process – the general stress response – is subject to a finely tuned network of regulation, since the bacterial cell must maintain the delicate balance of survival in the face of adverse conditions without exhausting resources needed for its continued metabolic survival.

APPENDIX 1

STRUCTURE-ACTIVITY RELATIONSHIPS OF FPSS ANALOGS

To determine which structural moieties of FPSS are necessary for its inhibition of $\sigma^B$ activity, we tested six analogs synthesized by our collaborators at Georgia State University (B. Wang) (Appendix Figure 1). We grew *B. subtilis* strain PB198 in BLB at 37°C to mid exponential phase, added 64 uM of each compound, then induced $\sigma^B$ activity by adding 0.3 M NaCl. We measured $\sigma^B$ activity indirectly with a *ctc-lacZ* reporter fusion using a fluorescence-based assay with 4-methylumbelliferyl β-D-galactopyranoside (4-MUG) as a substrate. β-galactosidase cleaves 4-MUG into the resultant hydrolysis product 4-methylumbelliferone (MU), which is fluorescent. We chose this substrate for greater sensitivity and for quantification, since standards of MU can be used for quantification. MU values from samples removed at 60 min after salt addition were used to determine $\sigma^B$ activity, relative to $\sigma^B$ activity of DMSO-treated control cultures.

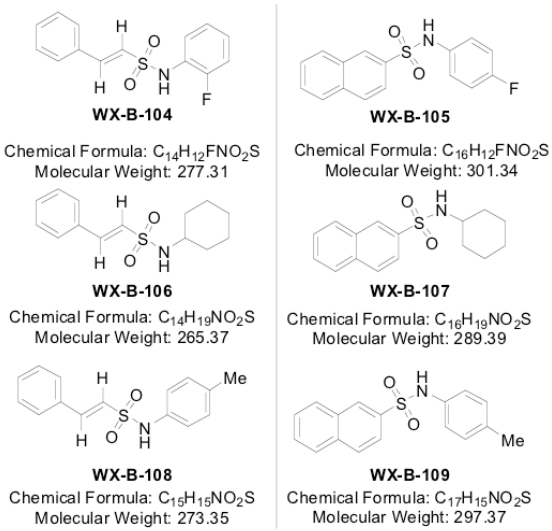


**Appendix Figure 1** Structures of FPSS analogs. Analogs of FPSS synthesized by B. Wang's group.

Initial experiments indicated compounds WX-B-105 and WX-B-109 to be growth inhibitors. Growth curves conducted with these compounds in *L. monocytogenes* 10403S showed severe growth inhibition by WX-B-105 when added to exponentially growing cells, and moderate growth inhibition by compound WX-B-109 (Appendix Figure 2). We excluded these compounds from further β-galactosidase assays investigating structure activity relationships.

β-galactosidase assays of the FPSS analogs showed compounds WX-B-104 and WX-B-108 to have comparable inhibitory effects on *B. subtilis* strain PB198 compared to FPSS

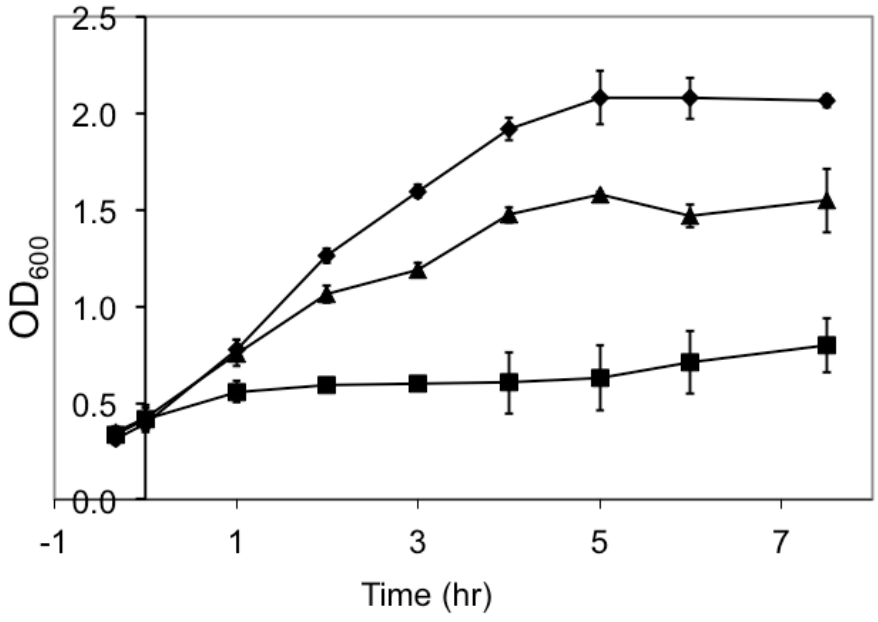


**Appendix Figure 2** Growth curves of *L. monocytogenes* 10403S with FPSS analogs WX-B-105 and WX-B-109. *L. monocytogenes* 10403S was grown 37°C in BHI (5 ml) to $OD_{600}$ 0.4, then 64 uM of DMSO (◆), WX-B-105 (■), or WB-B-109 (▲) was added at $t = 0$. Mean $OD_{600}$ values and range bars from two biological replicates are shown.

(Appendix Figure 3). Compounds WX-B-106 and WX-B-107 had little to no inhibitory effect on $\sigma^B$ activity, comparable to MU values of DMSO-treated cultures. These results suggest that the important structural moieties of FPSS include its fluorinated phenyl ring, which appears to be necessary for its inhibitory activity (Appendix Figure 4). The growth inhibition of WX-B-105 and WX-B-109 suggest that the combination of this phenyl ring with a naphthalene ring instead of a phenylethene group has growth inhibiting consequences.

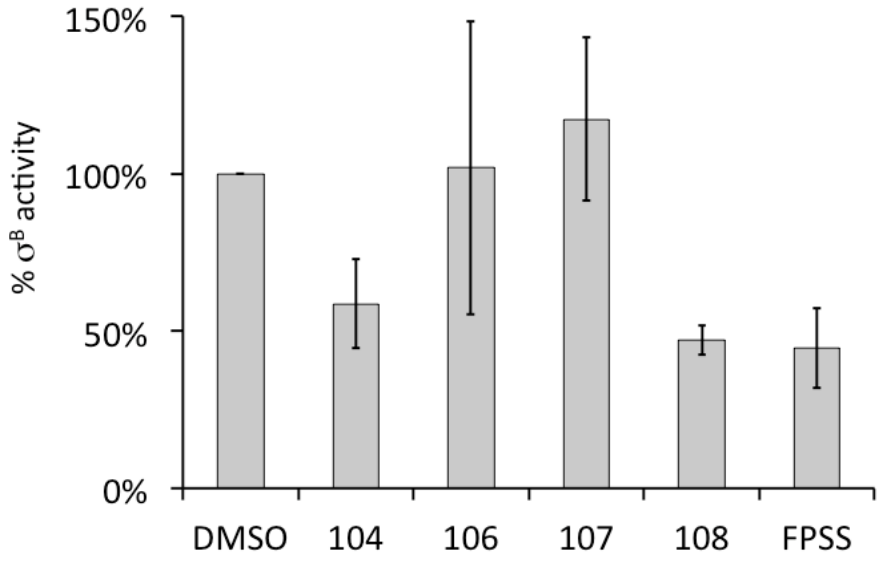


**Appendix Figure 3.** $\sigma^B$ activity of *B. subtilis* treated with FPSS analogs. $\sigma^B$ activity of *B. subtilis* PB198 (*amyE::ctc-lacZ trpC2)* 60 min after addition of 0.3 M NaCl. MU values of analog-treated cultures were normalized to MU values of DMSO-treated control included in each replicate. Mean MU values with range bars from two biological replicates are shown (four biological replicates of FPSS).

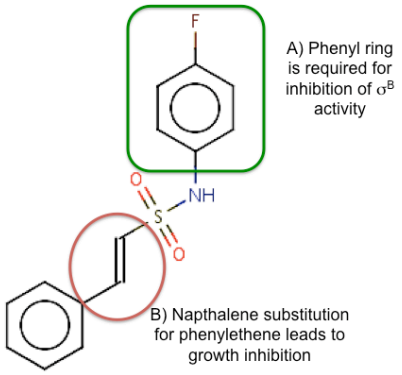


**Appendix Figure 4.** Structural features of FPSS that contribute to A) inhibition of $\sigma^B$ activity and B) growth inhibition.